CHAPTER 4

Ammonia Production Technologies

K.H.R. ROUWENHORST • P.M. KRZYWDA • N.E. BENES • G. MUL • L. LEFFERTS

INTRODUCTION

Ammonia (NH_3) is produced from nitrogen (N_2) and hydrogen (H_2), both naturally and synthetically (see Eq. 4.1) [1,2]. Often, breaking the N≡N triple bond is the rate-limiting step in nitrogen fixation, due to a high dissociation energy (941 kJ/mol). Whilst the synthetic ammonia production routes have developed over the past century, some organisms in nature fix nitrogen in the form of ammonia with nitrogenase [1–4]. Other sources of fixed nitrogen are atmospheric deposition, recycling of crop residues, and animal manures such as guano [5,6]. Furthermore, ammonium sulphate was produced as a by-product of coke and town gas production from coal at the end of the 19th century [7]. However, only half of the required nitrogen fixation could be obtained from these sources around the turn of the 20th century [5].

$$3H_2 + N_2 \rightleftharpoons 2NH_3 \ (\Delta H^o = -91.8 \ \text{kJ/mol}) \qquad \textbf{(4.1)}$$

This notion was addressed by Thomas R. Malthus in *An Essay on the Principle of Population* in 1798, in which he argued that the exponential increase in the human population would lead to starvation due to the finite resources of the earth and the exponential potential for population increase [8]. About a century later (in 1898), Sir William Crookes gave an historical speech at the British Association for the Advancement of Science in Bristol, in which he argued that the world population would starve by 1921 due to the depletion of natural nitrate fertilizer located in deposits in Chile [9]. Crookes called onto the scientists around the world to develop a synthetic process for nitrogen fixation and many heeded the call.

About half of the fixed nitrogen is nowadays produced via a synthetic method, namely the Haber–Bosch process, which is a synthetic thermochemical ammonia synthesis process [5,10]. As shown in Fig. 4.1, the world population has dramatically increased since the industrial realization of the Haber–Bosch process. Without the Haber–Bosch process, the world would be about 40% less populated [10]. Thus, the Haber–Bosch process is one of the most important discoveries of the 20th century [5,10]. The Haber–Bosch process consumes about 1%–2% of the energy, as well as 5% of the natural gas consumption worldwide, at the cost of 1.6% of the CO_2 emissions worldwide [10]. Furthermore, about half of the nitrogen in the human body has been processed via the Haber–Bosch process [10].

BIOLOGICAL NITROGEN FIXATION

Various bacteria, blue-green algae and water ferns can fix atmospheric nitrogen, either by themselves or in a symbiosis with a host plant [4], as first reported in 1888 [11,12]. For example, Rhizobium bacteria settle in the root nodules of legumes [13]. Blue-green algae are self-sufficient for nitrogen fixation by photosynthesis [4]. The enzyme nitrogenase performs the ammonia synthesis, which is due to the NIF gene (a family of proteins) present in these bacteria and algae [4,14]. However, not all organisms can synthesize ammonia and at sufficient rates. Therefore, synthetic ammonia synthesis technologies are required. Recently, bio-inspired catalysts have been researched for on-site fertilizer production on the seeds of plants [15]. Nitrogenase can serve as an inspiration for the design of these catalysts.

Three types of nitrogenases have been identified, the most commonly found being Mo-nitrogenase. The other types of nitrogenases are V-nitrogenase and Fe-only nitrogenase [1]. The protein cycles of Mo-nitrogenase are discussed in Ref. [1,3,16,17]. The enzymes of these nitrogenases stabilize transition states for ammonia synthesis, thereby allowing for ammonia synthesis at near ambient conditions (see Fig. 4.2). Dinitrogenase binds and destabilizes the N_2 molecules, whilst reductase reduces the dinitrogenase protein to form ammonia [11]. The enzyme structure in nitrogenase limits the access to electrons, thereby limiting the hydrogen evolution reaction. In the ideal case, ammonia is formed from air and water according to Eq. (4.2). In practice, one catalytic

Techno-Economic Challenges of Green Ammonia as an Energy Vector. https://doi.org/10.1016/B978-0-12-820560-0.00004-7

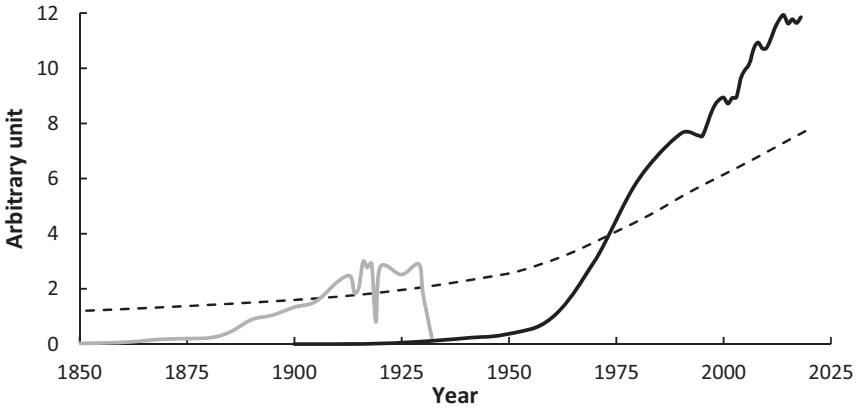

FIG. 4.1 The dependence of the human population on the Haber–Bosch process. Dotted black line: World population ($\times 10^7$ humans). Fully grey line: Annual Chilean nitrate export ($\times 10^3$ kt/y). Full black line: Ammonia production by the Haber–Bosch process ($\times 10^7$ $t_{fixed\text{-}N}$/y).

cycle involves eight electrons, as given by Eq. (4.3). Thus, two electrons are used for the formation of hydrogen, rather than ammonia.

$$0.5\ N_2 + 1.5\ H_2O \rightarrow NH_3 + 0.75\ O_2 \quad (\Delta F^0_{298} = 20.0^{-1} GJ/t_{NH3} \text{ and } \Delta H^0_{298} = 22.5\ GJ/t_{NH3}) \tag{4.2}$$

$$N_2 + 8\ H^+ + 8\ e^- \rightarrow 2\ NH_3 + H_2 \tag{4.3}$$

The competing hydrogen evolution reaction is an issue in electrocatalytic ammonia synthesis. Thus, biological nitrogen fixation can serve as inspiration for electrocatalysis. Current research focuses on the application of biological nitrogen fixation as well as the fundamental understanding of the mechanism in the nitrogenase enzyme [14].

The active site for biological nitrogen fixation is a $MoFe_7S_9N$ cluster (FeMo-cofactor), which produces ammonia from solvated protons, electrons, and nitrogen under ambient conditions [18]. The nitrogen is hydrogenated via an associative mechanism (i.e. molecular di-nitrogen is hydrogenated rather than nitrogen dissociation followed by hydrogenation) [19–22]. About 16 adenosine triphosphate or 26–30 GJ/t_{NH3} are required for ammonia synthesis under ambient conditions [17]. However, a maximum overall efficiency of about 10%–15% is estimated for the enzyme nitrogenase (150–225 GJ/t_{NH3}), and even lower for the bacteria as a whole [4].

HISTORY OF SYNTHETIC AMMONIA SYNTHESIS

Industrially, nitrogen has been fixed along various pathways, namely by a plasma-assisted nitrogen fixation process (the Birkeland–Eyde process), by a cyanamide process (the Frank–Caro process), and a thermochemical synthesis process (the Haber–Bosch process) [23]. The Birkeland–Eyde process and the Frank–Caro process are discussed elsewhere [1]. In the first 2 decades of the 20th century, these processes were employed in parallel [24]. From 1927 onward, the Haber–Bosch process started to win over from the Birkeland–Eyde process and Frank–Caro process, and from the 1940s onward, nitrogen has been fixed almost exclusively by the Haber–Bosch process due to its lower energy consumption per fixed nitrogen and upscaling potential [1,6].

The thermochemical ammonia synthesis process was published and patented by Haber and Le Rossignol in 1913 and 1916, which would be termed the Haber–Bosch process in the years to follow [25–27]. The feasibility of this process was demonstrated by Haber and Le Rossignol in 1908 with a tabletop system operating at

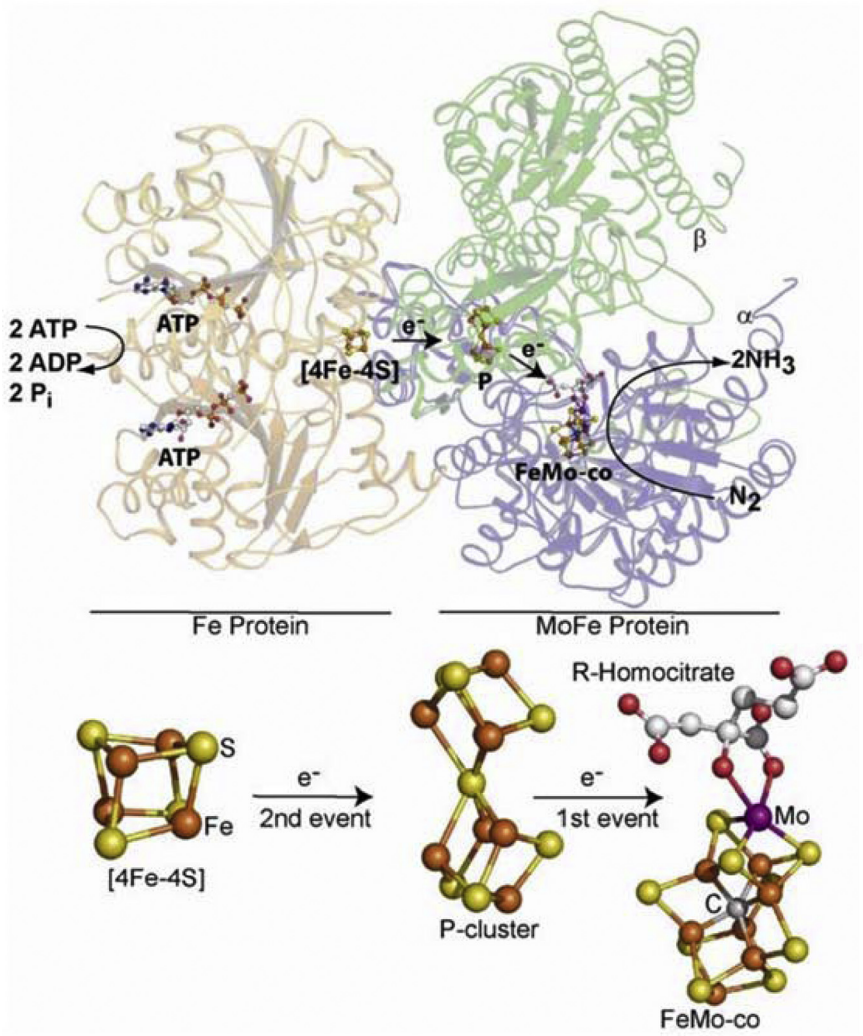

FIG. 4.2 Schematic of ammonia formation in nitrogenase. (Reprinted from Seefeldt LC, Hoffman BM, Dean DR. Electron transfer in nitrogenase catalysis. Curr Opin Chem Biol. 2012;16(1–2):19–25with permission of Elsevier Ltd.)

500–550°C, 100–200 atm and in the presence of an osmium catalyst, producing about two kg_{NH3}/d [24]. Nernst amongst others had concluded that ammonia synthesis was not feasible during the 14th General Convention of the Bunsen Society, only 1 year before [28]. However, Nernst' values for the thermodynamics proved erroneous and synthetic ammonia synthesis was feasible after all. Mittasch et al. developed and patented the use of a multicomponent ('*mehrstoff*') iron catalyst as a more abundant alternative to osmium for ammonia synthesis in 1909–12 and 15 [29,30]. After extensive research performed by many researchers [31], the surface mechanism over the multicomponent iron catalysts was only resolved by Ertl et al. towards the end of the 1970s [32]. Subsequent engineering challenges regarding burst-proof converter material development were dealt with by Bosch et al. in the 1910s [33]. Up to this point, no industrial processes were operated at hundreds of bars [33,34]. Optimizing the metallurgy in the chemical industry remains an

FIG. 4.3 Yara's ammonia plant in Philbara, Western Australia. Courtesy of Yara International ASA.

active field of research [35]. Other major contributors to the understanding of the Haber–Bosch process include Aika, Boudart, Dumesic, Emmett, Liu, Nielsen, Nørskov, Ostwald, Ozaki, Somorjai, Taylor, and Topsøe, amongst many, many others.

Within a decade, the thermodynamics were established, an abundant catalyst was developed, and the engineering challenges were solved [33]. For over 100 years, ammonia has been synthesized by the Haber–Bosch process, starting from 1913 at BASF in Oppau, Ludwigshafen (see Fig. 4.3) [29]. Although research was also conducted in the United States and in other countries within Europe in the 1910s, industrial plants in these countries were only running from the 1920s, mostly based on the German technologies developed in the 1910s [24,36]. In the early days, coal and lignite gasification was the dominant technology for hydrogen production. However, the emergence of low-cost methane with lower chlorine and sulphur content than coal and lignite allowed for more efficient operation with more active catalysts [37]. Methane is reformed with steam to produce a mixture of hydrogen, nitrogen and carbon oxides (see Fig. 4.4) [38].

Alternative process designs to the Haber–Bosch synthesis loop were proposed in the 1920–50 [36]. Amongst these, the Claude process was most radically different, operating at 900–1000 bar with multiple reactors and condensers in series, thereby eliminating the requirement for a recycle in the synthesis loop [39,40]. However, such process designs are impractical for energy-efficient operation due to the heat losses during compression, as well as due to the frequent temperature swings in the Claude process.

The development of ammonia synthesis has been focused on increasing the energy efficiency over the past century (from about 100 GJ/t_{NH3} in the 1920s to 27 GJ/t_{NH3}). Historical developments for ammonia synthesis include the transition from coal or lignite gasification (about 90–100 GJ/t_{NH3}) to steam methane reforming (50–55 GJ/t_{NH3}, 1930–50s), the introduction of centrifugal compressors to replace reciprocating compressors (40–45 GJ/t_{NH3}, around 1960), improved heat integration through process optimization and scale-up in single-train plants (28–40 GJ/t_{NH3}), as well as improved catalyst stability, selectivity and activity to allow for milder operating conditions (26–27 GJ/t_{NH3}) [1,7,41–45]. Further gains in energy efficiency are possible, as the theoretical minimum energy consumption for ammonia synthesis from natural gas is 20.9 GJ/t_{NH3} [4]. Nowadays, gains in energy consumptions are due to scale-up and technology optimization [37]. Whilst in the 2000s the maximum plant size was about 2000 t_{NH3}/d, nowadays the largest plants are 3300 t_{NH3}/d with a potential increase to 5000–6000 t_{NH3}/d in the foreseeable future [37,42]. As equipment sizes such as compressors are limited, new process designs are required for single train plants, such as the Uhde process, comprising of a two-stage ammonia synthesis loop [45]. Furthermore, autothermal reforming (ATR) is more economic than tubular reforming at such large scales due to the lower energy input and steel cost. At the other hand, an oxygen purification plant is required when solely operating with an autothermal reformer. At intermediate scales, a combination of a tubular reformer and an autothermal reformer is most economic (see Fig. 4.4). Potential future developments

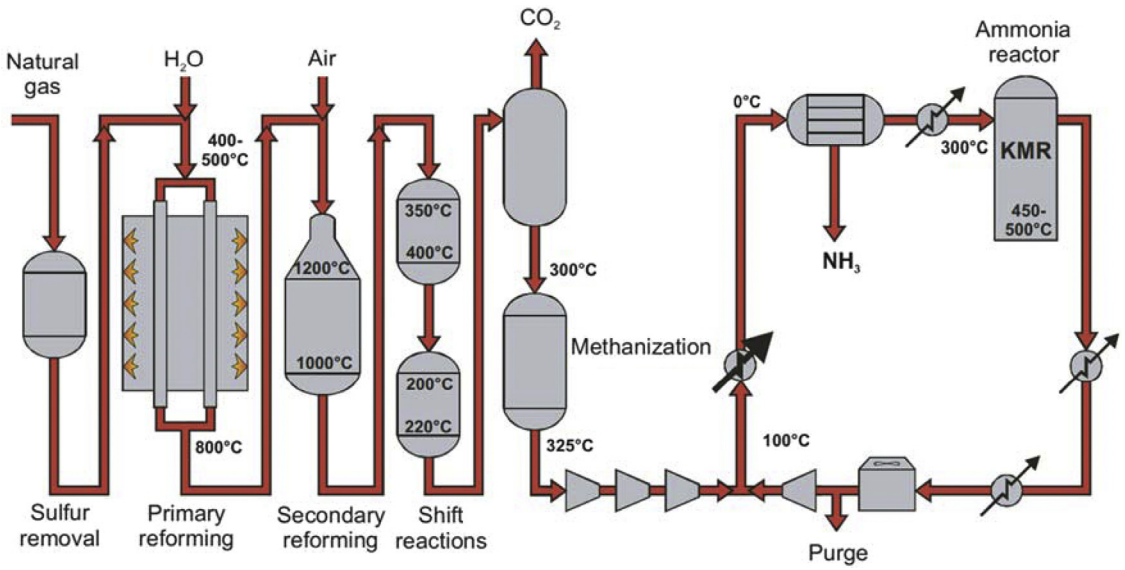

FIG. 4.4 Process scheme of steam methane reforming-based ammonia synthesis. (Reprinted from Hellman A, Honkala K, Dahl S, Christensen CH, Nørskov JK. Ammonia synthesis: state of the bellwether reaction. In: Comprehensive inorganic chemistry (II). 2nd ed. Elsevier Ltd;2013. with permission of Elsevier Ltd.)

include the development of more active catalysts, which may lower the temperature and pressure in the ammonia synthesis loop to about 30 bar (i.e. the pressure of the steam methane reforming section) [46], although this can increase the energy consumption for ammonia condensation and the refrigeration compression [7].

Synthetic ammonia is classified as *brown* ammonia, *blue* ammonia and *green* ammonia. Brown ammonia refers to ammonia synthesized with hydrogen production based on carbon sources, such as methane, naphtha, heavy fuel oil and coal. Fossil hydrogen produced from coal, natural gas and lignite is referred to as *black*, *grey*, and *brown* hydrogen, respectively [48]. Amongst these technologies, the ammonia synthesis process based on methane as a feedstock with steam methane reforming (SMR) for hydrogen synthesis is primarily used. A process scheme of a steam methane reforming-based ammonia synthesis process is shown in Fig. 4.4. Ammonia synthesis technologies emit about 2.0 t_{CO2}/t_{NH3} on average (see Table 4.1). The total CO_2 equivalent emissions have decreased from about 33.4 million t_{CO2} in 1990 to 23.9 million t_{CO2} in 2016 within the European Union [49]. About two-third of the CO_2 is produced during the reforming of hydrocarbons, whilst a third is required for the fuel combustion for the synthesis plant (about 7.2−9.0 GJ/t_{NH3} [50]). Brown ammonia synthesis technologies are discussed extensively in various references [4,44,51−56]. As listed in Table 4.1, the best synthetic ammonia production processes already outperform nitrogenase in nature in terms of energy efficiency (see Fig. 4.5). Although the Haber−Bosch process is an energy-intensive process, the net energy consumption is low. The synthesis pressure for the steam methane reforming section is typically 30 bar, whilst the synthesis loop operates at 100−300 bar.

Decarbonization of heating through electric heating is a recent trend for the chemical industry [57,58]. In the case of brown ammonia synthesis, electric heating for steam methane reforming is proposed to decrease the methane consumption for heating purposes [59]. The footprint of electrified steam methane reforming is about two orders of magnitude smaller than gas-fired steam methane reforming [59]. Furthermore, the start-up of electrified steam methane reforming is only a few minutes, as compared to hours or even days for the conventional, fire-heated steam methane reformers. Electrification of ammonia synthesis plants is attractive in areas with low cost, abundant renewable electricity, as was already pointed out by Ernst in the 1920s [23].

TABLE 4.1
Energy Requirement and CO_2 Footprint of Brown Ammonia, Blue Ammonia, and Green Ammonia Based on the Conventional High Pressure Ammonia Synthesis Loop. The Best Available Technology (BAT) Represents the BAT in the Year 2020, Whilst the Potential Represents the Year 2050.

	ENERGY REQUIREMENT (GJ/t_{NH3})		CO_2 FOOTPRINT (t_{CO2}/t_{NH3})		
	BAT	**Potential**	**BAT**	**Potential**	**Relative IInvestment**
Brown ammonia	**26**	**26**	**1.6**	**1.6**	**1.0**
SMR	26	26	1.6	1.6	1.0
Naphtha	35	–	2.5	–	1.1–1.2
Heavy fuel oil	38	–	3.0	–	1.5
Coal	42	–	3.6	–	1.8–2.1
Blue ammonia	**33**	**26**	**0.4**	**0.2**	**1.5**
Byproduct hydrogen	–	–	1.5–1.6	0.6	–
SMR with CCS	33	27	0.4	0.2	1.5
Coal with CCS	57	–	1.0–2.0	0.5	2.5–3.0
eSMR	–	26	–	1.1	1.0
Green ammonia	**33**	**26**	**0.1**	**0.0**	**1.2–1.5**
Low temperature electrolysis	33	31	0.1	0.0	1.2–1.5
High-temperature electrolysis	–	26	–	0.0	1.5–2.0
Biomass (with CCS)	–	33	1.1–1.2[a]	0.5[a]	1.2–3.0
Global average	**35**	**27**	**2.0**	**1.4**	

[a] The CO_2 emitted is part of a short carbon cycle, as opposed to the CO_2 emitted for natural gas, naphtha, heavy fuel oil, and coal feedstocks. Estimates based on [37,42,44,50,60–62,65,66,69–72].

Blue ammonia is classified as ammonia synthesized in a similar manner as brown ammonia, with a lower net carbon footprint. This reduced carbon footprint can be obtained by combining hydrogen production processes with carbon capture storage (CCS). Electrification of heating processes within steam methane reforming (eSMR) can also reduce the carbon footprint [59]. Hydrogen can also be obtained as a byproduct in other processes, resulting in a lower carbon footprint for ammonia synthesis. Ethylene crackers, chlorine plants, carbon black plants and plastic gasification plants are examples of sources for byproduct hydrogen with a reduced carbon footprint [62,63].

Green ammonia can be classified as ammonia synthesized with essentially zero carbon footprint. Green ammonia can be produced along various pathways, namely with conventional technology for the ammonia synthesis loop combined with electrolysis-based hydrogen (see Fig. 4.6) and with nonconventional technologies for ammonia synthesis. Before the availability of cheap natural gas in the 1950s and onwards, electrolysis-based ammonia synthesis with hydropower was one of the most used technologies, only second to coal gasification. Lastly, biomass-based hydrogen production with carbon capture storage can be considered as an alternative for small scale, green ammonia synthesis [64–67].

In the 1920s, the first electrolysis-based Haber–Bosch process started operation, with an energy consumption of about 46–48 GJ/t_{NH3} [23,40]. Four drivers can be identified for the production of green ammonia, namely the sustainability of the reactants, a low energy consumption, modular scalability, and economic viability [23,68,69]. Green ammonia technologies based on the conventional, high-pressure ammonia synthesis loop with electrolysis-based hydrogen are discussed in Section 4.4-4.9. The theoretical minimum energy required for ammonia synthesis from water and air is 22.5 GJ/t_{NH3} [44]. Nonconventional technologies are discussed in Section 4.10.

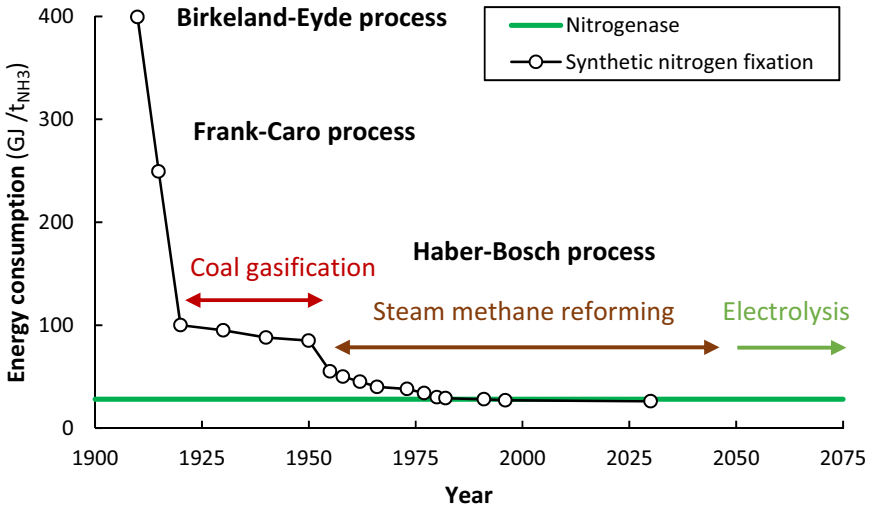

FIG. 4.5 Energy consumption nitrogenase and energy consumption of best available technology (BAT) for dominant synthetic nitrogen fixation processes. (Based on Patil BS, Hessel V, Seefeldt LC, Dean DR, Hoffman BM, Cook BJ, et al. Nitrogen fixation. In: Ullmann's encyclopedia of industrial chemistry. 2017; Smil V. Enriching the earth: Fritz Haber, Carl Bosch, and the transformation of world food production. Cambridge (MA); 2004; CEFIC. European chemistry for growth: unlocking a competitive, low carbon and energy efficient future [Internet]. 2013. Available from: http://www.cefic.org/Documents/RESOURCES/Reports-and-Brochure/Energy-Roadmap-The Report-European-chemistry-for-growth.pdf; Hansen JB, Han P. The SOC4NH3 project in Denmark. In: NH_3 event. Rotterdam (The Netherlands); 2019.)

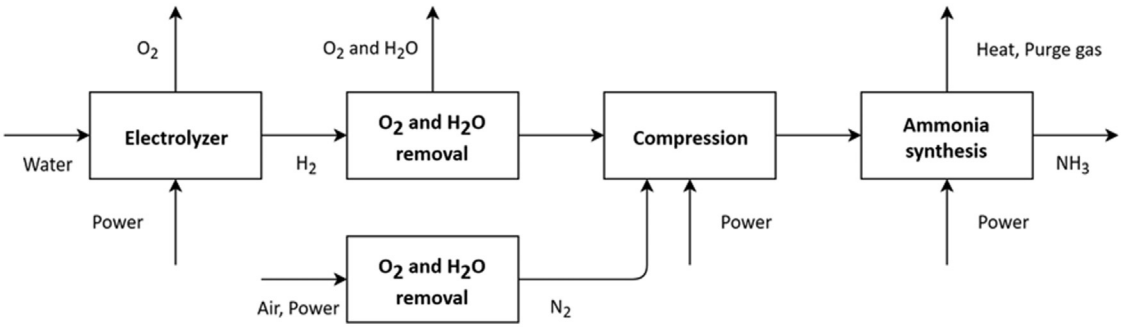

FIG. 4.6 Schematic of green ammonia synthesis process with electrolysis-based hydrogen production.

ELECTROLYSIS-BASED HYDROGEN PRODUCTION

Green hydrogen can be synthesized by electrolysis. The net reaction is given by Eq. (4.4), and the heat of reaction is $\Delta H_r^0 = 250\ \text{kJ/mol}_{H2}$, indicating a high energy requirement either through heating or electrical energy (or the combination of both) [73]. The thermal decomposition of water is not discussed here, as this is mainly relevant for the steam reforming of hydrocarbons.

$$2H_2O \rightarrow 2H_2 + O_2 \quad (4.4)$$

Electrolysis is performed in an electrolysis cell composed of an electrolyte (the ion conductor), active layers for the redox reactions, and a current and material collector (the electronic conductor), which enables the electricity supply, as well as the supply and collection of reactants and products [74]. Electrolysis systems also require gas cooling, purification, compression, and H_2 storage capacity [75]. Furthermore, safety and control systems are installed to condition the power from the power source [76]. Pretreatment of the feed water is performed by mechanical vapour compression,

TABLE 4.2
Electrolysis Technologies.

		Alkaline	PEM	Solid Oxide
Temperature (°C)		60–90	50–80	600–1000
Pressure (bar)		1–30	10–200	1–25
System energy consumption	(GJ/t_{NH3})	29–46	31–46	24–27
Current density (A/cm)		0.2–0.45	0.6–2.0	0.3–2.0
Hydrogen purity (vol.%)		>99.5	99.99	99.9
Maximum installed capacity (MW)		165	20	0.2
Load range (%)		10–110	0–160	20–100
Installed capital cost (k€ tp/d_{NH3})	2020 2030 Long term	165–465 135–285 65–235	365–600 215–500 65–300	935–1865 265–935 165–335
Electrolyte		20–40 wt.% KOH	Nafion	YSZ/SSZ
System size		Large	Compact	Compact
Stack lifetime (h ×1000)	2020 2030 Long term	60–90 90–100 100–150	30–90 60–90 100–150	10–30 40–60 75–100
Technology readiness level (TRL)		9	8–9	5–6

Estimates based on [48,61,73,79,85–87].

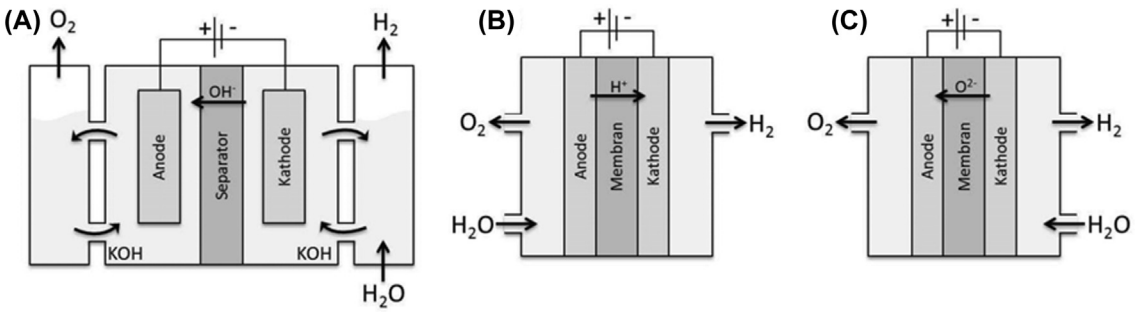

FIG. 4.7 Schematic representation of electrolysis systems: **(A)** alkaline electrolysis, **(B)** PEM electrolysis and **(C)** solid oxide electrolysis. (Reprinted from Steinmüller H, Reiter G, Tichler R, Friedl C, Furtlehner M, Lindorfer J, et al. Power to Gas - eine Systemanalyse: Markt- und Technologieschouting und -analyse [Internet]. Linz; 2014. Available from: https://www.ea.tuwien.ac.at/fileadmin/t/ea/projekte/PtG/Endbericht_-_Power_to_Gas_-_eine_Systemanalyse_-_2014.pdf with permission of TU Wien.)

reverse osmosis or electrodialysis, depending on the feed impurities, purity required and scale of application [77,78].

Various technologies for electrolysis are commercially available, such as alkaline electrolysis and proton exchange membrane (PEM) electrolysis (see Table 4.2). Some technologies are in the demonstration stage, such as solid oxide electrolysis. Other technologies are researched in academia, such as anion exchange membrane electrolysis [73]. The efficiency and capital cost of the system depend on the scale of the application. All commercial systems have load responses in the seconds range in hot standby [79], which is required for adequate coupling with intermittent renewable electricity sources. However, in cold standby, PEM electrolysis is the only technology capable of ramping within seconds. The schematic representation of alkaline electrolysis, PEM electrolysis and solid oxide electrolysis are shown in Fig. 4.7.

Alkaline electrolysis operates with electrodes immersed in a liquid electrolyte (20–40 wt.% KOH), separated by a diaphragm. OH^- ions pass through the

diaphragm, forming hydrogen at the cathode (Ni or Ni–Mo), and oxygen and water at the anode (Ni or Ni–Co). From the 1920s up to the 1990s, alkaline electrolysers were typically used to produce hydrogen in countries with hydropower resources such as Egypt, Norway and Peru, after which steam methane reforming took over [23,24,48]. Novel approaches to enhance the performance (and energy efficiency) include the decoupling of the hydrogen evolution and oxygen evolution reactions by a two-step cycle [81], and the combination of a battery function and an electrolyser function in a single unit [82,83].

In the case of PEM electrolysis protons pass through the membrane. At the cathode (Pt or Pt–Pd), the protons are recombined to form hydrogen and at the anode (RuO_2 or IrO_2) protons and oxygen are produced. Because of the corrosive acidic condition of the membrane, noble metals are used for the electrodes, leading to high capital costs for PEM electrolysis [73]. Platinum replacements such as molybdenum disulphide and phosphides may lower the costs with a performance close to platinum [84]. Improving the stability of such materials is one of the key research focuses.

Solid oxide electrolysis operates with steam rather than liquid water, reducing the electrical energy demand for hydrogen production. Thus, solid oxide electrolysers can operate at a lower energy input than alkaline electrolysis and PEM electrolysis (a minimum energy input of about 250 kJ/mol_{H2} instead of 285 kJ/mol_{H2}). At the cathode (Ni or FeCr), hydrogen is produced, whilst oxygen anions pass through the yttria-stabilized zirconia (YSZ) or scandia-stabilized zirconia (SSZ) membrane to recombine to oxygen over the perovskite-type lanthanum strontium manganese or anthanum strontium cobalt ferrite anode. A benefit of solid oxide electrolysers is the possibility of producing the hydrogen and nitrogen feed in a single unit, thereby omitting the need for a separate nitrogen production unit [61]. This is facilitated by the combustion of oxygen from air with part of the produced hydrogen. Solid oxide electrolysers are expected to be commercially available at the MW scale in 2025–30 [61,73,88]. Current research focuses on cost reduction and increasing the performance at reduced temperatures (from about 1000 to 600°C), thereby increasing the lifetime of the stack [89]. Apart from oxygen anion-conducting membranes, proton-conducting membranes are also investigated, potentially allowing for operation at lower temperatures (400–700°C) and hydrogen production without moisture content [90–92].

Combinations of electrolysis-based hydrogen and hydrogen derived from methane are also proposed. For instance, a hybrid plant with a solid oxide electrolyser and an ATR can be beneficial, as purified oxygen is required for the autothermal reformer and supplied by the solid oxide electrolyser. An autothermal reformer operates via partial combustion of methane with purified oxygen and is especially attractive for large-scale ammonia synthesis due to the expensive oxygen purification plant, which is only economically viable at large scales. In a solid oxide electrolyser, purified oxygen is produced in any case, potentially making autothermal reforming feasible at smaller scales. Such a configuration can save up to 22% in terms of natural gas consumption [88].

BIOMASS-BASED HYDROGEN PRODUCTION

Biomass-based hydrogen production is an alternative for electrolysis-based hydrogen production for small-scale ammonia synthesis [64–67]. In industrialized countries, about 9%–13% of the total energy supply is facilitated by biomass, making it the most used renewable to date [93]. In developing countries, this figure is as high as 20%–35% [93]. By the end of the 1990s, about 40 GW biomass capacity was installed worldwide [93]. Typical biomass-based facilities are limited by the logistics (i.e. the supply of biomass), implying plant capacities are usually below 50 MW [94]. The key metric for the cost of hydrogen is the cost of biomass, which strongly depends on the type of biomass and the location.

Biomass-based hydrogen can be produced via both thermochemical processes and biochemical processes [98,101]. Various biomass-based hydrogen synthesis technologies are listed in Table 4.3. A benefit of biomass-based hydrogen production is the compatibility with the technologies used in conventional brown hydrogen production process. The products of thermochemical or biochemical processing of the biomass are the feedstock of the steam methane reforming reactor, as used in brown ammonia synthesis. A drawback of biomass-based hydrogen production is the complex processing of the biomass [48]. Furthermore, the technical potential of biomass to satisfy the demand for hydrogen is orders of magnitude smaller than that of renewable electricity resources, such as tidal, solar and wind, due to the limited availability of biomass [48]. Typical sources of biomass include bagasse, crops, straw, switchgrass, wood and wood chips [100–103]. The typical products of biomass processing are biogas, bio-oil and biochar [98]. An alternative for natural biomass feedstocks is the recycling of municipal waste [104]. An example of a waste-to-ammonia process is

TABLE 4.3
Technologies for Biomass-Based Hydrogen Production. For Reference, the Best Steam Methane Reformers Operate at 26 GJ/t_{NH3}.

		THERMOCHEMICAL		BIOCHEMICAL	
		Pyrolysis	**Gasification**	**Anaerobic**	**Fermentation**
Temperature (°C)		350–750	500–1150	20–80	30–70
Pressure (bar)		1–5	225–350	1	1
Energy consumption	(kWh/m_{H2}^3) (GJ/t_{NH3})	– –	7.1–10.1 50–72	– –	– –
Hydrogen yield (vol.%)		–	20–65	–	–
Biomass conversion products		Bio-oil, gas, char	H_2, CO, CO_2, CH_4	Biogas	Acids, alcohols, gases
Capacity range (MW)		0.1	0.1–100	<10	<2
Load range (%)		–	–	–	–
Cost of hydrogen (€/kg)	2020 Potential	– –	>1.3 0.6–1.1	– –	– –
TRL		3–5	5–7	6–9	9

Estimates based on [48,93,95–100].

the use of recycled plastic, as is in operation in Japan for selective catalytic reduction purposes [105].

In the case of thermochemical processes, the biomass is either converted into bio-oil, gas and char via pyrolysis or into a mixture of hydrogen, carbon monoxide, carbon dioxide and methane via gasification [48,99]. A benefit of thermochemical processes over biochemical processes is that no microorganisms need to be added for the conversion [98]. Furthermore, biochemical processes have slow kinetics and large reactors due to the near-ambient operation [100].

Pyrolysis is the thermal decomposition of biomass at high temperatures (350–750°C) in the absence of a reactive, oxidative environment. The major product of pyrolysis is bio-oil (45–70 wt.%), the remainder being gases (10–35 wt.%) and char (15–25 wt.%) [98]. The direct production of hydrogen from pyrolysis is insufficient for commercial applications, even in the presence of a catalyst. Therefore, the products of pyrolysis need to be processed to syngas in a steam reformer.

Biomass gasification is a direct pathway for syngas production, as all of the biomass feedstock can be converted directly to gaseous products [97,99]. Biomass gasification gained attention in the 1980s [93]. This process scheme is similar to that of coal gasification, which allows for some blending in biomass in coal feedstocks to minimize the carbon footprint. Chemical and physical reactions occurring in the biomass gasification process include drying, pyrolysis, reduction and combustion [98]. There are some demonstration plants for biomass gasification [48]. Current technological challenges include catalyst poisoning due to the formation of tars [48]. Sorbents such as CaO can be used to remove CO_2 in situ, thereby shifting the equilibrium position for the water gas shift reaction [98]. In the case of steam gasification, the thermal energy-to-hydrogen efficiencies can attain 35%–52% [98].

In the case of biochemical processes, microorganisms convert biomass into biogas via anaerobic digestion or into acids, alcohols and gases via fermentation [48,98]. Anaerobic digestion converts biomass into biogas in the absence of oxygen, whilst in the presence of microorganisms. The process operates at near-ambient conditions (20–80°C). The biogas produced from anaerobic digestion typically contains primarily methane (50–75 wt.%), as well as a substantial portion of CO_2 (25–50 wt.%). Anaerobic digestion is one of the most technologically advanced biomass conversion technologies, but only part of the biomass can be processed, such as process sewage sludge, agricultural waste, food processing waste, household waste and energy crops [48].

The fermentation of biomass is can produce various products in the presence of enzymes, such as acids, alcohols and gases. The non-edible cellulosic parts of plants can be processed in the case of fermentation [48]. A drawback of such biochemical processes is the near-ambient operation, implying slow kinetics and large reactors [100]. Lastly, vegetable oil from energy crops can be converted into glycerol via

transesterification, which can be converted into syngas [98]. The typical operation conditions for transesterification of vegetable oils are 50–80°C and ambient pressure, in the presence of a base [100].

Biogas from biomass can be combined with renewable electricity as well. An example of such a system is anaerobic digestion for biogas production combined with electrified tubular steam reforming reactors. Another example is the combination of a biogas reactor with a solid oxide electrolyser and an autothermal reformer.

NITROGEN PURIFICATION

Purified nitrogen gas is produced from the air using various technologies, namely an air separation unit (ASU, cryogenic distillation), pressure swing adsorption (PSA), membrane permeation and hydrogen combustion [106]. In steam methane reforming, the air is usually introduced in the hydrogen production section, and the oxygen is combusted with part of the hydrogen. Hydrogen combustion can be employed in a solid oxide electrolyser to generate the heat for the hydrogen production from water [61,107]. The three other technologies can be employed in combination with alkaline or PEM electrolysers, where the hydrogen and nitrogen are produced in separate units (see Table 4.4).

The preferred alternative depends on the required nitrogen purity and the scale of application [108]. For both pressure swing adsorption and membrane permeation, a deoxo system is required to remove residual oxygen content [106]. Oxygen is removed by catalytic combustion with hydrogen, after which the water is removed in a regenerative dryer [106]. Oxygen must be removed before the gas mixture enters the synthesis loop, as oxygen compounds are detrimental for the ammonia synthesis catalyst. Nitrogen purification is discussed in various references [106,108,109].

AMMONIA SYNTHESIS LOOP

Ammonia synthesis from nitrogen and hydrogen is an exothermic process favored by a decrease in temperature and an increase in pressure (see Fig. 4.8). However, due to the limited activity of industrially applied iron-based catalysts for breaking the N≡N triple bond and the desorption limitations for ammonia [111], typical operating conditions are 350–550°C and 100–450 bar [44,78,112,113]. As shown in Fig. 4.8, near-complete conversion to ammonia is not achievable under industrially relevant conditions. Thus, a significant recycle is required in the Haber–Bosch process.

A typical industrial ammonia synthesis process is shown in Fig. 4.4. After the production of hydrogen and nitrogen feed in the steam methane reforming section, the nitrogen and hydrogen feed is compressed to 100–450 bar and combined with the recycle. This stream is fed into the ammonia synthesis reactor at about 300–350°C into a multiple bed reactor and feed is converted to about 15–20 mol.% ammonia with an outlet temperature of about 450–500°C [47]. Then, ammonia is separated from the nitrogen and hydrogen gases by condensation at −20 to 30°C. About 2–5 mol.% ammonia is fed back to the ammonia synthesis reactor with the recycle stream [44], which is due to the substantial ammonia vapour pressure at separation conditions (see Fig. 4.9). Some industrial processes

TABLE 4.4
Nitrogen Purification Technologies.

		ASU (Cryogenic)	PSA	Membrane
Temperature (°C)		−195 to −170	20–35	40–60
Pressure (bar)		1–10	6–10	6–25
Purity (wt.%)		99.999	99.8	99.5[a]
Energy consumption	(kWh/kg_{N2}) (GJ/t_{NH3})	0.1 0.3	0.2–0.3 0.7–1.0	0.2–0.6 0.7–2.0
Capacity range (Nm^3/h)		250–50000	25–3000	3–3000
Load range (%)		60–100	30–100	–
Investment cost (k€/tpd_{NH3})		<8	4–25	25–45
TRL		9	9	8–9

[a] In most cases membranes are used for nitrogen enrichment of air, rather than the production of highly purified nitrogen.
Estimates based on [78,106,108–110].

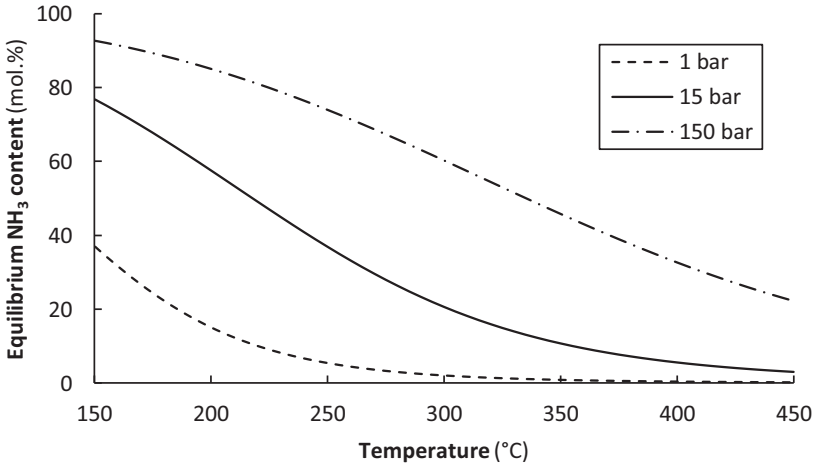

FIG. 4.8 Ammonia equilibrium mole fraction for various temperatures and pressures. H_2:N_2 = 3:1, no inert.

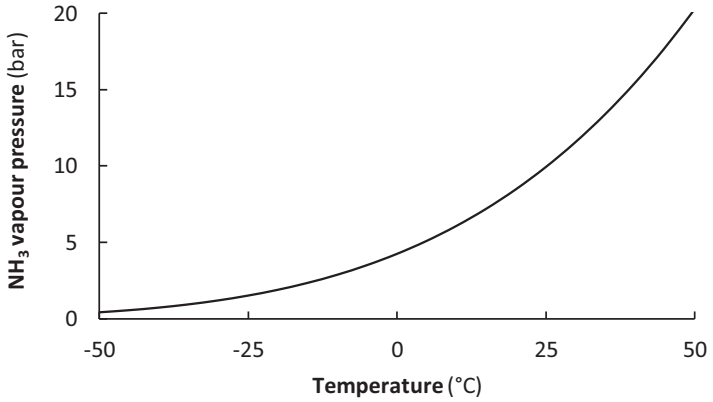

FIG. 4.9 Ammonia vapour pressure as function of temperature. (Antoine parameters reproduced from Stull DR. Vapor pressure of pure substances. Organic and inorganic compounds. Ind Eng Chem. 1947;39(4): 517–540.)

combine the feed with the recycle before the ammonia synthesis reactor, whereas other processes combine the feed with the recycle before the condenser [44].

Catalysts

After the development of the multiple promoted iron catalyst by Mittasch et al. in 1909–12 from Gallivare magnetite (an iron ore from Sweden), the industrially most used catalyst has remained remarkably similar. Whilst the catalyst formulation in the first part of the 20th century was mostly focused on stability against chemical poisoning by sulphur and chlorine compounds, afterwards the focus has been on the catalytic activity due to a reduced fraction of catalyst poisons in the synthesis loop. Iron catalysts derived from magnetite ore (Fe_3O_4) with structural promoters for stability enhancements (Al_2O_3, CaO, MgO, SiO_2) and electronic promoters for activity enhancement (K_2O) are mostly used in industry due to the very high thermal stability and chemical stability against oxygen species. The catalyst is activated by reducing the iron oxide to metallic iron, whilst the promoters remain in their oxide phases. The reaction mechanism via dissociative nitrogen adsorption, subsequent hydrogenation, and desorption of ammonia from iron-based catalysts is well understood [31,32,47,115,116], and the reaction rates of industrial catalysts can be modeled with microkinetic models over a wide range of conditions [47,117,118]. Ultrahigh vacuum surface science with ideal Fe surfaces was successfully applied to predict

the catalytic reaction over iron-based catalysts under industrial conditions, bridging a 'pressure gap' of nine orders of magnitude [117,119].

The first development in iron-based catalyst was the introduction of about 5 wt.% Co to the iron oxide. The introduction of Co to the iron oxide lowers the reduction temperature, which increases the exposure of the most active Fe(111) plane for ammonia synthesis and decreases ammonia desorption limitations [44,120]. Another development is the use of wüstite ($Fe_{1-x}O$) rather than magnetite during the preparation [121], which changes the distribution of promoters in the catalyst. As compared to magnetite-based catalysts, wüstite-based catalysts are known to have a lower reduction temperature and less hydrogen inhibition at low temperatures [121]. However, the thermal stability of wüstite-based catalysts is lower than that of magnetite-based catalysts [122]. This is due to a lower stabilizing effect of Al_2O_3 in wüstite-based catalysts, which is replaced by MgO and CaO [121]. Recent academic contributions to industrial iron-based catalysts include the addition of Co to wüstite-based catalyst [123], the addition of iron nanoparticles to maximize the iron surface area [124], and the addition of rare earth metals to the iron oxide precursor [125].

Ruthenium-based catalysts are also industrially applied for ammonia synthesis. Ruthenium-based catalysts are more active than iron-based catalysts at low pressures and at high conversions, due to less ammonia desorption limitations [126,127]. Ruthenium-based catalysts were developed and patented in the industry in the 1970 and 1980s [44], whilst academic research was also conducted (especially in Japan) [128–132]. A multiple promoted ruthenium catalyst supported on activated carbon was developed, which is used in the Kellogg Advanced Ammonia Process (KAAP). An energy saving of about 1.17 GJ/t_{NH3} was achieved as compared to iron-based processes [44]. Furthermore, the capital cost of the KAAP process is lower than conventional processes, due to the lower operating pressure and the single-stage synthesis gas compressor, albeit at a higher catalyst cost [33,54]. A drawback of ruthenium-based catalysts is the scarcity, making scale-up to all ammonia synthesis plants difficult [133]. Processes with ruthenium-based catalysts generally operate at lower pressures as well as lower H_2:N_2 ratios than those with iron-based catalysts, due to the hydrogen inhibition on ruthenium-based catalysts [44,112].

As opposed to bulk iron-based catalysts, ruthenium-based catalysts consist of ruthenium nanoparticles supported on an activated carbon (AC) support or oxide support [44,47,116]. Alkali (Cs, K) and alkaline earth metals (Ba) are introduced to electronically increase the activity by orders of magnitude [134,135]. The KAAP process uses a Ru/AC catalyst with Ba and K promoters. Methanation of the carbon support is an issue for Ru/AC catalysts, causing a shorter catalyst lifetime. The Ba reduces the rate of methanation of the support, stabilizes the nanoparticles and maximizes the number of active sites for ammonia synthesis [136]. Alkali promoters (Cs, K) enhance the nitrogen dissociation rate and lower the surface coverage of NH_X species on the catalyst species [115,136].

Process Conditions

The choice of the catalyst has little influence on the operating efficiency of the synthesis loop [53,137]. However, the operating temperatures and pressures vary depending on the choice of catalyst (see Table 4.5). This becomes especially relevant upon scale-down and intermittent operation, as milder operating conditions lead to less heat losses upon decreasing degree of heat integration. Furthermore, green hydrogen production implies a change in heat and mass flows in the process, thereby requiring different heat integration schemes [56,138]. Various catalysts are often combined in a single reactor with different beds [139,140]. Typically, ammonia synthesis reactors are multiple-bed adiabatic reactors [45,55]. The first beds operate at high temperatures (up to 500–550°C), whilst later beds operate at milder temperatures. Thus, highly stable catalysts at high temperatures are mostly preferred for the first beds, whereas the activity at mild conditions is increasingly important for the last beds.

SCALE-DOWN AND INTERMITTENCY

Recent trends in ammonia synthesis technologies are further scale-up for minor improvements in energy consumption (mega conventional, mostly for *brown* and *blue* ammonia production), and scale-down for coupling with intermittent, renewable energy sources (small decentralized, for *green* ammonia) [88]. Decentralization of ammonia synthesis processes is mainly conducted along two pathways, namely by using the conventional electrolysis-based Haber-Bosch technology, and by using nonconventional technology with milder reaction and separation conditions [46]. The nonconventional technologies are discussed in section 4.10.

Up to the 1990s, electrolysis-based Haber–Bosch process was operated in various places with hydropower, such as Norway and Peru [143]. Thus, electrolysis-based Haber–Bosch processes are proven technology at large-

TABLE 4.5
Comparison of SMR-Based Ammonia Synthesis Processes With Commercial Iron-Based and Ruthenium-Based Catalysts.

	IRON			RUTHENIUM
	Fe_3O_4	Fe_3O_4 with Co	$Fe_{1-x}O$	Ru–Ba–K/AC
Year	1913	1979	1986	1992
Temperature (°C)	360–520	350–500	300–500	325–450
Pressure (bar)	120–450	100–300	100–250	70–100
Energy consumption (GJ/t_{NH3})	28	28	27–28	26–27
H_2:N_2 ratio	2–3	2–3	2–3	1.5–2
Catalyst lifetime (y)	>14	–	6–10	≤10
Relative activity	1.0	1.2	1.5	2–10
Thermal stability	High	Medium/Low	Medium	Low
Relative catalyst cost	1.0	1.5	1.1	150–230

Based on [4,44,78,112,141,142].

scale operation (300 t_{NH3}/d with alkaline electrolysers of 135 MW capacity). Currently, only one large-scale, alkaline electrolysis-based Haber–Bosch plant with hydropower resources remains operational in Cusco, Peru (built in 1962). The current aim is to operate these electrolysis-based Haber–Bosch processes as energy efficient as possible and at the scale of single wind turbines or at the scale of solar or wind farms. Demonstration plants were recently opened in various countries, including Japan and the United Kingdom. Demonstration plants in the United States include solar-powered systems and wind-powered systems located in areas with extensive farmlands [144–148]. Commercial PEM electrolysis-based Haber–Bosch plants operating with a PSA unit and a high-pressure ammonia synthesis loop are in operation in various countries including Argentina, China and Switzerland [149,150]. A benefit of small-scale plants (≤50 t_{NH3}/d) is that these are not considered as industrial sites, implying regulatory obstacles are usually smaller [151].

Upon scale-down, heat losses increase and the energy consumption increases (see Fig. 4.10). A large-scale ammonia plant (≥1000 t_{NH3}/d) consumes about 2–7 GJ/t_{NH3} for pressurizing, heating, pumping and utilities [56]. At intermediate scales (3–20 t_{NH3}/d), this energy consumption increases to typically 13–14 GJ/t_{NH3} [152,153]. At ammonia synthesis scales down to 5 t_{NH3}/d, losses in high-pressure synthesis processes are primarily due to scale effects. At very small scales (<0.1 t_{NH3}/d), heat is even required to keep the ammonia synthesis reactor at the synthesis temperature due to radial heat losses, and hydrogen and nitrogen production also becomes less efficient [147,154,155]. Thus, milder operating conditions in the synthesis loop are required for effective scale-down.

As shown in Fig. 4.10, the energy consumption is a function of the ammonia synthesis capacity. The energy consumption of electrolysis-based Haber–Bosch processes can be estimated based on Eq. (4.5), which is valid in the range 10^1–10^6 kg_{NH3}/h capacity.

$$E = (52.58 * \log_{10}(\text{capacity in kg/h}))^{-0.30} \quad (4.5)$$

Intermittent solar power and wind power cause variations in electricity supply. Therefore, the synthesis loop should either be able to ramp up and down fast, or batteries should be installed to operate the synthesis loop at constant load. The latter option is technically feasible, but expensive [69]. Ramp up and down can be achieved to some extent by varying the H_2:N_2 ratio within the synthesis loop [46]. Nitrogen can be used as an inert in the synthesis loop when low amounts of hydrogen are present. However, ammonia must be present in the synthesis loop to enable condensation. Upon ramping down, the energy consumption per amount of ammonia produced can drastically increase [78], although control strategies have been proposed with a minimum increase in energy consumption [156]. To put ramping up and down in perspective: the cold start-up time of large-scale plant takes one to 2 days [70]. Thus, shut-down can be considered when electricity supply is not available for a few weeks (i.e. beyond the storage time of a battery). Again, milder

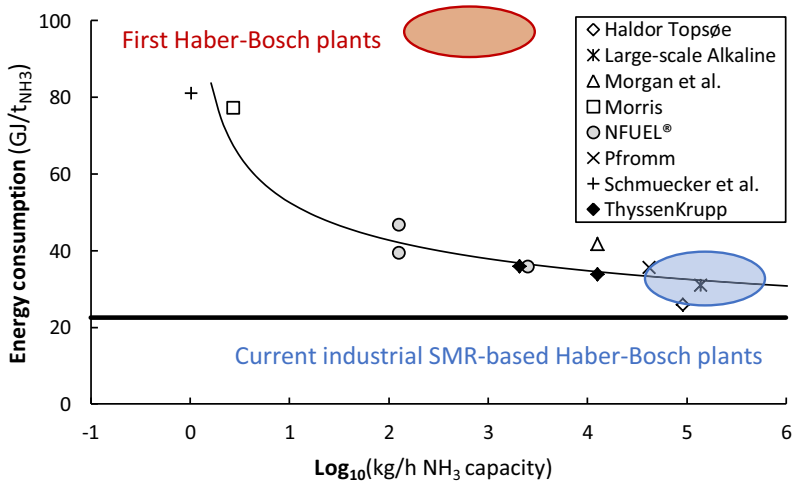

FIG. 4.10 Energy consumption of various electrolysis-based Haber-Bosch processes (academic and industrial estimates). The bold line represents the thermodynamic minimum energy consumption (22.5 GJ/t_{NH3}). (Reproduced and modified from Rouwenhorst KHR, Van Der Ham AGJ, Mul G, Kersten SRA. Islanded ammonia power systems: technology review & conceptual process design. Renew Sustain Energy Rev. 2019;114.)

conditions in the synthesis loop are expected to enable intermittent operation at lower energy losses. Furthermore, the separation of ammonia in the gas phase rather than by condensation can be beneficial for intermittent operation [46].

COST OF ELECTROLYSIS-BASED HABER–BOSCH PROCESSES

The installed capital cost of an electrolysis-based Haber–Bosch plant consists of equipment for hydrogen production, nitrogen production, ammonia synthesis and ammonia storage. Various cost-scaling relations were proposed for alkaline electrolysis-based and PEM electrolysis-based Haber–Bosch processes with a PSA for nitrogen purification [108,157,158]. The installed cost of various electrolysis-based Haber–Bosch processes as well as some proposed scaling-relations is shown in Fig. 4.11.

The installed costs of various electrolysers and nitrogen purification units are listed in Tables 4.2 and 4.4. About half to two-third of the investment is required for the electrolyser, depending on the process scale [77,78]. The cost of electrolysers is expected to decrease in the next decade, as listed in Table 4.2. The cost of electrolysers scales with a factor 0.6 with an installed capacity in the range 0.1–50 MW [157]. At larger scales of 50–1000 MW, the cost-scaling increases from 0.6 to 0.85 for PEM electrolysis-based Haber–Bosch plants [65].

A cost-scaling relation based on installed costs of ammonia synthesis loops is given by Eq. (4.6), where C_{IHB} is the installed cost in € and X is the ammonia capacity in t_{NH3}/d (1 MW ≈ 3 t_{NH3} d^{-1}). The cost-scaling relation is valid in the range 1–20 MW.

$$C_{IHB} = 2.0 \times 10^6 \times X^{0.6} \quad (4.6)$$

The most accurate cost-scaling relation including hydrogen production, nitrogen production, ammonia synthesis and ammonia storage was proposed by Morgan et al. [157]. The cost-scaling relation is given by Eq. (4.7), where C_{Itot} is the installed cost in € and X is the ammonia capacity in t_{NH3}/d (1 MW ~ 3 t_{NH3}/d). This cost-scaling relation is valid in the range of 0.1–50 MW. For comparison, a biogas-based plant with a capacity of 22.5 t_{NH3}/d has an investment cost of 14.4 M€ [161]. Furthermore, an SMR-based plant with a capacity of 1800 t_{NH3}/d has an investment cost of about 199 M€ [4].

$$C_{Itot} = 3.3 \times 10^6 \times X^{0.6} \quad (4.7)$$

The operating costs of an electrolysis-based Haber–Bosch process can be divided into the owner's costs and the electricity costs. About 75%–95% of the electricity is required for hydrogen production in the electrolyser

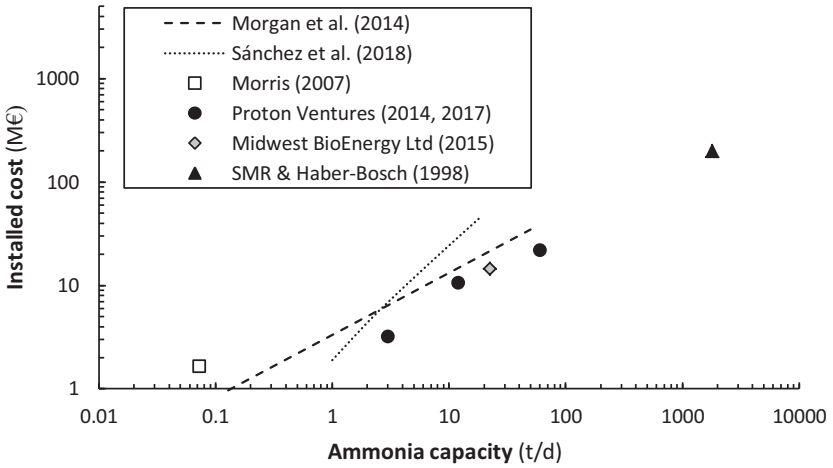

FIG. 4.11 Estimated and realized installed cost of electrolysis-based Haber–Bosch processes with PSA for nitrogen production. The estimated installed cost of Morgan et al. Sánchez et al., and Morris plant include equipment for H_2 production, N_2 production, NH_3 synthesis and storage. The quota from Proton Ventures only includes the NH_3 synthesis loop. The Midwest BioEnergy Ltd. plant is based on biogas rather than electrolysis. As a point of reference, a 1800 t_{NH3}/d SMR-based ammonia plant is included as well (lump turnkey cost of plant). (Based on [4,78,108,157,159,160].)

in a large-scale electrolysis-based Haber–Bosch process [61,137,150,162]. As shown in Fig. 4.10, the electricity consumption and cost depends on the scale and location of the plant. The owner's costs are 120 k€/y/tpd for a 3 t_{NH3}/d plant [78].

Hydrogen production is the major cost contributor for ammonia synthesis. Various alternatives can be considered, depending on the location. The cost of brown hydrogen produced from steam methane reforming is 845–1585 €/t (excluding CCS, costs increase to 1305–2145 €/t with CCS) [48]. The cost of electrolysis-based, renewable hydrogen ranges from below 1440 €/t to above 3605 €/t, depending on the cumulative solar and wind load hours at a given location [48]. Electrified steam methane reforming can be considered when the electricity cost is below 15–25 €/MWh, depending on the cost of natural gas at a given location. As compared to electrolysis, a benefit of electrified steam methane reforming is the compatibility with existing steam methane reforming plants for hydrogen production, as well as the lower capital investment.

Biomass-based ammonia with thermochemical processing typically costs 380–1875 €/t, depending on the scale of application, the source of the biomass and the location [64,101–103]. The cost of ammonia produced from recycled municipal waste is as high as 2135 €/t [104].

NONCONVENTIONAL TECHNOLOGIES

Even though green ammonia synthesis is feasible with the technology existing for about a century, nonconventional technologies are widely researched to allow for scale-down, intermittent operation, and potentially higher energy efficiencies [56]. Nonconventional technologies focus on improving the catalytic ammonia synthesis reaction at milder conditions, as well as on enhancing ammonia separation using sorbents. Research varies from fundamental concepts to the use of commercial materials at the pilot plant scale. Examples of research areas include nonconventional heterogeneous catalysis, adsorbents, absorbents, non-thermal plasma technology, electrochemical synthesis, photochemical synthesis, homogeneous catalysis, as well as chemical looping approaches [69,163–167]. The nonconventional technologies typically allow for scale-down and operation in remote areas. Thus, the economic risks of the innovations are smaller as compared to conventional, large-scale plants, and a faster pace of innovation may occur.

Discoveries of new catalytic systems is nowadays a combination of experimental work in the laboratory, and computer-aided experiments [163,168,169]. Comparative assessment with calculated ammonia synthesis for heterogeneous catalysts has become reliable in recent years [170]. Cross-cutting approaches amongst enzyme catalysis, homogeneous catalysis

TABLE 4.6
Best Reported and Potential Energy Requirement of Various Non-conventional Technologies.

	ENERGY REQUIREMENT (GJ/t_{NH3})		
	Reported	**Potential**	**Relative Cost of Ammonia**
Benchmark electrolysis-based Haber–Bosch process	33	26	1.0
Electrolysis-based Haber–Bosch processes with	46–50	30–35	1.0–1.5
Absorbent-enhanced synthesis loop	47–50	30–35	1.0–1.5
Adsorbent-enhanced synthesis loop	46–50	30–35	1.0–1.5
Non-thermal plasma technology	155	60–70	2.0–4.5
Electrochemical and photochemical synthesis	135	27–29	–
Electrochemical synthesis	135	27–29	–
Photochemical synthesis	–	200[a]	–
Other technologies	64	55	–
Electro-thermochemical looping	64	55	–
Redox cycles	–	79[b]	–
Homogeneous catalysis	900	159	–

[a] About 199 GJ/t_{NH3} is required as direct solar energy.
[b] About 35 GJ/t_{NH3} is required as direct solar energy.
Estimates based on [14,60,61,150,166,174–177].

and heterogeneous catalysis also allow for new insights and potential pathways towards ammonia synthesis under milder conditions and at sufficiently high rates [163,171]. An example of this is the similarity between heterogeneous catalysis over ruthenium-based catalysts and enzyme catalysis in $MoFe_6S_9$ complexes [171]. Furthermore, progress is made for in situ and operando spectroscopy, which increases the understanding of the ammonia synthesis reaction under relevant conditions [163].

The nonconventional technologies researched are listed in Table 4.6. It should be noted that some technologies have been investigated even before the Haber–Bosch process, such as plasma technology and thermochemical looping, being commercialized as the Birkeland–Eyde process and the Frank–Caro process (see Fig. 4.5) [1,43]. Furthermore, novel approaches such as single-atom catalysis have also been proposed for various categories of catalytic ammonia synthesis [172,173].

Nonconventional Heterogeneous Catalysis

Heterogeneously catalysed ammonia synthesis has been studied for over a century. However, new discoveries are still common for the bellwether reaction in heterogeneous catalysis [178,179]. The search for new efficient heterogeneous catalysts for ammonia synthesis in the 21st century is different from that in the 20th century. Whilst thousands of catalysts were experimentally tested in lab reactors in the facilities of Mittasch in the early days [30], nowadays predictive computer-aided experiments are performed, based on scaling relations amongst transition metals and first-principle calculation [168,169,180–184]. Even though early attempts for the volcano curve in ammonia synthesis date from the 1970s [185], predictive theory provided additional evidence on the most active transition metals for ammonia synthesis from the early 2000s onwards. As follows from the volcano curve (see Fig. 4.12), the binding strength of nitrogen is a descriptor for the ammonia synthesis rate and Fe, Ru and Os are the best transition metals for ammonia synthesis [126,186,187]. Metals binding nitrogen very strongly have a low barrier for N_2 activation, but the activity is low due to the desorption limitations of ammonia from the surface. On the other hand, metals binding nitrogen weakly have too high activation barriers for N_2 dissociation. The optimum activity is found in between these extremes (i.e. the top of the volcano). Whilst the choice of the transition metal is of fundamental importance, the electronic

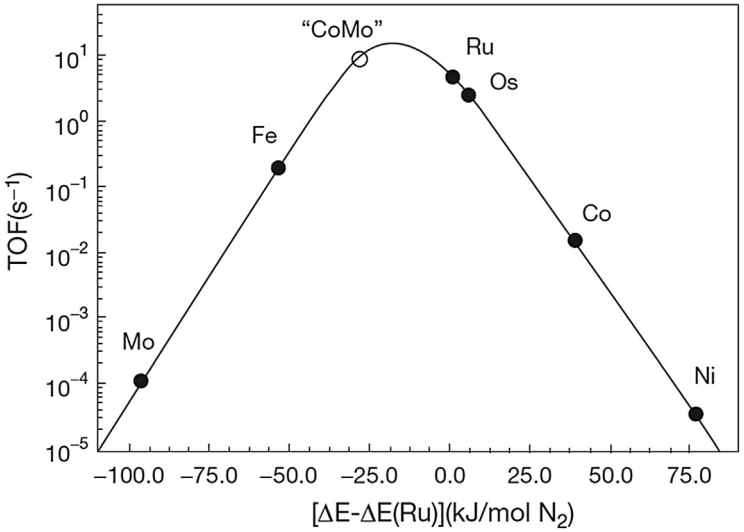

FIG. 4.12 Calculated turnover frequencies for ammonia synthesis as a function of the adsorption energy of nitrogen (at 400°C, 50 bar, H_2:N_2 = 3:1% and 5% NH_3). (Reprinted from Jacobsen CJH, Dahl S, Clausen BGS, Bahn S, Logadottir A, Nørskov JK. Catalyst design by interpolation in the periodic table: bimetallic ammonia synthesis catalysts. J Am Chem Soc. 2001;123(34):8404–8405 with permission of the American Chemical Society.)

factor influenced by the support and promoters can also alter the activity by orders of magnitude [116,134].

Bimetallic catalysts represent the first generation of the discoveries combined with computational activity trends. By combining two transition metals, the resulting binding energy for nitrogen is of an intermediate strength (see Fig. 4.12), giving rise to an interpolation in the periodic table [186]. Examples of such bimetallic catalysts with activities on par or better than industrial Fe and Ru catalysts are Co–Mo catalysts [186,188,189], Co–Re catalysts [190,191] and Fe–Co catalysts [192,193].

The Co–Mo catalysts are the most active of a series of nitride structures (Co_3Mo_3N, Fe_3Mo_3N, and Ni_3Mo_3N), which show higher activities than industrial iron-based catalysts, especially in the low-temperature regime (325–400°C) [194]. The activity enhancement in the low-temperature regime can be understood from nitrogen adsorption via a Mars-van Krevelen mechanism rather than a Langmuir–Hinshelwood mechanism [195–197]. A drawback of Co_3Mo_3N is the high-temperature nitrification process for the catalyst preparation, which makes the production of catalysts with high surface areas difficult [47]. Similar to Fe and Ru-based catalysts, the activity of bimetallic nitride catalysts is enhanced by the addition of various alkali promoters [194]. Bimetallic rhenium-containing catalysts such as Co-Re are primarily of scientific interest, as Re is far too expensive (even more expensive than Ru) and activities are not higher than for Fe or Ru catalysts. Similarly, studies on barium promoted Fe–Co alloys supported on carbon offer scientific insights on the reduced ammonia inhibition due to the presence of Co, whilst the observed activity is not higher than that of industrial Fe catalysts [192].

A major portion of recent research has focused on improving ruthenium-based catalysts [112]. Whilst mechanistic understanding has substantially increased over the past decades regarding the effect of nanoparticle sizes and the distribution of sizes (i.e. the structural factor) [180,198–202], most research now focuses on the electronic factor by altering the support and promoter formulation [203]. The first focus area is the development of oxide-supported ruthenium-based catalysts to replace activated carbon as a support [44]. Activated carbon is known to be prone to methanation in the presence of hydrogen [44,51]. A wide range of oxides, as well as nitrides, has been tested [129–131]. A general observed trend is an increased activity for ammonia synthesis with decreasing electronegativity of the oxide supports [135]. The catalytic activity can be enhanced further by the addition of alkali (Cs, K) and alkaline earth metals (Ba), which enhance the nitrogen dissociation rate and lower the surface coverage of NH_X species on the catalyst species [115,136].

Over the past decade, Co and Ru catalysts with substantially enhanced electronic properties have been developed, leading to catalysts with hydrogenation as the rate step-limiting rather than the N_2 dissociation step [204]. Examples of these catalysts are Co and Ru on $12CaO.7Al_2O_3$ electride [204–208], metallic electrides [209,210] and $Ba–Ca(NH_2)_2$ (ammines) [211–213]. The electride supports act as electron-donating support for these ruthenium-based catalysts with ammonia synthesis rates order of magnitude higher than conventional oxide-supported catalysts [205]. Furthermore, hydrogen can be stored in the electride cages, thereby minimizing the hydrogen poisoning effect usually observed for ruthenium-based catalysts [207]. The ammine (NH_2) structure in the support and the Ba layer on the Ru particles enhance the ammonia synthesis rate, such that the hydrogenation rate is the rate-limiting step rather than N_2 dissociation [211]. Researchers in Japan aim to commercialize the $Ru/Ba–Ca(NH_2)_2$ catalyst for low-pressure (10 bar) ammonia synthesis in the upcoming decade [214]. Furthermore, transition metals combined with metal hydrides have been developed, which separate the N_2 dissociation and hydrogenation steps, resulting in a high catalytic activity at low temperatures (200–350°C) and pressures (1–10 bar) [69,215].

Nowadays science-based approaches are used to predict potential catalysts [168,180–183]. Computational methods can be used to search for nonconventional catalyst structures not on the scaling line of transition metals [169,183]. Ammonia synthesis catalysts based on three-dimensional structures rather than two-dimensional transition metal planes can be discovered. Furthermore, inspiration can be obtained from nitrogenase structures for the development of single metal atom catalysts. Such catalysts operate with an associative mechanism instead of a dissociative mechanism [18], which may eventually allow for ammonia synthesis under mild conditions. A few practical issues associated with such catalysts are transport limitations to such sites and the lack of high active site densities due to low loadings.

Absorbent-Enhanced Haber-Bosch and Adsorbent-Enhanced Haber-Bosch

Academic research has focused on enhancing the activity of ammonia synthesis catalysts to lower the ammonia synthesis temperature and pressure [216], as more active catalysts allow for a lower operating temperature and consequently a lower operating pressure, matching pressure of H_2 and N_2 production pressure [46]. This can save about 1 GJ/t_{NH3} for the syngas compression step [33]. However, even when substantially more active catalysts are developed, the separation efficiency by condensation is limited by the ammonia vapour pressure (see Fig. 4.9). Other ammonia separation technologies are required to lower the operating pressure to 10–30 bar.

A proposed solution is an absorbent- or adsorbent-enhanced ammonia synthesis loop operating at 10–30 bar [46,56,217,218]. This technology utilizes an absorbent or adsorbent to remove ammonia more completely from the hydrogen and nitrogen than by condensation (see Table 4.7). This allows for the operation of the synthesis loop at lower pressures, less temperature swing within the synthesis loop, as well as less feed compression [46,152,154,155,219]. Combining non-conventional heterogeneous catalysts

TABLE 4.7
Comparison of Ammonia Separation Technologies.

	Condensation	Activated Carbon	Metal Halides	Zeolites
Separation temperature (°C)	−20 to 30	20–50	150–250	20–100
Desorption temperature (°C)	–	200	350–400	200–250
Pressure (bar)	100–450	20–50	10–30	10–30
Energy consumption (GJ/t_{NH3}	3–5	15–35	6–11	8
Ammonia at outlet (mol.%)	2–5	0.5––2.0	0.1––0.3	0.1–0.3
Ammonia capacity (wt.%)	100	2–5	5–30	5–15
Ammonia density (kg/m^{-2})	680	10–25	100–600	30–90
Chemical stability	–	High	Low/Medium	High
TRL	9	3	4–5	4–5

Based on [46,225,232–234].

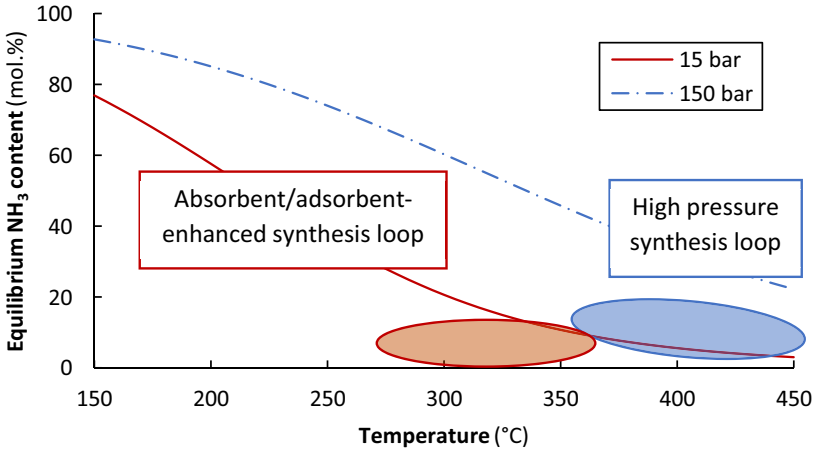

FIG. 4.13 Comparison in conditions for ammonia synthesis for **conventional** high-pressure synthesis loop with condensation and low-pressure synthesis loop with nonconventional catalysts and absorbent/adsorbent. Ammonia equilibrium mole fraction for various temperatures and pressures are also indicated. H_2: $N_2 = 3{:}1$, no inert.

with an absorbent or adsorbent for separation allows for reducing the temperature swing within the process even more [46,56]. Typical ammonia synthesis conditions for the high-pressure synthesis loop and the absorbent- or adsorbent-enhanced synthesis loop are shown in Fig. 4.13. Ammonia separation with membranes was also proposed [220–222]. However, due to low selectivities at low partial pressures of ammonia, as well as poor thermal stability, membranes have not been researched widely [7].

This technology, the absorbent- or adsorbent-enhanced Haber-Bosch process, is considered a low hanging fruit for the upcoming decades, as a large decrease in pressure can be achieved with little technological innovation [46,69]. The ammonia synthesis loop can operate at the same pressure as the hydrogen and nitrogen production units [46]. Furthermore, the catalysts are generally more active at the low ammonia concentrations in the absorbent- or adsorbent-enhanced ammonia synthesis loop than at the high ammonia concentrations in the conventional ammonia synthesis loop [126,223]. The resulting energy consumption of a small-scale absorbent- or adsorbent-enhanced Haber–Bosch process is lower than that of a small-scale, high-pressure Haber-Bosch process [46,152,154,224,225].

Interactions of absorbents and adsorbents with ammonia include electrostatic interactions, metal ammine formation and ammonium ion formation [142]. A wide range of solid and fluid materials has been proposed for ammonia separation, such as activated carbon, covalent organic frameworks, deep eutectic solvents, ionic liquids, metal-organic frameworks, metal halides, oxides, porous organic polymers and zeolites [225–232]. Ammonia capacities of up to 55 wt.% have been reported for metal halide sorbents [233]. The wide range of materials researched indicates the academic interest to improve the ammonia separation and storage method. Hereafter, activated carbon, metal halides and zeolites are discussed, as these materials are applied in industry for various processes and the material cost is typically low [232]. Furthermore, the mechanisms for ammonia separation on these sorbents are well understood and reasonable ammonia capacities have been reported. The ammonia separation characteristics of condensation, activated carbon, metal halides and zeolites under process conditions are listed in Table 4.7.

Activated carbon is widely used as a catalyst support and for separations. Various types of activated carbon have been investigated for ammonia separation [142,232]. Surface-modified activated carbon materials can reversibly store up to 5 wt.% ammonia [142,232]. The introduction of metal oxides on the surface increases the ammonia capacity due to an increase in electrostatic attractions [232]. On the other hand, the hydrogen present in the loop removes functional groups at elevated temperatures, thereby lowering the ammonia capacity irreversibly [232]. Both the reversible and irreversible ammonia adsorption increases by treating the activated carbon material with acid or metal oxides [232]. Due to the low reversible ammonia storage capacity, activated carbons are not desirable ammonia adsorbents.

Metal halides are also proposed for ammonia absorption and storage due to their high ammonia storage capacity of up to 6−8 mol of ammonia per mole of metal halide, thereby forming metal ammine complexes [217−219,223,233,235−244]. The incorporation of ammonia into calcium chloride proceeds according to $CaCl_2+6NH_3 \rightarrow Ca(NH_3)_6Cl_2$. The cation affinity to ammonia determines the minimum partial pressure of ammonia required for absorption [237]. Inert supports are used to stabilize the nanoporous metal halide structures and these supports prevent agglomeration of particles [218,233,236,242,245,246]. Nanopores are introduced during the desorption of ammonia [242,244,247]. Due to the high volumetric ammonia density (see Table 4.7), metal halides can also be used to storage ammonia after separation from the hydrogen and nitrogen [46]. The absorption in metal halides is kinetically limited, whilst the desorption is diffusion limited [219,243]. Metal halides have a low ammonia vapour pressure at ambient conditions, making these sorbents safe alternatives for ammonia storage as compared to liquefied ammonia storage [248]. The absorption and desorption cycle can be operated in both a pressure swing approach and temperature swing approach [219,237,249]. Pressure swing absorption may be more economically feasible than temperature swing absorption [234], but so far temperature swing absorption is most successfully applied [218,233]. The investment in an absorbent- or adsorbent-enhanced ammonia synthesis loop is similar to that of conventional ammonia synthesis loops [56,158]. In case a solid oxide fuel cell is used for electricity generation from ammonia in an islanded system, the heat of the solid oxide fuel cell can be utilized for the desorption of ammonia from the metal halide, thereby increasing the round-trip efficiency [46]. The current challenge is the stabilization of metal halides on inert supports, giving a high reversible ammonia absorption rate and capacity over multiple cycles whilst maintaining a high surface area and nanoporosity [233].

Zeolite materials have also been proposed for ammonia adsorption. About 5−15 wt.% ammonia can be adsorbed on zeolites, depending on the zeolite structure and ion exchange used [227,232,250]. Ammonia can be adsorbed at low temperatures, whilst the adsorption capacity decreases with increasing temperature, facilitating the desorption [227]. The ammonia adsorption and desorption from zeolites are described by the Langmuir−Freundlich isotherm [227,251]. Recently, technology with commercial molecular sieves was also developed and patented [224,252]. Both chemisorption and physisorption phenomena can occur during ammonia separation from nitrogen and hydrogen using zeolites [253], even in the presence of water impurities in the stream [254]. Ammonia adsorption can be due to ammine complex formation with an alkali metal ion, ammonium ion formation with a proton, as well as electrostatic attractions with ions on the zeolite [255]. Various ion-exchange faujasites structures have been investigated [255]. The current challenge is to develop zeolite materials with a higher reversible ammonia adsorption capacity, which may be achieved by investigating various zeolite families, other than faujasites.

Non-Thermal Plasma Technology

Plasma technology is a novel solution for the activation of molecules with stable bonds such as the N≡N triple bond [256−259], especially in combination with a catalyst [260]. Whilst high temperature and pressure are conventionally used to activate catalysts and molecules on the surface, plasma can also be used to accelerate the ammonia synthesis rate in combination with a catalyst, even at low temperatures [69,175]. A plasma is an ionized gas with electrons, photons, activated molecules, as well as positive, negative and neutral radical species [175]. Thermal and non-thermal plasmas exist, where the former operates at high temperatures (>1000°C), whilst the latter has the electrons at elevated temperatures and the other species at near ambient conditions. In the case of non-thermal plasmas, vibrationally excited and electronically excited species are prominent [256]. Thermal plasmas not practical, as the equilibrium ammonia content is low at these conditions and catalysts are not stable at such high temperatures. Current research mostly focuses on atmospheric, non-thermal plasma-catalysis in a dielectric barrier discharge, whilst fundamental studies are also performed at low pressures in radiofrequency plasma-reactors [261,262]. Plasma-catalysis requires a multidisciplinary approach [263]. The effects of the plasma on the catalyst and vice versa are often mutual, leading to a high level of complexity [264,265].

In conventional heterogeneous catalysis over transition metals there are so-called scaling relations (see section 4.10.1), which put fundamental limitations on the operating conditions [168]. Either the nitrogen adsorption or ammonia desorption is inhibiting operation at low temperatures. This can be overcome by combining a plasma with a catalyst, as plasma can activate nitrogen via vibrational or electronic excitation [266], thereby changing both the kinetics and thermodynamics of the reaction [267,268]. Given

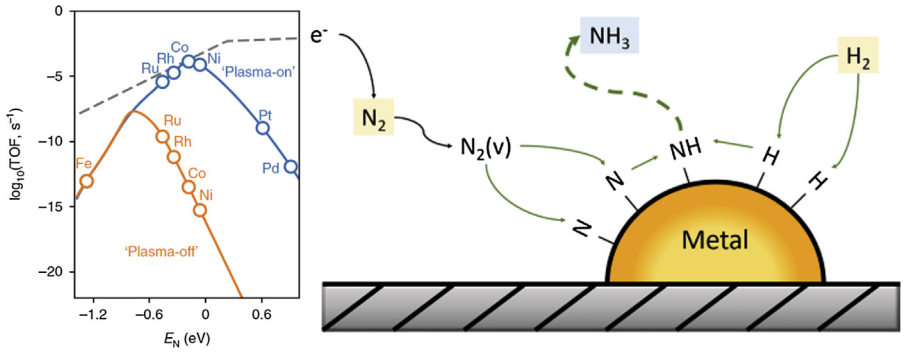

FIG. 4.14 Left: Effect of plasma-induced N_2 activation on the catalytic activity at $T = 200°C$ and 1 bar. The dashed line represents the maximum possible hydrogenation rate. (Reprinted from Mehta P, Barboun P, Herrera FA, Kim J, Rumbach P, Go DB, et al. Overcoming ammonia synthesis scaling relations with plasma-enabled catalysis. Nat Catal. 2018;1(4):269–275 with permission of Springer Nature Limited. Right: Proposed mechanism for plasma-enhanced **catalytic** ammonia synthesis via plasma-activated N_2 dissociation. Reprinted from Rouwenhorst KHR, Kim H-H, Lefferts L. Vibrationally excited activation of N_2 in plasma-enhanced catalytic ammonia synthesis: a kinetic analysis. ACS Sustain Chem Eng. 2019 with permission of the American Chemical Society.)

that the hydrogenation reactions are sufficiently fast over the catalytic surface, plasma-catalysis can be used to synthesize ammonia over late-transition metals with nitrogen adsorption limitations at near ambient conditions. Activation of nitrogen molecules causes a shift in the volcano curve for ammonia synthesis towards more noble metals, as shown in Fig. 4.14. The activation barrier for ammonia synthesis over Ru-based catalysts was found to decrease from 60 to 115 kJ/mol to 20–40 kJ/mol, which can be attributed to N_2 activation in the plasma [268].

Investment cost benefits are not expected for a 180 t_{NH3}/d plasma-based plant as compared to a benchmark Haber-Bosch plant [176]. However, small-scale applications with highly intermittent energy supply may provide a niche market for processes with non-thermal plasma technology with low operating temperatures and pressures combined with an absorbent or adsorbent for separation [269], given that the energy input for plasma-catalysis can be decreased substantially. The best-reported energy input for plasma-catalysis is about 95 GJ/t_{NH3} at about 0.2 mol.% ammonia [270], whilst the energy consumption must be decreased to about 18–24 GJ/t_{NH3} at about 1.0 mol.% ammonia for small-scale application [175,268]. From this, it follows that a catalyst would be required in any case to assist nitrogen dissociation, as the full nitrogen dissociation by the plasma would require 28 GJ/t_{NH3} [268]. Current strategies to produce more ammonia at a lower energy input include plasma-reactor optimization such as pulsed plasmas, a change in operating pressure, and catalyst optimization. Inspiration for catalyst design can be obtained from heterogeneous catalysts [268].

Electrochemical Synthesis

Due to the emergence of low cost, renewable electricity, electrochemical conversions have recently gained considerable interest [57,271]. For this reason, electrochemical ammonia synthesis is widely researched [15], inspired on the biological nitrogen fixation, where proton-coupled electron transfer occurs under mild conditions in the enzyme nitrogenase (see section 4.2) [272]. Electrochemical ammonia synthesis has several potential advantages over the Haber–Bosch process [273], such as the compact design due to the integration of hydrogen production from water and nitrogen reduction in a single process unit. Furthermore, the formation of gaseous hydrogen can be totally bypassed by using water oxidation as a counter reaction in an electrochemical cell, which delivers protons for the nitrogen reduction reaction (NRR).

Electrochemical ammonia synthesis involves the oxidation of hydrogen (Eq. 4.8) or water (Eq. 4.9) on the anode, transport of protons through a liquid or solid electrolyte, and transport of electrons via an external circuit to the cathode, where nitrogen is reduced to ammonia (Eq. 4.10). An example of an electrochemical cell is shown in Fig. 4.15.

$$3H_2 \rightarrow 6H^+ + 6e^- \tag{4.8}$$

$$3H_2 \rightarrow 6H^+ + 6e^- + 3/2O_2 \tag{4.9}$$

$$N_2 + 6H^+ + 6e^- \rightarrow 2NH_3 \tag{4.10}$$

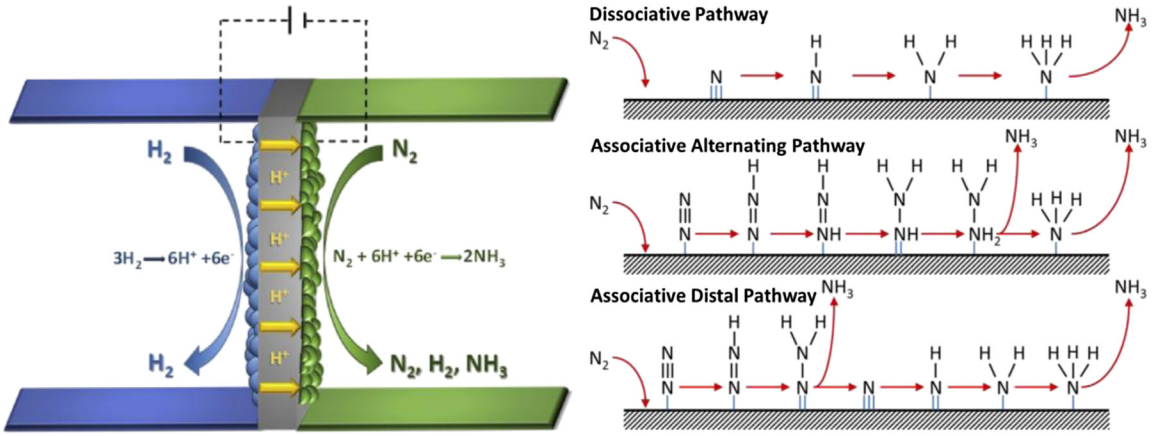

FIG. 4.15 Left: Example of an electrochemical cell for high-temperature ammonia synthesis using a solid electrolyte. (Reprinted from Kyriakou V, Garagounis I, Vasileiou E, Vourros A, Stoukides M. Progress in the electrochemical synthesis of ammonia. Catal Today. 2017;286:2–13 with permission of Elsevier Ltd. Right: Proposed reaction mechanisms for the electrochemical nitrogen reduction reaction. Reprinted from Shipman MA, Symes MD. Recent progress towards the electrosynthesis of ammonia from sustainable resources. Catal Today. 2017;286:57–68 with permission of Elsevier Ltd.)

The reaction mechanism for the electrochemical nitrogen reduction reaction is currently debated. Various alternatives reaction mechanisms for nitrogen activation on a solid surface have been proposed, as shown in Fig. 4.15. The mechanism depends on the catalyst used and the operating conditions [272,274]. In the case of the dissociative pathway, dinitrogen is dissociated to atomic nitrogen on the surface, after which hydrogenation occurs to ammonia, with subsequent desorption. This mechanism is predicted to occur at elevated temperatures due to the high activation barrier for breaking the triple N≡N bond. Thus, associative pathways with the breaking of the nitrogen bond only after partial hydrogenation to N_2H_X species are more likely to occur at low temperatures. This mechanism is similar to that of nitrogenase (see Section 4.2) [272]. Hydrazine was detected for Au nanorods in an alkaline electrolyte [275]. Furthermore, surface-enhanced infrared absorption spectroscopy on Au in an alkaline electrolyte showed weak signals for N_2H_x species [276], which suggests that an associative pathway may be relevant for the nitrogen reduction reaction on Au surfaces in alkaline electrolytes. Apart from these mechanisms, a Mars-van Krevelen mechanism may occur in the case of metal nitride catalysts, in which N from the catalyst lattice is hydrogenated to ammonia, leaving an N vacancy on the surface, which can be regenerated with a nitrogen atom [277]. The Mars-van Krevelen mechanism was reported on a VN catalyst, based on quantitative $^{14}N_2/^{15}N_2$ isotope exchange experiments [278]. All in all, little experimental data is currently available to substantiate which mechanism is dominant for electrochemical ammonia synthesis, especially considering the low ammonia concentrations.

Various approaches to electrochemical ammonia synthesis can be distinguished based on the temperature of operation, namely high-temperature solid-state electrolyte reactors (400–750°C, high-temperature electrochemical ammonia synthesis), molten salt reactors and composite membrane reactors (100–500°C, intermediate temperature electrochemical ammonia synthesis), and liquid electrolyte reactors and low-temperature solid-state electrolyte reactors (20–100°C, low-temperature electrochemical ammonia synthesis) [279,280]. Solid-state electrolytes are probably most promising, as these separate the hydrogen feed from the ammonia production [279,281].

Solid-state ammonia synthesis is usually investigated at high temperatures (>500°C) to ensure high proton conductivity within the solid oxide electrolytes. A dense electrolyte is placed in between two porous electrodes and ions are transported through the solid oxide electrolytes (usually H^+ or O^{2-} ions), as shown in Fig. 4.15. Perovskite materials are generally used as electrolytes, but fluorite- or pyrochlore-type structures have also been reported [279,282]. The high temperature aids the nitrogen activation and enhances the reaction kinetics, but it has a negative influence on the thermodynamic equilibrium, thereby limiting the attainable conversion to ammonia [271,283,284].

Furthermore, high operating temperatures can cause issues due to material degradation [13]. The reported ammonia formation rate is in the order of magnitude of 10^{-9} mol/s/cm and the Faradaic efficiency of the process is usually below 50%, based on the amount of electrochemically supplied hydrogen [13,271]. The highest reported Faradaic efficiency is around 80% [285,286]. When water is used as the proton source, the Faradaic efficiency drops to below 1% [271,284,287]. Research efforts focus on the development of more stable electrolytes, with a higher conductivity at milder operating conditions.

To overcome problems with ammonia decomposition at higher temperatures, as well as material stability issues, intermediate temperature electrochemical ammonia synthesis is studied, which operates at 100−500°C. Molten salts and composite membranes with the addition of a eutectic mixture of alkali metal salts are usually used as electrolytes [279,288−292]. It should be noted that composite membranes have been operated at temperatures of up to 650°C [293], which is considered high-temperature electrochemical ammonia synthesis. The mixture of eutectic solvents ensures a good ionic conductivity at lower temperatures. A common approach is to reduce dinitrogen to N^{3-} on the cathode, which often migrates towards the anode, where it reacts with hydrogen to form ammonia [294]. However, the addition of a Li_3N precursor (i.e. a nitrogen source) to the electrolyte in most of the studies makes it difficult to estimate the real efficiency of the process [290,295]. Ammonia formation rates in the range 10^{-11}−10^{-8} mol/s/cm with Faradaic efficiencies mostly below 10% have been reported [271]. The highest reported Faradaic efficiency of 80% was found to be unstable, and dropped to 10% after some time [296], which may indicate a nitrogen-containing precursor being present in the system rather than a catalytic effect. A disadvantage of molten salt electrolytes is their corrosiveness, leading to a low stability of the electrode materials [297].

Low-temperature electrochemical ammonia synthesis (20−100°C) recently gained interest [298,299], with about 100 academic publications per year. For low-temperature systems, ammonia decomposition is not an issue. Polymer electrolytes with high H^+ conductivity have been used, such Nafion [300,301] or sulphonated polysulphone [302]. The reported ammonia formation rate is in the range 10^{-10}−10^{-8} mol/s/cm at 80°C, but Faradaic efficiencies below 1% are generally reported [271,303]. Studies at room temperatures are performed with liquid electrolytes, which are usually aqueous-based electrolytes [273,304,305], whilst organic solvents [306,307] and ionic liquids [308] have also been used. An advantage of aqueous-based electrolytes is that water can be used directly as the proton source [271]. Acidic electrolytes are suitable for reduction reactions, as protons are abundantly available, whilst an alkaline environment can suppress the hydrogen evolution reaction, which competes with the nitrogen reduction reaction to ammonia [309].

A wide variety of catalysts was tested, starting from noble metals such as Ag, Ag, Pd, Pt, Rh and Ru [275,300,310−316], after which metal oxides based on Ce, Co, Fe, Mo, Mn, Nb, Ta, Ti and V [317−328], metal sulphides based on Co, Fe and Mo [329−332], and metal carbides based on Mo [333] were also studied experimentally. Another group of catalysts consists of transition metal nitride materials such as CrON, Mo_2N and VN [334−336], for which the possibility of a Mars-Van Krevelen mechanism is considered [277]. The activity of organometallic complexes based on Al and Ti [337,338], and metal-free catalysts such as B, BN, P and polymeric carbon nitride [339−342] were also evaluated. Limited reports are available about single-atom catalysts for the nitrogen reduction reaction, such as Au, Fe, and Ru [343−346]. Various reviews provide a more detailed description of low-temperature electrochemical ammonia synthesis [13,273,304,309,347−349].

Despite many recent academic publications, low ammonia production rates of 10^{-12}−10^{-9} mol/s/cm with Faradaic efficiencies below 10% are generally reported at room temperature. Various publications reported higher Faradaic efficiencies [323,343,350−352], even up to 67.8% [353]. However, the presented Faradaic efficiencies are usually measured at low current densities (sometimes below −0.1 mA/cm) and at low ammonia concentrations (usually <1 ppm). Thus, any ammonia contamination in the system causes a large error in the apparent ammonia synthesis rate and Faradaic efficiency [354].

Ammonia is a common impurity in the air [355], it can easily dissolve in water and adsorb at a wide variety of surfaces [356], which makes it very easy to find it as contamination. It means that researchers working on the nitrogen reduction reaction should pay extra attention to those contaminations. Ammonia can be found in gas tubes, glassware, gloves, nitrogen streams and even human breath. Trace contaminations can appear at certain stages of the experiment, such as membrane pre-treatment, improper reactor cleaning, sample post-treatment, storage and ammonia detection [354]. Moreover, nitrogen-containing compounds present as contaminations in nitrogen streams, such as nitrates,

nitrites, amines and nitrogen oxides, can be converted electrochemically to ammonia [354,357]. Special attention should be paid for catalyst and electrode preparation. Various catalysts precursors consist of nitrate salts, contain additives necessary to form a certain morphology (like polyvinylpyrrolidone), or HNO_3 is used for pH adjustments. Lastly, ammonia is sometimes used during catalyst preparation. All of those situations should be avoided as much as possible. For all those reasons, special attention should be paid for proper control experiments, including quantitative $^{15}N_2$ experiments to prove the origin of detected ammonia during an electrochemical experiment [354,358–361].

There are several reasons why electrochemical ammonia synthesis is so difficult. First of all, the inert nature of dinitrogen with a high dissociation energy of 941 kJ/mol makes activation difficult, especially in ambient conditions and at sufficient rates. Moreover, there is a high energy gap between the highest occupied molecular orbital and the lowest unoccupied molecular orbital in the dinitrogen molecule of 10.82 eV, which is not favourable for electron transfer [273]. Another issue is the low nitrogen solubility in water, which results in limited availability of nitrogen near the electrode surface. To deal with this issue, electrode and reactor engineering can play a role. Moreover, the reaction kinetics are slow at low temperature, whilst ammonia decomposition and material degradation are issues at elevated temperatures. When water is used as a proton source, the competing hydrogen evolution reaction is usually dominant over the nitrogen reduction reaction [362], which is due to the similar equilibrium potential (Eqs. 4.11 and 4.12) [273]. Furthermore, in the case of aqueous electrolytes, the water availability near the electrode surface is higher than the nitrogen availability. The hydrogen evolution reaction only requires two electrons (Eq. 4.12), whilst the nitrogen reduction reaction requires six electrons (Eq. 4.11) [18,84].

$$N_2 + 6H_2O + 6e^- \rightarrow 2NH_3 + 6OH^- \quad (E^0 = -0.736\ \text{V vs. SHE at pH 14}) \quad (4.11)$$

$$2H_2O + 2e^- \rightarrow H_2 + 2OH^- \quad (E^0 = -0.828\ \text{V vs. SHE at pH 14}) \quad (4.12)$$

A thermodynamic analysis of the nitrogen reduction reaction shows certain limitations due to multiple proton–electron transfer steps involving several intermediates (see Fig. 4.15). Strongly adsorbed, stable intermediates make nitrogen hydrogenation and difficult [272]. The adsorption energies of reaction intermediates are correlated with one another via so-called scaling relations [363]. When there is an unfavourable scaling relation between two intermediates, it is difficult to find a catalyst that can ensure all steps to be thermodynamically downhill in the reaction pathway [273]. In the case of the nitrogen reduction reaction, the scaling relation between the N_2H and NH_2 intermediates is not favourable. Therefore, a minimum overpotential of 0.4 V is required for the reaction to proceed [272]. So far, there is no catalyst to overcome this issue and significant overpotentials have to be applied, which makes the hydrogen evolution reaction much more favourable on most transition metals (see Fig. 4.16) [362].

Various groups have reported Density functional theory (DFT) calculations to assess the trends in the nitrogen reduction reaction along the dissociative and associative reaction mechanisms over stepped surfaces and flat surfaces of transition metals (see Fig. 4.16). Ru, Mo, Fe, Rh and Re are the most active surfaces for the nitrogen reduction reaction [18], although the hydrogen evolution reaction is also favourable over these metals [177,362]. Thus, these surfaces will be covered with H-adatoms in case of aqueous electrolytes, which blocks the active site for the nitrogen adsorption, increasing the selectivity towards the hydrogen evolution reaction [177]. On the other hand, surfaces of Ti, Zr, Sc and Y were found to bind N-adatoms more strongly than H-adatoms, which implies ammonia can be produced if sufficiently bias is applied (between −1 V and −1.5 V vs. SHE) [18]. Other types of catalysts were also considered in DFT calculations, such as metal oxides [364], nitrides [365], sulphides [366] and single-atom catalysts [367–370].

Despite substantial theoretical and experimental research on electrochemical nitrogen reduction, no breakthrough has been achieved in finding a suitable catalyst to date [371]. Further research should focus on the development of new materials and strategies to reduce nitrogen at lower overpotentials, causing less problems with the hydrogen evolution reaction. Bimetallic surfaces should be considered to help optimize the binding strength of intermediates at different catalyst sites, thereby decreasing the overpotential for rate-determining step. Single-atom catalysts can play an important role when trying to mimic nature. They can bind molecules more precisely, but their manufacturing is still a challenge. Simultaneously, the possibility of suppressing the hydrogen evolution reaction should be evaluated to improve the selectivity towards ammonia. This can be achieved by decreasing the amount of H^+ near the electrode surface, such that the nitrogen coverage can be increased. A strategy for this is the use of non-aqueous electrolytes [372,373]. Furthermore, more insight into the relevant

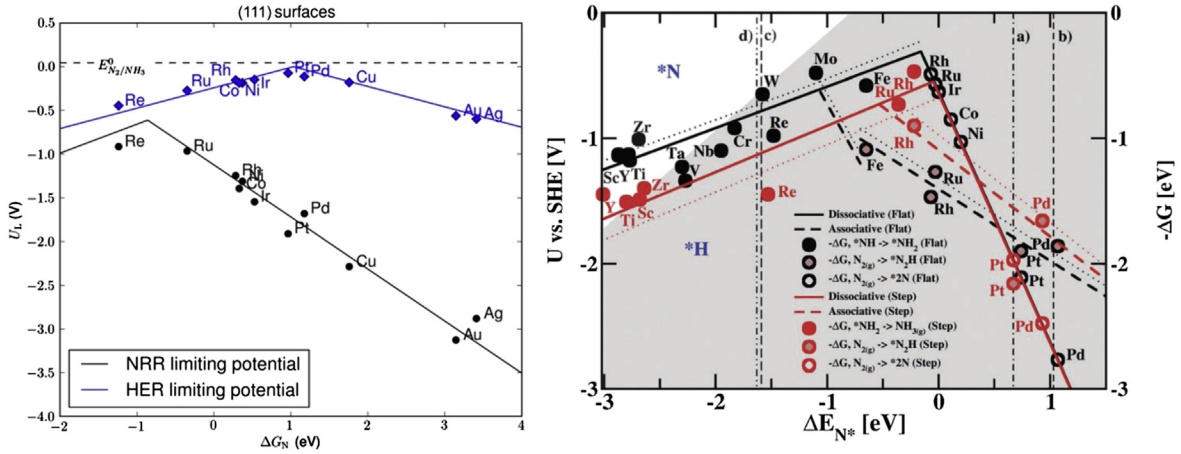

FIG. 4.16 Left: limiting potential for the nitrogen reduction reaction and hydrogen evolution reaction over step sites on transition metals. (Reprinted from Montoya JH, Tsai C, Vojvodic A, Jens KN. The challenge of electrochemical ammonia synthesis: a new perspective on the role of nitrogen scaling relations. ChemSusChem. 2015;8(13):2180–2186 with permission of John Wiley & Sons, Inc. Right: Volcano plots for transition metal surfaces for the nitrogen reduction reaction via the dissociative and associative reaction mechanisms. Reprinted from Skúlason E, Bligaard T, Gudmundsdóttir S, Studt F, Rossmeisl J, Abild-Pedersen F, et al. A theoretical evaluation of possible transition metal electro-catalysts for N_2 reduction. Phys Chem Chem Phys. 2012;14(3):1235–1245 with permission of the Royal Society of Chemistry.)

reaction mechanism is required for catalyst development.

A lot of complex strategies are required for electrochemical ammonia synthesis to become feasible for practical application, which is an interesting scientific challenge. To make electrochemical ammonia synthesis economically feasible, a current density of 300 mA/cm with a Faradaic efficiency of 90% is desired, which gives an ammonia production rate of approximately 10^{-6} mol/s/cm [13]. For now, electrochemical ammonia synthesis should not be considered as a potential replacement of the Haber–Bosch process for large-scale ammonia production, but rather as a technology for small-scale, intermittent ammonia production. When aqueous electrolytes are used, this would allow for localized, on-demand ammonia production for fertilizer application.

Photochemical Synthesis

Photocatalysis provides an interesting approach for the conversion of molecular nitrogen to ammonia, which has attracted widespread attention in recent years [374]. Similar to the electrochemical ammonia synthesis, the main advantage of this approach is the possibility to use water as a reducing agent for nitrogen fixation in ambient conditions. Instead of an electrocatalyst, a semiconductor is used. There are three main steps in the photochemical reaction. First, light is absorbed by a semiconductor, which produces charge carriers. For this step to occur, the energy of absorbed photons needs to be equal or higher than the energy gap of the semiconductor. Then, the electrons are promoted from the valence band to the conduction band of the semiconductor, which results in photo-generated electrons and holes in the valence band. Afterwards, the electrons and holes migrate to the surface of semiconductor, where redox reactions can take place. Water can be oxidized to O_2 and H^+ by surface holes when the valence band is more positive than 1.23 V versus NHE (normal hydrogen electrode), whilst N_2 can be reduced by electrons from the conduction band and hydrogenated by water-liberated H^+ [375,376]. The mechanism of the nitrogen reduction reaction on semiconductors is not fully understood, but it is suggested that it follows an associative pathway rather than a dissociative pathway, similar to nitrogenase and electrochemical ammonia synthesis (see Fig. 4.15) [272,304].

Two types of solar-driven nitrogen fixation approaches can be distinguished [298]. In the photochemical process, semiconductor nanoparticles are suspended in an aqueous solution and both redox half-reactions happen on the different sites of the same particles (see Fig. 4.17). The downside of this

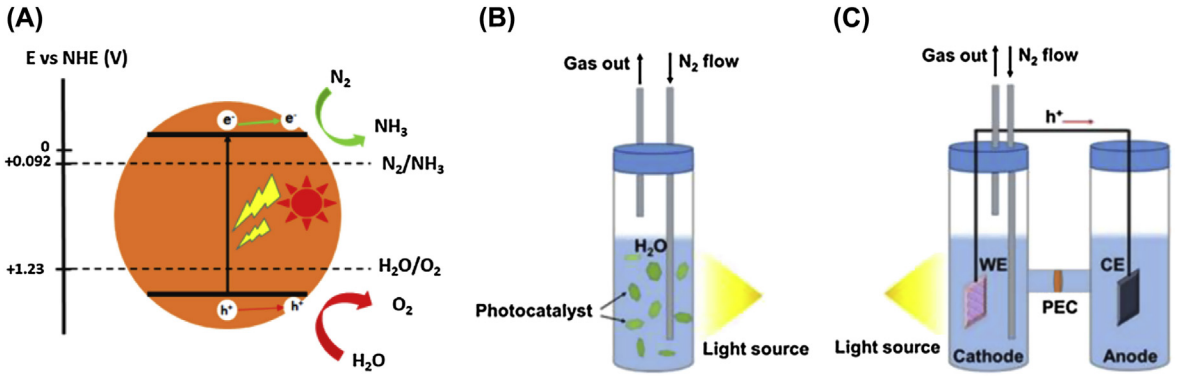

FIG. 4.17 **(A)** Schematic representation of semiconductor for NRR. Typical reactor configuration used in **(B)** photochemical and, **(C)** photo(electro)chemical NRR. (**(A)** Reproduced from Vu MH, Sakar M, Do TO. Insights into the recent progress and advanced materials for photocatalytic nitrogen fixation for ammonia (NH3) production. Catalysts. 2018;8(12). **(B)** and **(C)** Reprinted from Zhang S, Zhao Y, Shi R, Waterhouse GIN, Zhang T. Photocatalytic ammonia synthesis: recent progress and future. Energy. 2019;1(2):100013 with permission of Elsevier Ltd.)

reactor type is the possibility of re-oxidation of the produced ammonia by photo-generated holes on the semiconductor. Another possibility of this approach is the combination of a photocatalyst with an electrochemical cell (see Fig. 4.17). The photoelectrode (i.e. the photocathode or photoanode) creates holes as well as electrons after light absorption, and then the charge is separated between two electrodes with an external bias applied. That causes both redox half-reactions to occur at two different electrodes, which hinders the recombination of holes and electrons, thereby increasing the solar conversion efficiency [298,377].

Early attempts of photo-nitrogen fixation utilized TiO_2 semiconductors as the photocatalyst with various different doping variations [378–381]. Other oxides based on Fe, V and W as well as sulphides were also investigated [382–386]. A major group of test materials was based on Bi-oxyhalides, as well as graphitic carbon nitride materials [387–391]. Research is mainly focusing on the modification of known catalysts by varying oxygen-, nitrogen-, sulphur vacancies, as well as on co-catalysts, morphology and heterojunction engineering [377]. Despite a significant number of studies, no efficient photochemical system for ammonia synthesis was developed. All tested systems have a low production rate and usually there is no quantum efficiency reported. Moreover, the information is presented in varying units, using different conditions, as well as different light sources, which makes the performance difficult to compare. Therefore, standards and benchmarks were proposed to report data in a consistent manner [392].

The issues with solar-driven nitrogen fixation are similar to the ones in the case of electrochemical synthesis, which originates from inertness of the nitrogen molecule and the unfavourable electron transfer kinetics to nitrogen at in ambient conditions (see section 4.10.4). Similarly, an aqueous environment causes issues with the competing hydrogen evolution reaction, as well as transport of nitrogen to the active sites of the catalyst due to its low solubility in commonly used electrolytes. When no external bias is applied, the produced ammonia can be oxidized by photo-generated holes on the semiconductor as well, as both electrons and holes can recombine before the redox reaction occurs. Thus, the overall efficiency is decreased along various pathways. Another issue is the poor stability of the photocatalyst and the low utilization of the light, which leads to a low solar-to-ammonia conversion [304,374,375]. Finally, due to low conversion values, special attention should be paid to proper control experiments to avoid false results, as described for electrochemical ammonia synthesis (see section 4.10.4) [354].

For now, there is no reason to think about photo fixation of nitrogen as a future industrial process. The focus should be on fundamental research, both theoretical and experimental, such as potential reaction mechanisms, finding catalysts which can bind and activate nitrogen in ambient conditions and materials that capture solar energy more efficiently [375,392]. There is limited data available about photoelectrochemical systems, which can aid for efficient charge separation after photoexcitation, implying more research is required

[298,377]. It is estimated that an energy efficiency of 0.1% for solar-to-ammonia is required to evaluate the process as a potential alternative for ammonia synthesis [392], which has only been reported in a few cases [393].

Homogeneous Catalysis

Volpin et al. [394,395] reported the first homogeneous nitrogen reduction reactions in the 1960s. Various homogeneous nitrogen fixation reactions, catalytic and non-catalytic, were reported in the decades to follow [12,14]. Some of the most significant contributions include single atom transition metal Mo complexes, which reduce N_2 to ammonia at ambient conditions [396–398], at the same energy input as biological N_2 fixation. Other studied systems include Fe complexes [399–401] and Zr complexes [402]. The nature of the reaction intermediates has been studied with a mechanistic comparison to biological nitrogen fixation [3,403,404], and various ligands have been investigated for the Mo complex [405]. A strategy for a high ammonia selectivity (i.e. similar to nitrogenase) is the use of a solvent with a low solubility for the reactants, thereby limiting the rate of the hydrogen evolution reaction [396].

So far, homogeneous catalysis has not found practical application due to low yields (up to 8–12 equivalents of ammonia per equivalent of the catalyst [396,397]), fast catalyst deactivation, and expensive catalyst compounds [3,14]. Furthermore, the reactions are complex, and selective formation of ammonia is difficult without the use of excessive amounts of solvent [14]. Thus, homogeneous catalysts for ammonia synthesis are currently most useful for understanding nitrogenase [406]. Synthetic nitrogenase-like complexes may find applications for on-site fertilizer production on the seeds of plants [163].

Chemical Looping Approaches

Ammonia can also be synthesized by chemical looping approaches. The main advantage of this kind of approach is the possibility of independent control of nitrogen activation and ammonia formation (i.e. the nitrogen reduction can be performed in the absence of reactive protons [407]). Chemical looping approaches involve separate thermodynamically stable reaction intermediates. This allows for optimizing the operating conditions of each step separately. Three main approaches for chemical looping have been proposed for ammonia synthesis, namely hydrogen chemical looping, water chemical looping, and alkali or alkaline earth metal hydride chemical looping, as well as their combination with electrocatalysis (see Fig. 4.18) [15,299,408]. A general benefit of chemical looping approaches is that mild pressures down to atmospheric pressures can be applied.

The water chemical looping approach is based on the nitridation, oxidation, and reduction of a metal in a cycle. The metal nitride is hydrolysed with steam into ammonia and a metal oxide. The metal oxide is subsequently reduced and nitridated for the next cycle [15,299,409]. An example of a hydrogen chemical looping cycle is the reduction and subsequent nitridation of Al_2O_3 to AlN in the presence of nitrogen and

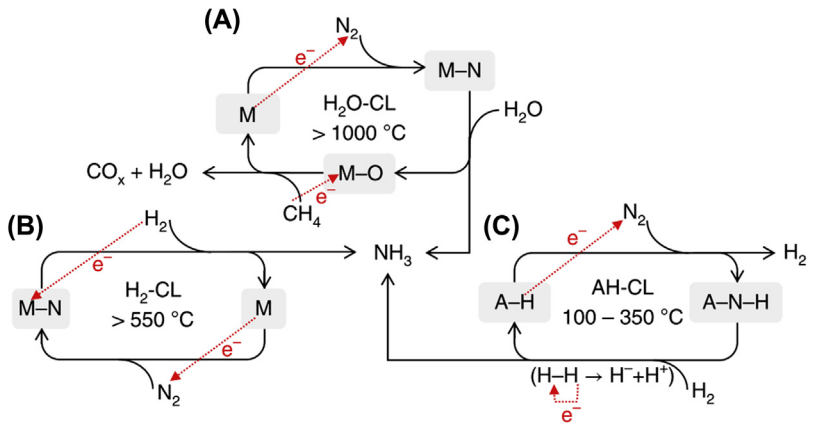

FIG. 4.18 Schematic representation of chemical looping approaches for ammonia synthesis: **(A)** water chemical looping cycles, **(B)** hydrogen chemical looping cycles, and **(C)** alkali or alkaline earth metal hydride cycles. (Reprinted from Gao W, Guo J, Wang P, Wang Q, Chang F, Pei Q, et al. Production of ammonia via a chemical looping process based on metal imides as nitrogen carriers. Nat Energy. 2018;3(12):1067–1075 with permission of Springer Nature Limited.)

methane, with subsequent hydrolysation to Al_2O_3 whilst forming ammonia [410]. Other systems were also studied [411,412], such as MoO_2-based and MgO-based systems [408,413]. An advantage of water chemical looping systems is the direct hydrogenation of nitrogen with water, which implies a separate hydrogen production step is not required. A disadvantage of water chemical looping systems is the high temperature required for reduction of the metal oxides (usually >1000°C), as well as the use of sacrificial agents like CO and CH_4.

The hydrogen chemical looping approach is very similar to the water chemical looping approach. It also involves a metal nitride as a nitrogen source for ammonia synthesis. In the hydrogen chemical looping cycle, a metal undergoes nitridation in a nitrogen stream, after which it is reduced back to the metallic state in presence of hydrogen, whilst forming ammonia. Several metal nitrides were studied, such as Mo_2N, Ca_3N_2, Sr_2N and Mn_xN_y [414–417]. However, a reduction from the metal nitride to the metal only occurs at high temperatures (>500°C).

In the case of alkali or alkaline earth metal hydride cycles, nitrogen is reduced by a metal hydride rather than a pure metal. In this process, a metal imide is formed, which is subsequently reduced back to the metal hydride in the presence of hydrogen whilst forming ammonia and closing the loop [409,418]. Ammonia can be formed at temperatures as low as 100°C and at atmospheric pressure over a Ni–BaH_2/Al_2O_3 system [409].

An example of an electrochemically assisted chemical cycle is lithium-mediated ammonia synthesis [419,420]. As discussed in Section 4.10.4, hydrogen evolution is a competing reaction for electrochemical ammonia synthesis. A cyclic, lithium mediated ammonia synthesis approach separates the nitrogen activation from the hydrogenation step, thereby eliminating the issue of the competing hydrogen evolution reaction. The first step is the electrochemical reduction of Li^+ to metallic Li, which deposits on the electrode. Then, the electrode with the Li layer is exposed to a nitrogen atmosphere at room temperature and atmospheric pressure. Since Li has very strong reducing properties, it reacts with nitrogen to form Li_3N. Subsequently, Li_3N is treated with water or another proton source, which produced ammonia and Li^+ salt, thereby closing the loop (see Fig. 4.19) [174,299]. Electrochemically assisted, lithium-mediated ammonia synthesis has also been operated in a molten salt electrolyte at 450°C, attaining energy requirements as low as 64 GJ/t_{NH3} [407]. However, the theoretical minimum energy consumption is

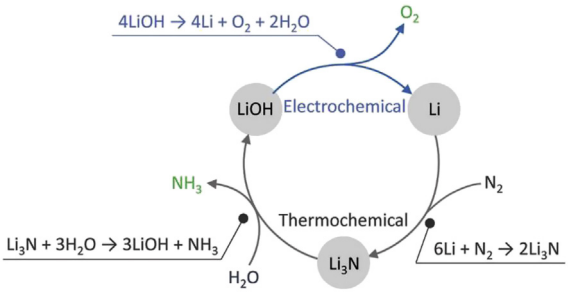

FIG. 4.19 Schematic representation of Li electrochemical/thermochemical cycling for ammonia synthesis. (Reprinted from Jiao F, Xu B. Electrochemical ammonia synthesis and ammonia fuel cells. Adv Mater. 2018;1–5 with permission of John Wiley & Sons, Inc.)

55 GJ/t_{NH3}, leaving little space for improvements [407]. Other variations were also studied, including a continuous process, in which nitrogen is bubbled through a tetrahydrofuran electrolyte with ethanol and Li [292,421]. This allows for ammonia synthesis at ambient conditions due to the difference in reaction rates between Li-nitridation and ethanol reduction on Li [422,423]. Current research focuses on systems with different metals to reduce energy consumption.

SUMMARY

As presented in this chapter, the Haber-Bosch process is one of the most impactful inventions in human history. The Haber-Bosch process has prevented mass starvation in the past century, and it potentially has a substantial role to play in the hydrogen economy. This technology for large-scale, high-pressure ammonia synthesis has been optimized from an energy consumption of about 100 GJ/t_{NH3} in the 1930s down to about 26 GJ/t_{NH3} nowadays. Currently, most ammonia is produced from fossil fuels, although green ammonia synthesis via the electrolysis-based Haber-Bosch process is also mature technology with a century of operational experience. The current challenge is to match green ammonia synthesis with intermittent renewables, such as solar and wind energy. Academic research focuses on ammonia synthesis under mild conditions, potentially allowing for intermittent and decentralized green ammonia production. The areas of research are diverse, but most academic research focuses on the electrochemical reduction of atmospheric nitrogen to ammonia, allowing for producing ammonia directly from air and water. However, so far this remains an unsolved technologic challenge.

REFERENCES

[1] Patil BS, Hessel V, Seefeldt LC, Dean DR, Hoffman BM, Cook BJ, et al. Nitrogen fixation. In: Ullmann's encyclopedia of industrial Chemistry; 2017.

[2] Appl M. Ammonia, 1. Introduction. In: Ullmann's encyclopedia of industrial chemistry; 2011.

[3] Foster SL, Bakovic SIP, Duda RD, Maheshwari S, Milton RD, Minteer SD, et al. Catalysts for nitrogen reduction to ammonia. Nat Catal 2018;1(July).

[4] Appl M. In: Appl M, editor. Ammonia: principles and industrial practice. 1st ed. Weinheim (Germany): Wiley-VCH Verlag GmbH; 1999.

[5] Smil V. Detonator of the population explosion. Nature 1999;400(6743):415.

[6] Smil V. Enriching the earth: Fritz Haber, Carl Bosch, and the transformation of world food production. 2004. Cambridge (MA).

[7] Nielsen SE. Ammonia synthesis: catalyst and technologies. ACS Symp Ser 2009;1000:15–39.

[8] Malthus TR. An Essay on the principle of population. 1798.

[9] Hager T. The alchemy of air: a jewish genius, a doomed tycoon, and the scientific discovery that fed the world but fueled the rise of Hitler. New York (NY): Harmony Books; 2008.

[10] Erisman JW, Sutton MA, Galloway J, Klimont Z, Winiwarter W. How a century of ammonia synthesis changed the world. Nat Geosci 2008;1(10):636–9.

[11] Burris RH, Roberts GP. Biological nitrogen fixation. Annu Rev Nutr 1993;13:317–35.

[12] Bazhenova TA, Shilov AE. Nitrogen fixation in solution. Coord Chem Rev 1995;144(C):69–145.

[13] McPherson IJ, Sudmeier T, Fellowes J, Tsang SCE. Materials for electrochemical ammonia synthesis. Dalton Trans 2019;48(5):1562–8.

[14] Cherkasov N, Ibhadon AO, Fitzpatrick P. A review of the existing and alternative methods for greener nitrogen fixation. Chem Eng Process Process Intensif [Internet] 2015;90:24–33. Available from: https://doi.org/10.1016/j.cep.2015.02.004.

[15] Nørskov J, Chen J, Bullock M, Chorkendorff I, Jaramillo T, Jones A, et al. Sustainable Ammonia Synthesis Exploring the scientific challenges associated with discovering alternative, sustainable processes for ammonia production. Dulees, VA: DOE Roundtable Rep; 2016.

[16] Seefeldt LC, Hoffman BM, Dean DR. Electron transfer in nitrogenase catalysis. Curr Opin Chem Biol 2012;16(1–2):19–25.

[17] Burgess BK, Lowe DJ. Mechanism of molybdenum nitrogenase. Chem Rev 1996;96(7):2983–3011.

[18] Skúlason E, Bligaard T, Gudmundsdóttir S, Studt F, Rossmeisl J, Abild-Pedersen F, et al. A theoretical evaluation of possible transition metal electro-catalysts for N_2 reduction. Phys Chem Chem Phys 2012;14(3):1235–45.

[19] Dance I. Calculated details of a mechanism for conversion of N_2 to NH_3 at the FeMo cluster of nitrogenase. Chem Commun 1997;(2):165–6.

[20] Rod TH, Hammer B, Nørskov JK. Nitrogen adsorption and hydrogenation on a MoFe6S9 complex. Phys Rev Lett 1999;82(20):4054–7.

[21] Rod TH, Nørskov JK. Modeling the nitrogenase FeMo cofactor. J Am Chem Soc 2000;122(51):12751–63.

[22] Hoffman BM, Dean DR, Seefeldt LC. Climbing nitrogenase: toward a mechanism of enzymatic nitrogen fixation. Acc Chem Res 2009;42(5):609–19.

[23] Ernst FA. Industrial chemical monographs: fixation of atmospheric nitrogen. London (UK): Chapman & Hall, Ltd.; 1928.

[24] Travis AS. Nitrogen capture: the growth of an international industry (1900–1940). Springer International Publishing; 2018.

[25] Haber F, Le Rossignol R. The production of synthetic ammonia. Ind Eng Chem 1913;5(4):328–31.

[26] Haber F, Le Rossignol R. Production of ammonia [internet]. Germany; 1202995. 1916. Available from: https://patents.google.com/patent/US1202995A/.

[27] Sheppard D, Robert Le R. 1884–1976: engineer of the "Haber" process. R Soc J Hist Sci 2017;71:263–96.

[28] Nernst W. Über das Ammoniakgleichgewicht. Zeitschrift fur Elektrochemie und Angew Phys Chemie 1907;13(32).

[29] Farber E. From Chemistry to philosophy: the way of Alwin Mittasch (1869–1953). Chymia 1966;11:157–78.

[30] Mittasch A, Frankenburg W. Early studies of multicomponent catalysts. Adv Catal 1950;2(C):81–104.

[31] Ozaki A, Taylor H, Boudart M. Kinetics and mechanism of the ammonia synthesis. Proc R Soc A Math Phys Eng Sci 1960;258(1292):47–62.

[32] Ertl G. Surface science and catalysis—studies on the mechanism of ammonia synthesis: the P. H. Emmett award address. Catal Rev 1980;21(2):201–23.

[33] Prieto G, Schüth F. The Yin and Yang in the development of catalytic processes: catalysis research and reaction engineering. Angew Chem Int Ed 2015;54(11):3222–39.

[34] Bosch C. The development of the chemical high pressure method during the establishment of the new ammonia industry. 1932. Available from: https://www.nobelprize.org/uploads/2018/06/bosch-lecture.pdf.

[35] Murkin C, Brightling JR. Eighty years of steam reforming. Johnson Matthey Technol Rev 2016;60(4):263–9.

[36] van Rooij A. Engineering contractors in the chemical industry. The development of ammonia processes, 1910–1940. Hist Technol 2005;21(4):345–66.

[37] Brightling JR. Ammonia and the fertiliser industry: the development of ammonia at Billingham. Johnson Matthey Technol Rev 2018;62(1):32–47.

[38] Rostrup-Nielsen JR. Catalytic steam reforming. In: AJ S, Boudart M, editors. Catalysis: science and technology. 1st ed. Berlin Heidelberg: Springer-Verlag; 1984. p. 1–117.

[39] The Claude process for ammonia synthesis. Nature 1921;107(2702):765.

[40] West JH. The Claude synthetic ammonia process and plant. J Soc Chem Ind 1921;40(22).

[41] Philibert C. Renewable Energy for Industry: from green energy to green materials and fuels [Internet]. Paris Cedex (France). 2017. Available from: https://www.iea.org/publications/insights/insightpublications/Renewable_Energy_for_Industry.pdf.
[42] European Fertilizer Manufacturers' Association. Production of Ammonia [Internet]. Best available techniques for pollution prevention and control in the European fertilizer industry. Brussels (Belgium). 2000. Available from: https://www.ocinitrogen.com/Media.Library/Ammonia.process-BA.Production.of.ammonia.(2000)-Brochure.pdf.
[43] Patil BS, Wang Q, Hessel V, Lang J. Plasma N_2-fixation: 1900–2014. Catal Today [Internet] 2015;256:49–66. Available from: https://doi.org/10.1016/j.cattod.2015.05.005.
[44] Liu H. Ammonia synthesis catalysts: innovation and practice. World Scientific; 2013.
[45] Pattabathula V. Ammonia. In: Kirk-othmer encyclopedia of chemical technology; 2019.
[46] Rouwenhorst KHR, Van Der Ham AGJ, Mul G, Kersten SRA. Islanded ammonia power systems: technology review & conceptual process design. Renew Sustain Energy Rev 2019;114.
[47] Hellman A, Honkala K, Dahl S, Christensen CH, Nørskov JK. Ammonia synthesis: state of the bellwether reaction. In: Comprehensive inorganic chemistry (II). 2nd ed. Elsevier Ltd; 2013.
[48] International Energy Agency. The Future of hydrogen: seizing today's opportunities. 2019.
[49] CEFIC. Facts & figures of the European chemical industry [Internet]. 2018. Available from: https://cefic.org/app/uploads/2018/12/Cefic_FactsAnd_Figures_2018_Industrial_BROCHURE_TRADE.pdf.
[50] Bazzanella AM, Ausfelder F. Technology study: low carbon energy and feedstock for the European chemical industry [Internet]. Dechema: Gesellschaft für Chemische Technik und Biotechnologie e.V; 2017. Available from: https://dechema.de/dechema_media/Technology_study_Low_carbon_energy_and_feedstock_for_the_European_chemical_industry-p-20002750.pdf.
[51] Appl M. Ammonia, 3. Production plants. In: Ullmann's encyclopedia of industrial chemistry; 2012. p. 295–338.
[52] Eggeman T. Updated by staff. Ammonia. Kirk-othmer encycl chem technol [Internet]. 2010. p. 1–33. Available from: https://doi.org/10.1002/0471238961.0113131503262116.a01.pub3.
[53] Jennings JM. Catalytic ammonia synthesis: fundamentals and practice. 1st ed. New York: Plenum Press; 1991.
[54] Nielsen A. In: Nielsen A, editor. Ammonia: catalysis and manufacture. 1st ed. Berlin Heidelberg: Springer-Verlag; 1995.
[55] Appl M. Ammonia, 2. Production processes. In: Ullmann's encyclopedia of industrial chemistry; 2012. p. 295–338.
[56] Smith C, Hill AK, Torrente-Murciano L. Current and future role of Haber–Bosch ammonia in a carbon-free energy landscape. Energy Environ Sci 2020;13(2):331–44.
[57] Van Geem KM, Galvita VV, Marin GB. Making chemicals with electricity. Science 2019;364(6442):734–5.
[58] Schiffer ZJ, Manthiram K. Electrification and decarbonization of the chemical industry. Joule [Internet] 2017;1(1):10–4. Available from: https://doi.org/10.1016/j.joule.2017.07.008.
[59] Wismann ST, Engbæk JS, Vendelbo SB, Bendixen FB, Eriksen WL, Aasberg-Petersen K, et al. Electrified methane reforming: a compact approach to greener industrial hydrogen production. Science 2019;364(6442):756–9.
[60] CEFIC. European chemistry for growth: unlocking a competitive, low carbon and energy efficient future [Internet]. 2013. Available from: http://www.cefic.org/Documents/RESOURCES/Reports-and-Brochure/Energy-Roadmap-The Report-European-chemistry-for-growth.pdf.
[61] Hansen JB, Han P. The SOC4NH3 project in Denmark. In: NH_3 event. Rotterdam (The Netherlands); 2019.
[62] Elgowainy A. Resourcing byproduct hydrogen from industrial operations. In: H2@Scale workshop. Houston (TX); 2017.
[63] Brown T. Innovations in ammonia. In: H_2@Scale R&D consortium kick-off meeting.
[64] Arora P, Hoadley AFA, Mahajani SM, Ganesh A. Small-scale Ammonia production from biomass: a techno-enviro-economic perspective. Ind Eng Chem Res 2016;55(22):6422–34.
[65] Demirhan CD, Tso WW, Powell JB. Sustainable ammonia production through process synthesis and global optimization. AIChE J 2019;65(7).
[66] Arora P, Sharma I, Hoadley A, Mahajani S, Ganesh A. Remote, small-scale, 'greener' routes of ammonia production. J Clean Prod [Internet] 2018;199:177–92. Available from: https://doi.org/10.1016/j.jdepro.2018.06.130.
[67] Frattini D, Cinti G, Bidini G, Desideri U, Ciof R, Jannelli E. A system approach in energy evaluation of different renewable energies sources integration in ammonia production plants. Renew Energy 2016;99:472–82.
[68] Soloveichik G. Future of Ammonia production: improvement of Haber-Bosch process or electrochemical synthesis?. In: NH_3 fuel conference [Internet]. Minneapolis (MN); 2017. Available from: https://nh3fuelassociation.org/2017/10/01/future-of-ammonia-production-improvement-of-haber-bosch-process-or-electrochemical-synthesis/.
[69] Soloveichik G. Electrochemical synthesis of ammonia as a potential alternative to the Haber – Bosch process. Nat Catal 2019;2(May):377–80.
[70] European Commission. Reference document on best available techniques for the manufacture of large volume inorganic chemicals - ammonia, acids and fertilisers [Internet]. 2007. Available from: http://eippcb.jrc.ec.europa.eu/reference/BREF/lvic_aaf.pdf.
[71] International Energy Agency, Associations IC of C. DECHEMA Gesellschaft fur Chemische Technik und Biotechnologie e.v. Technology Roadmap: Energy and GHG Reductions in the Chemical Industry via Catalytic Processes [Internet]. 2013. Available from: https://www.iea.org/publications/freepublications/publication/TechnologyRoadmapEnergyandGHGReductionsintheChemicalIndustryviaCatalyticProcesses.pdf.

[72] Zhou W, Zhu B, Li Q, Ma T, Hu S, Griffy-brown C. CO_2 emissions and mitigation potential in China's ammonia industry. Energy Pol 2010;38(7):3701–9.
[73] Buttler A, Spliethoff H. Current status of water electrolysis for energy storage, grid balancing and sector coupling via power-to-gas and power-to-liquids: a review. Renew Sustain Energy Rev 2018;82(September 2017):2440–54.
[74] Olivier P, Bourasseau C, Bouamama PB. Low-temperature electrolysis system modelling: a review. Renew Sustain Energy Rev 2017;78(May):280–300.
[75] Koponen J. Review of water electrolysis technologies and design of renewable hydrogen production systems (MSc thesis) [Internet]. Lappeenranta (Finland); 2015. Available from: https://www.doria.fi/bitstream/handle/10024/104326/MScThesis_JKK.pdf.
[76] Ursua A, Gandia LM, Sanchis P. Hydrogen production from water electrolysis: current status and future trends. Proc IEEE [Internet] 2012;100(2):410–26. Available from: http://ieeexplore.ieee.org/ielx5/5/6132586/05898382.pdf?tp=&arnumber=5898382&isnumber=6132586%5Cnhttp://ieeexplore.ieee.org/xpls/abs_all.jsp?arnumber=5898382.
[77] Morgan ER. Techno-economic feasibility study of ammonia plants powered by offshore wind [internet]. University of Massachusetts Amherst; 2013. Available from: https://scholarworks.umass.edu/cgi/viewcontent.cgi?article=1704&context=open_access_dissertations.
[78] Bañares-Alcántara R, Dericks III G, Fiaschetti M, Grünewald P, Lopez JM, Tsang E, et al. Analysis of islanded ammonia-based energy storage systems [internet]. Oxford (United Kingdom). 2015. Available from: http://www.eng.ox.ac.uk/systemseng/publications/Ammonia-based_ESS.pdf.
[79] Schmidt O, Gambhir A, Staffell I, Hawkes A, Nelson J, Few S. Future cost and performance of water electrolysis: an expert elicitation study. Int J Hydrogen Energy [Internet] 2017;42(52):30470–92. Available from: https://doi.org/10.1016/j.ijhydene.2017.10.045.
[80] Steinmüller H, Reiter G, Tichler R, Friedl C, Furtlehner M, Lindorfer J, et al. Power to Gas - eine Systemanalyse: markt- und Technologieschouting und -analyse [Internet]. Linz; 2014. Available from: https://www.ea.tuwien.ac.at/fileadmin/t/ea/projekte/PtG/Endbericht_-_Power_to_Gas_-_eine_Systemanalyse_-_2014.pdf.
[81] Dotan H, Landman A, Sheehan SW, Malviya KD, Shter GE, Grave DA, et al. Decoupled hydrogen and oxygen evolution by a two-step electrochemical–chemical cycle for efficient overall water splitting. Nat Energy 2019;4:786–95.
[82] Mulder FM, Weninger BMH, Middelkoop J, Ooms FGB, Schreuders H. Efficient electricity storage with a battolyser, an integrated Ni–Fe battery and electrolyser. Energy Environ Sci [Internet] 2017;10(3):756–64. Available from: http://xlink.rsc.org/?DOI=C6EE02923J.
[83] Weninger BMH, Mulder FM. Renewable hydrogen and electricity dispatch with multiple Ni-Fe electrode storage. ACS Energy Lett 2019;4(2):567–71.
[84] Seh ZW, Kibsgaard J, Dickens CF, Chorkendorff I, Nørskov JK, Jaramillo TF. Combining theory and experiment in electrocatalysis: insights into materials design. Science 2017;355(6321).
[85] Carmo M, Fritz DL, Mergel J, Stolten D. A comprehensive review on PEM water electrolysis. Int J Hydrogen Energy 2013;38(12):4901–34.
[86] Bertuccioli L, Chan A, Hart D, Lehner F, Madden B, Standen E. Development of water electrolysis in the European Union: final report [Internet]. 2014. Available from: http://www.fch.europa.eu/sites/default/files/study electrolyser_0-Logos_0_0.pdf.
[87] RVO, Gas TKI. Overzicht van Nederlandse waterstofinitiatieven, -plannen en -toepassingen: input voor een routekaart waterstof [Internet]. 2017. Available from: https://topsectorenergie.nl/sites/default/files/uploads/TKI Gas/publicaties/Overzicht waterstofinitiatieven TKI Gas dec 2017.pdf.
[88] Hansen JB, Han PA. Roadmap to all electric ammonia plants. In: NH_3 fuel conference. Pittsburgh (PA); 2018.
[89] Ouweltjes JP, Berkeveld L, Rietveld B. Recent progress in the development of solid oxide electrolyzers at ECN. In: Stolten D, Grube T, editors. 18th world hydrogen energy conference [Internet]. Essen (Germany): Forschungszentrum Jlich GmbH, Zentralbibliothek, Verlag; 2010. Available from: http://juser.fz-juelich.de/record/135448/files/HP3b_2_Lefebvre-Joud-_Ouweltjes_.pdf.
[90] Vøllestad E, Strandbakke R, Tarach M, Catalán-Martínez D, Fontaine ML, Beeaff D, et al. Mixed proton and electron conducting double perovskite anodes for stable and efficient tubular proton ceramic electrolysers. Nat Mater 2019;18(7):752–9.
[91] Duan C, Kee R, Zhu H, Sullivan N, Zhu L, Bian L, et al. Highly efficient reversible protonic ceramic electrochemical cells for power generation and fuel production. Nat Energy 2019;4(3):230–40.
[92] Lei L, Zhang J, Yuan Z, Liu J, Ni M, Chen F. Progress report on proton conducting solid oxide electrolysis cells. Adv Funct Mater 2019:1–17.
[93] Faaij A. Modern biomass conversion technologies. Mitig Adapt Strategies Glob Change 2006;11(2):343–75.
[94] IRENA. Renewable power generation costs in 2018. 2019. Abu Dhabi.
[95] Holladay JD, Hu J, King DL, Wang Y. An overview of hydrogen production technologies. Catal Today 2009;139(4):244–60.
[96] Mathieu P, Dubuisson R. Performance analysis of a biomass gasifier. Energy Convers Manag 2002;43(9–12):1291–9.
[97] Ni M, Leung DYC, Leung MKH, Sumathy K. An overview of hydrogen production from biomass. Fuel Process Technol 2006;87(5):461–72.
[98] Dou B, Zhang H, Song Y, Zhao L, Jiang B, He M. Sustainable Energy & Fuels Hydrogen production from the

thermochemical conversion of biomass: issues and challenges. Sustain Energy Fuels 2019;3:314–42.
[99] Navarro RM, Peña MA, Fierro JLG. Hydrogen production reactions from carbon feedstocks: fossil fuels and biomass. Chem Rev 2007;107(10):3952–91.
[100] Serrano-Ruiz JC, Ruiz-Ramiro MP, Faria J. Biological feedstocks for biofuels. In: An introduction to green Chemistry methods; 2013. p. 116–30.
[101] Sánchez A, Martín M, Vega P. Biomass based sustainable ammonia production: digestion vs gasification. ACS Sustainable Chem Eng 2019;7(11):9995–10007.
[102] Arora P, Hoadley AFA, Mahajani SM, Ganesh A. Multi-objective optimization of biomass based ammonia production - potential and perspective in different countries. J Clean Prod 2017;148:363–74.
[103] Andersson J, Lundgren J. Techno-economic analysis of ammonia production via integrated biomass gasification. Appl Energy 2014;130:484–90.
[104] Paixão VP, Secchi AR, Melo PA. Preliminary design of a municipal solid waste biorefinery for environmentally friendly NH_3 production. Ind Eng Chem Res 2018; 57(45):15437–49.
[105] Showa Denko KK. ECOANN ™ [internet]. 2018 [cited 2018 May 18]. Available from: http://www.sdk.co.jp/english/products/104/105/ecoann.html.
[106] Hardenburger TL, Ennis M. Nitrogen. Kirk-Othmer Encycl Chem Technol. 2005:1–23.
[107] Hansen JB, Hendriksen PV. The SOC4NH3 project. Production and use of ammonia by solid oxide cells. In: Eguchi K, Singhal SC, editors. ECS transactions. Kyoto (Japan). Electrochemical Society Inc.; 2019. p. 2455–65.
[108] Sánchez A, Martín M. Scale up and scale down issues of renewable ammonia plants: towards modular design. Sustain Prod Consum 2018;16:176–92.
[109] Bocker N, Grahl M. Nitrogen. Ullmann's Encycl Ind Chem. 2013:1–27. encyclopedia article.
[110] Sánchez A, Martín M. Optimal renewable production of ammonia from water and air. J Clean Prod 2018;178: 325–42.
[111] Vojvodic A, Medford AJ, Studt F, Abild-Pedersen F, Khan TS, Bligaard T, et al. Exploring the limits: a low-pressure, low-temperature Haber-Bosch process. Chem Phys Lett 2014;598:108–12.
[112] Liu H. Ammonia synthesis catalyst 100 years: practice, enlightenment and challenge. Cuihua Xuebao/Chinese J Catal [Internet] 2014;35(10):1619–40. Available from: https://doi.org/10.1016/S1872-2067(14)60118-2.
[113] Schlögl R. Inorganic reactions: ammonia synthesis. In: Ertl G, Knözinger H, Weitkamp J, editors. Handbook of heterogeneous catalysis. 2nd ed. Weinheim (Germany): Wiley-VCH Verlag GmbH & Co. KGaA; 2008. p. 1697–748.
[114] Stull DR. Vapor pressure of pure substances. Organic and inorganic compounds. Ind Eng Chem 1947;39(4):517–40.
[115] Ertl G. Mechanisms of heterogeneous catalysis. In: Reactions at solid surfaces. 1st ed. Hoboken (NJ): John Wiley & Sons, Inc.; 2009. p. 123–39.
[116] Dahl S, Logadottir A, Jacobsen CJH, Norskov JK. Electronic factors in catalysis: the volcano curve and the effect of promotion in catalytic ammonia synthesis. Appl Catal Gen 2001;222(1–2):19–29.
[117] Stoltze P, Nørskov JK. Bridging the "pressure gap" between ultrahigh-vacuum surface physics and high-pressure catalysis. Phys Rev Lett 1985;55(22):2502–5.
[118] Sehested J, Jacobsen CJH, Törnqvist E, Rokni S, Stoltze P. Ammonia synthesis over a multipromoted iron catalyst: extended set of activity measurements, microkinetic model, and hydrogen inhibition. J Catal 1999;188(1): 83–9.
[119] Stoltze P, Nørskov JK. A description of the high-pressure ammonia synthesis reaction based on surface science. J Vac Sci Technol A Vacuum, Surfaces, Film [Internet] 1987;5(4):581–5. Available from: http://avs.scitation.org/doi/10.1116/1.574677.
[120] Kaleńczuk RJ. Cobalt promoted fused iron catalyst for ammonia synthesis. Int J Inorg Mater 2000;2(2–3): 233–9.
[121] Liu H, Han W. Wüstite-based catalyst for ammonia synthesis: structure , property and performance. Catal Today 2017;297:276–91.
[122] Lendzion-Bieluñ Z, Arabczyk W, Figurski M. The effect of the iron oxidation degree on distribution of promotors in the fused catalyst precursors and their activity in the ammonia synthesis reaction. Appl Catal Gen 2002; 227(1–2):255–63.
[123] Ł C, Lendzion-Bieluń Z. Wustite based iron-cobalt catalyst for ammonia synthesis. Catal Today 2017;286: 114–7.
[124] Li L, Han W-F, Li L-H, Liu H-Z. Modification of wüstite based ammonia synthesis catalyst with fine Fe particles. J Mol Catal [Internet 2017;31(3). Available from: http://www.jmcchina.org/ch/reader/create_pdf.aspx?file_no=20170302.
[125] Yu X, Lin B, Lin J, Wang R, Wei K. A novel fused iron catalyst for ammonia synthesis promoted with rare earth gangue. J Rare Earths [Internet] 2008;26(5):711–6. Available from: https://doi.org/10.1016/S1002-0721(08)60168-4.
[126] Jacobsen CJH, Dahl S, Boisen A, Clausen BS, Topsøe H, Logadottir A, et al. Optimal catalyst curves: connecting density functional theory calculations with industrial reactor design and catalyst selection. J Catal 2002; 205(2):382–7.
[127] Hinrichsen O, Rosowski F, Muhler M, Ertl G. The microkinetics of ammonia synthesis catalyzed by cesium-promoted supported ruthenium. Chem Eng Sci 1996; 51(10):1683–90.
[128] Aika K, Hori H, Ozaki A. Activation of nitrogen by alkali metal promoted transition metal I. Ammonia synthesis over ruthenium promoted by alkali metal. J Catal 1972;27(3):424–31.
[129] Aika K-I, Shimazaki K, Hattori Y, Ohya A, Ohshima S, Shirota K, et al. Support and promoter effect of ruthenium catalyst. I. Characterization of alkali-promoted

ruthenium/alumina catalysts for ammonia synthesis. J Catal 1985;92(2):296–304.
[130] Aika K, Ohya A, Ozaki A, Inoue Y, Yasumori I. Support and promoter effect of ruthenium catalyst: II. Ruthenium/alkaline earth catalyst for activation of dinitrogen. J Catal 1985;92(2):305–11.
[131] Aika K, Kumasaka M, Oma T, Kato O, Matsuda H, Watanabe N, et al. Support and promoter effect of ruthenium catalyst. III. Kinetics of ammonia synthesis over various Ru catalysts. Appl Catal 1986;28(C):57–68.
[132] Aika K, Takano T, Murata S. Preparation and characterization of chlorine-free ruthenium catalysts and the promoter effect in ammonia synthesis. 3. A magnesia-supported ruthenium catalyst. J Catal 1992;136(1):126–40.
[133] Laursen AB, Sehested J, Chorkendorff I, Vesborg PCK. Availability of elements for heterogeneous catalysis: predicting the industrial viability of novel catalysts. Chin J Catal 2018;39(1):16–26.
[134] Aika K. Role of alkali promoter in ammonia synthesis over ruthenium catalysts—effect on reaction mechanism. Catal Today [Internet 2017;286:14–20. Available from: https://doi.org/10.1016/j.cattod.2016.08.012.
[135] Ozaki A. Development of alkali-promoted ruthenium as a novel catalyst for ammonia synthesis. Acc Chem Res 1981;14(1):16–21.
[136] Kowalczyk Z, Krukowski M, Raróg-Pilecka W, Szmigiel D, Zielinski J. Carbon-based ruthenium catalyst for ammonia synthesis: role of the barium and caesium promoters and carbon support. Appl Catal Gen 2003;248(1–2):67–73.
[137] Pfromm PH. Towards sustainable agriculture: fossil-free ammonia. J Renew Sustain Energy 2017;9(3).
[138] Cinti G, Frattini D, Jannelli E, Desideri U, Bidini G. Coupling solid oxide electrolyser (SOE) and ammonia production plant. Appl Energy [Internet] 2017;192:466–76. Available from: https://doi.org/10.1016/j.apenergy.2016.09.026.
[139] The Catalyst Group. Ammonia production: catalyst and process technology advances yielding cost efficiencies and CO_2 reductions (Multi-client study proposal). PA, United States): Spring House; 2016.
[140] Pan H, Li Y, Jiang W, Liu H. Effects of reaction conditions on performance of Ru catalyst and iron catalyst for ammonia synthesis. Chin J Chem Eng 2011;19(2):273–7.
[141] Brown DE, Edmonds T, Joyner RW, McCarroll JJ, Tennison SR. The genesis and development of the commercial BP doubly promoted catalyst for ammonia synthesis. Catal Lett 2014;144(4):545–52.
[142] Liu CY. Development of materials for ammonia separation-storage in a small scale ammonia synthesis. Tokyo University of Technology; 2002.
[143] Stevens R. Decarbonize. In: NH_3 event. Rotterdam (The Netherlands); 2019.
[144] Corporation JGC. Ammonia synthesis demonstration plant begins operation [Internet]. 2018. Available from: http://www.jgc.com/en/ViewPdf/view/1940.
[145] Nayak-Luke R, Bañares-Alcántara R. Long-term chemical energy storage: electrofuels for weekly/monthly storage. In: Perspectives on energy storage systems [Internet]. Copenhagen (Denmark); 2018. Available from: http://www.iea-isgan.org/wp-content/uploads/2018/05/Presentations-CEM0-Side-Event-Perspectives-on-Energy-Storage-Systems-2018-05-24-1.pdf.
[146] Reese M, Marquart C, Malmali M, Wagner K, Buchanan E, McCormick A, et al. Performance of a small-scale Haber process. Ind Eng Chem Res 2016;55(13):3742–50.
[147] Cesaro Z, Bañares-Alcántara R. Siemens demonstrator update & investigation into ammonia for energy infrastructure in developing countries. In: NH_3 event. Rotterdam (The Netherlands); 2019.
[148] Schmuecker J, Toyne D. Making demonstration ammounts of renewable ammonia and using it to fuel a farm tractor. In: NH_3 event. Rotterdam (The Netherlands); 2019.
[149] Patil A, Laumans L, Vrijenhoef H. Solar to ammonia - via Proton's NFuel units. Procedia Eng [Internet] 2014;83:322–7. Available from: https://doi.org/10.1016/j.proeng.2014.09.023.
[150] Proton Ventures BV. Sustainable ammonia for food and power. Nitrogen+Syngas [Internet] 2018;1–10. Available from: http://www.protonventures.com/wp-content/uploads/2018/09/NS-354-Small-scale-plant-design-PROTON-VENTURES-3-1.pdf.
[151] Bennani Y, Perl A, Patil A, van Someren CEJ, Heijne LJM, van Steenis M. Power-to-Ammonia: rethinking the role of ammonia - from a value product to a flexible energy carrier (FlexNH3) [Internet]. 2016. Available from: https://projecten.topsectorenergie.nl/storage/app/uploads/public/5b1/550/ded/5b1550ded80e0784988187.pdf.
[152] Palys M, McCormick A, Daoutidis P. Design optimization of a distributed Ammonia generation system. In: NH_3 fuel conference [internet]. Minneapolis (MN); 2017. Available from: https://nh3fuelassociation.org/2017/10/01/design-optimization-of-a-distributed-ammonia-generation-system/.
[153] te Roller E. Ammoniak biedt sleutel tot duurzame toekomst. Nederlandse Procestechnologen [Internet]. 2016. Available from: http://www.voltachem.com/images/uploads/NPT_Power2Ammonia.pdf.
[154] Palys MJ, Kuznetsov A, Tallaksen J, Reese M, Daoutidis P. Design optimization of an ammonia-based distributed sustainable agricultural energy system. In: NH_3 fuel conference [internet]. Pittsburgh (PA); 2018. Available from: https://nh3fuelassociation.org/2018/12/08/design-optimization-of-an-ammonia-based-distributed-sustainable-agricultural-energy-system/.
[155] Smith C, Malmali M, Liu C-Y, McCormick A, Cussler EL. Ammonia absorption and desorption in ammines. In: NH_3 fuel conference. Pittsburgh (PA); 2018.
[156] Ostuni R, Zardi F. Method for load regulation of an ammonia plant [Internet]. Switzerland. US9463983B2. 2012. Available from: https://patents.google.com/patent/US9463983.

[157] Morgan E, Manwell J, McGowan J. Wind-powered ammonia fuel production for remote islands: a case study. Renew Energy [Internet] 2014;72:51–61. Available from: https://doi.org/10.1016/j.renene.2014.06.034.
[158] Palys M, McCormick A, Cussler E, Daoutidis P. Modeling and optimal design of absorbent enhanced ammonia synthesis. Processes 2018;6(7):91.
[159] Vrijenhoef JP. Opportunities for small scale ammonia production. In: International Fertiliser Society [Internet]. London (UK); 2017. p. 1–16. Available from: http://www.protonventures.com/wp-content/uploads/2017/07/Paper-Opportunities-for-small-scale-ammonia-production_ProtonVentures_HansVrijenhoef.pdf.
[160] Reese M. Ammonia from wind, an update. In: NH_3 fuel conference. San Francisco (CA); 2007.
[161] Brown T. Midwest BioEnergy [Internet]. Monmouth, IL: Ammonia Industry; 2019 [cited 2019 Sep 9]. Available from: https://ammoniaindustry.com/monmouth-il-midwest-bioenergy/.
[162] Morgan ER, Manwell JF, McGowan JG. Sustainable ammonia production from U.S. Offshore wind farms: a techno-economic review. ACS Sustainable Chem Eng 2017;5(11):9554–67.
[163] U.S. Department of energy. Sustainable ammonia synthesis. 2016. Dulles (VA).
[164] Martin AJ, Shinagawa T, Perez-Ramirez J. Electrocatalytic reduction of nitrogen: from Haber-Bosch to ammonia artificial leaf. Inside Chem 2019;5(2):263–83.
[165] Chen JG, Crooks RM, Seefeldt LC, Bren KL, Bullock RM, Darensbourg MY, et al. Beyond fossil fuel–driven nitrogen transformations. Science 2018;360(6391).
[166] Wang L, Xia M, Wang H, Huang K, Qian C, Maravelias CT, et al. Greening ammonia toward the solar ammonia refinery. Joule 2018:1–20.
[167] Ye L, Nayak-Luke R, Bañares-Alcántara R, Tsang E. Reaction: "green" ammonia production. Inside Chem 2017;3(5):712–4.
[168] Medford AJ, Vojvodic A, Hummelshøj JS, Voss J, Abildpedersen F, Studt F, et al. From the Sabatier principle to a predictive theory of transition-metal heterogeneous catalysis. J Catal 2015;328:36–42.
[169] Nørskov JK, Bligaard T, Rossmeisl J, Christensen CH. Towards the computational design of solid catalysts. Nat Chem 2009;1:37–46.
[170] Medford AJ, Wellendorff J, Vojvodic A, Studt F, Abildpedersen F, Jacobsen KW, et al. Assessing the reliability of calculated catalytic ammonia synthesis rates. Science 2014;345(6193):197–200.
[171] Rod TH, Logadóttir A, Nørskov JK. Ammonia synthesis at low temperatures. J Chem Phys 2010;112(12):5343–7.
[172] Wang A, Li J, Zhang T. Heterogeneous single-atom catalysis. Nat Rev Chem 2018;2(6):65–81.
[173] liu xin, Jiao Y, Zheng Y, Jaroniec M, Qiao S-Z. Building up a picture of the electrocatalytic nitrogen reduction activity of transition metal single atom catalysts. J Am Chem Soc 2019;141(24):9664–72.
[174] Jiao F, Xu B. Electrochemical ammonia synthesis and ammonia fuel cells. Adv Mater 2018;1–5.
[175] Kim H-H, Teramoto Y, Ogata A, Takagi H, Nanba T. Plasma catalysis for environmental treatment and energy applications. Plasma Chem Plasma Process 2016;36(1):45–72.
[176] Hu J, Tian H, Luo Y, Bai X, Shekhawat D, Wildfire C, et al. Microwave catalysis for ammonia synthesis under mild reaction conditions. In: NH_3 fuel conference. Pittsburgh (PA); 2018.
[177] Singh AR, Rohr BA, Statt MJ, Schwalbe JA, Cargnello M, Nørskov JK. Strategies toward selective electrochemical ammonia synthesis. ACS Catal 2019;9:8316–24.
[178] Boudart M. Ammonia synthesis: the bellwether reaction in heterogeneous catalysis. Top Catal 1994;1(3–4):405–14.
[179] Schlögl R. Catalytic synthesis of ammonia - a "never-ending story"? Angew Chem Int Ed 2003;42(18):2004–8.
[180] Honkala K, Hellman A, Remediakis IN, Logadottir A, Carlsson A, Dahl S, et al. Ammonia synthesis from first-principles calculations. Science 2005;307(5709):555–8.
[181] Jones G, Bligaard T, Abild-Pedersen F, Nørskov JK. Using scaling relations to understand trends in the catalytic activity of transition metals. J Phys Condens Matter 2008;20(6).
[182] Wang S, Petzold V, Tripkovic V, Kleis J, Howalt JG, Skúlason E, et al. Universal transition state scaling relations for (de)hydrogenation over transition metals. Phys Chem Chem Phys 2011;13(46):20760–5.
[183] Singh AR, Montoya JH, Rohr BA, Tsai C, Vojvodic A, Nørskov JK. Computational design of active site structures with improved transition-state scaling for ammonia synthesis. ACS Catal 2018;8(5):4017–24.
[184] Hansgen DA, Vlachos DG, Chen JG. Using first principles to predict bimetallic catalysts for the ammonia decomposition reaction. Nat Chem 2010;2(6):484–9.
[185] Aika K, Yamaguchi J, Ozaki A. Ammonia synthesis over rhodium, iridium and platinum promoted by potassium. Chem Lett 1973;2(2):161–4.
[186] Jacobsen CJH, Dahl S, Clausen BGS, Bahn S, Logadottir A, Nørskov JK. Catalyst design by interpolation in the periodic table: bimetallic ammonia synthesis catalysts. J Am Chem Soc 2001;123(34):8404–5.
[187] Logadottir A, Rod TH, Nørskov JK, Hammer B, Dahl S, Jacobsen CJH. The Brønsted-Evans-Polanyi relation and the volcano plot for ammonia synthesis over transition metal catalysts. J Catal 2001;197(2):229–31.
[188] Kojima R, Aika K-I. Cobalt molybdenum bimetallic nitride catalysts for ammonia synthesis. Chem Lett 2000;(5):514–5.
[189] Hargreaves JSJ. Nitrides as ammonia synthesis catalysts and as potential nitrogen transfer reagents. Appl Petrochemical Res 2014;4(1):3–10.
[190] Kojima R, Aika K-I. Cobalt rhenium binary catalyst for ammonia synthesis. Chem Lett 2000;8:912–3.
[191] Kojima R, Aika KI. Rhenium containing binary catalysts for ammonia synthesis. Appl Catal Gen 2001;209(1–2):317–25.

[192] Hagen S, Barfod R, Fehrmann R, Jacobsen CJH, Teunissen HT, Chorkendorff I. Ammonia synthesis with barium-promoted iron-cobalt alloys supported on carbon. J Catal 2003;214(2):327–35.
[193] Hagen S, Barfod R, Fehrmann R, Jacobsen CJH, Teunissen HT, Stahl K, et al. New efficient catalyst for ammonia synthesis: barium-promoted cobalt on carbon. Chem Commun 2002;11:1206–7.
[194] Kojima R, Aika KI. Cobalt molybdenum bimetallic nitride catalysts for ammonia synthesis: Part 2. Kinetic study. Appl Catal Gen 2001;218(1–2):121–8.
[195] Mckay D, Gregory DH, Hargreaves JSJ, Hunter SM, Sun X. Towards nitrogen transfer catalysis: reactive lattice nitrogen in cobalt molybdenum nitride. Chem Commun 2007;7(29):3051–3.
[196] Zeinalipour-Yazdi CD, Hargreaves JSJ, Catlow CRA. Nitrogen activation in a Mars-van Krevelen mechanism for ammonia synthesis on Co_3Mo_3N. J Phys Chem C 2015; 119(51):28368–76.
[197] Zeinalipour-Yazdi CD, Hargreaves JSJ, Catlow CRA. Low-T mechanisms of ammonia synthesis on Co_3Mo_3N. J Phys Chem C 2018;122(11):6078–82.
[198] Leterme C, Fernández C, Eloy P, Gaigneaux EM, Ruiz P. The inhibitor role of NH_3 on its synthesis process at low temperature, over Ru catalytic nanoparticles. Catal Today 2017;286:85–100.
[199] Fernández C, Pezzotta C, Gaigneaux EM, Bion N, Duprez D, Ruiz P. Disclosing the synergistic mechanism in the catalytic activity of different-sized Ru nanoparticles for ammonia synthesis at mild reaction conditions. Catal Today 2015;251:88–95.
[200] Fernández C, Sassoye C, Debecker DP, Sanchez C, Ruiz P. Effect of the size and distribution of supported Ru nanoparticles on their activity in ammonia synthesis under mild reaction conditions. Appl Catal Gen 2014; 474:194–202.
[201] Jacobsen CJH, Dahl S, Hansen PL, Törnqvist E, Jensen L, Topsøe H, et al. Structure sensitivity of supported ruthenium catalysts for ammonia synthesis. J Mol Catal Chem 2000;163(1–2):19–26.
[202] Gavnholt J, Schiøtz J. Structure and reactivity of ruthenium nanoparticles. Phys Rev B Condens Matter 2008; 77(3):1–10.
[203] Saadatjou N, Jafari A, Sahebdelfar S. Ruthenium nanocatalysts for ammonia synthesis: a review. Chem Eng Commun 2015;202(4):420–48.
[204] Kobayashi Y, Kitano M, Kawamura S, Yokoyama T, Hosono H. Kinetic evidence: the rate-determining step for ammonia synthesis over electride-supported Ru catalysts is no longer the nitrogen dissociation step. Catal Sci Technol 2017;7(1):47–50.
[205] Hara M, Kitano M, Hosono H. Ru-loaded C12A7:e^- electride as a catalyst for ammonia synthesis. ACS Catal [Internet] 2017;7(4):2313–24. Available from: http://pubs.acs.org/doi/pdf/10.1021/acscatal.6b03357.
[206] Kitano M, Inoue Y, Yamazaki Y, Hayashi F, Kanbara S, Matsuishi S, et al. Ammonia synthesis using a stable electride as an electron donor and reversible hydrogen store. Nat Chem 2012;4(11):934–40.
[207] Kitano M, Kanbara S, Inoue Y, Kuganathan N, Sushko PV, Yokoyama T, et al. Electride support boosts nitrogen dissociation over ruthenium catalyst and shifts the bottleneck in ammonia synthesis. Nat Commun [Internet] 2015;6:1–9. Available from: https://doi.org/10.1038/ncomms7731.
[208] Inoue Y, Kitano M, Tokunari M, Taniguchi T, Ooya K, Abe H, et al. Direct activation of cobalt catalyst by $12CaO \cdot 7Al_2O_3$ electride for ammonia synthesis. ACS Catal 2019;9(3):1670–9.
[209] Gong Y, Wu J, Kitano M, Wang J, Ye T, Li J, et al. Ternary intermetallic LaCoSi as a catalyst for N_2 activation. Nat Catal 2018;1(3):178–85.
[210] Wu J, Li J, Gong Y, Kitano M, Inoshita T, Hosono H. Communications intermetallic catalysts hot paper intermetallic electride catalyst as a platform for ammonia synthesis communications angewandte. Angew Chem Int Ed 2019;58(3):825–9.
[211] Kitano M, Inoue Y, Sasase M, Kishida K, Kobayashi Y, Nishiyama K, et al. Self-organized ruthenium-barium core-shell nanoparticles on a mesoporous calcium amide matrix for efficient low-temperature ammonia synthesis. Angew Chem Int Ed 2018;57(10):2648–52.
[212] Inoue Y, Kitano M, Kishida K, Abe H, Niwa Y, Sasase M, et al. Efficient and stable Ammonia synthesis by self-organized flat Ru nanoparticles on calcium amide. ACS Catal 2016;6(11):7577–84.
[213] Gao W, Wang P, Guo J, Chang F, He T, Wang Q, et al. Barium hydride-mediated nitrogen transfer and hydrogenation for ammonia synthesis: a case study of cobalt. ACS Catal 2017;7(5):3654–61.
[214] Degnan T. New catalytic developments may promote development of smaller scale ammonia plants. Focus Catal 2018;2018(4):1.
[215] Wang P, Chang F, Gao W, Guo J, Wu G, He T, et al. Breaking scaling relations to achieve low-temperature ammonia synthesis through LiH-mediated nitrogen transfer and hydrogenation. Nat Chem [Internet] 2017;9(1):64–70. Available from: https://doi.org/10.1038/nchem.2595.
[216] Vojvodic A, James A, Studt F, Abild-pedersen F, Suvra T, Bligaard T, et al. Exploring the limits: a low-pressure , low-temperature Haber – Bosch process. Chem Phys Lett [Internet] 2014;598:108–12. Available from: https://doi.org/10.1016/j.cplett.2014.03.003.
[217] Cussler E, McCormick A, Reese M, Malmali M. Ammonia synthesis at low pressure. J Vis Exp [Internet] 2017:126. Available from: https://www.jove.com/video/55691/ammonia-synthesis-at-low-pressure.
[218] Wagner K, Malmali M, Smith C, McCormick A, Cussler EL, Zhu M, et al. Column absorption for reproducible cyclic separation in small scale Ammonia synthesis. AIChE J 2017;63(7):3058–68.
[219] Smith C, McCormick AV, Cussler EL. Optimizing the conditions for ammonia production using absorption. ACS Sustainable Chem Eng 2019;7:4019–29.

[220] Tricoli V, Cussler EL. Ammonia selective hollow fibers. J Membr Sci 1995;104(1−2):19−26.
[221] Phillip WA, Martono E, Chen L, Hillmyer MA, Cussler EL. Seeking an ammonia selective membrane based on nanostructured sulfonated block copolymers. J Membr Sci 2009;337(1−2):39−46.
[222] Daniel V, Laciak L, Quinn R, Pez GP, Appleby JB, Puri PS. Selective permeation of ammonia and carbon dioxide by novel membranes. Separ Sci Technol 1990; 25(13−15):1295−305.
[223] Malmali M, Reese M, McCormick AV, Cussler EL. Converting wind energy to ammonia at lower pressure. ACS Sustainable Chem Eng 2017;6(1):827−34.
[224] Beach J, Kintner J, Welch A. Rapid ramp NH_3 prototype reactor update. In: NH_3 fuel conference. Pittsburgh (PA); 2018.
[225] Beach JD, Kintner JD, Welch AW. Removal of gaseous NH_3 from an NH_3 reactor product stream [Internet]. United States. 2018. Available from: https://patentimages.storage.googleapis.com/62/ef/a4/83ada6d54f30fe/US20180339911A1.pdf.
[226] Wang J, Zeng S, Chen N, Shang D, Zhang X, Li J. Research progress of ammonia adsorption materials. Guocheng Gongcheng Xuebao/The Chinese J Process Eng. 2019;19(1):14−24.
[227] Helminen J, Helenius J, Paatero E, Turunen I. Comparison of sorbents and isotherm models for NH_3-gas separation by adsorption. AIChE J 2000;46(8):1541−55.
[228] Rieth AJ, Dinca M. Controlled gas uptake in metal-organic frameworks with record ammonia sorption. J Am Chem Soc 2018;140(9):3461−6.
[229] Li Y, Ali MC, Yang Q, Zhang Z, Bao Z, Su B, et al. Hybrid deep eutectic solvents with flexible hydrogen- bonded supramolecular networks for highly efficient uptake of NH_3. ChemSusChem 2017;10(17):3368−77.
[230] Zeng S, Liu L, Shang D, Feng J, Dong H, Xu Q, et al. Efficient and reversible absorption of ammonia by cobalt ionic liquids through Lewis acid−base and cooperative hydrogen bond interactions. Green Chem 2018;20(9): 2075−83.
[231] Doonan CJ, Tranchemontagne DJ, Glover TG, Hunt JR, Yaghi OM. Exceptional ammonia uptake by a covalent organic framework. Nat Chem 2010;2(3):235−8.
[232] Liu CY, Aika K. Modification of active carbon and zeolite as ammonia separation materials for a new de-NOx process with ammonia on-site synthesis. Res Chem Intermed 2002;28(5):409−17.
[233] Malmali M, Le G, Hendrickson J, Prince J, McCormick A, Cussler E. Better absorbents for ammonia separation. ACS Sustainable Chem Eng 2018;6(5):6536−46.
[234] Liu CY, Aika K. Effect of the Cl/Br molar ratio of a $CaCl_2$-$CaBr_2$ mixture used as an ammonia storage material. Ind Eng Chem Res. 2004;43(22):6994−7000.
[235] Zhang T, Miyaoka H, Miyaoka H, Ichikawa T, Kojima Y. Review on ammonia absorption materials: metal hydrides, halides, and borohydrides. ACS Appl Energy Mater 2018;1(2):232−42.
[236] Liu CY, Aika K. Ammonia absorption on alkaline earth halides as ammonia separation and storage procedure. Bull Chem Soc Jpn 2004;77(1):123−31.
[237] Liu CY, Aika K. Ammonia absorption into alkaline earth metal halide mixtures as an ammonia storage material. Ind Eng Chem Res [Internet] 2004;43(23):7484−91. Available from: http://pubs.acs.org/doi/abs/10.1021/ie049874a.
[238] Vegge T, Sørensen RZ, Klerke A, Hummelshøj JS, Johannessen T, Nørskov JK. Indirect hydrogen storage in metal ammines. In: Solid-state hydrogen storage: materials and chemistry; 2008. p. 533−64.
[239] Chakraborty D, Petersen HN, Elkjær C, Cagulada A, Johannessen T. Solid ammonia as energy carrier: current status and future prospects. Fuel Cell Bull 2009; 2009(10):12−5.
[240] Malmali M, Wei Y, McCormick A, Cussler EL. Ammonia synthesis at reduced pressure via reactive separation. Ind Eng Chem Res 2016;55(33):8922−32.
[241] Himstedt HH, Huberty MS, McCormick AV, Schmidt LD, Cussler EL. Ammonia synthesis enhanced by magnesium chloride absorption. AIChE J 2015; 61(4):1364−71.
[242] Huberty MS, Wagner AL, McCormick A, Cussler E. Ammonia absorption at Haber process conditions. AlChE J 2012;58(11):3526−32.
[243] Smith C, Malmali M, Liu CY, McCormick AV, Cussler EL. Rates of ammonia absorption and release in calcium chloride. ACS Sustainable Chem Eng 2018;6(9):11827−35.
[244] Christensen CH, Sørensen Z, Johannessen T, Quaade UJ, Honkala K, Elmøe TD, et al. Metal ammine complexes for hydrogen storage. J Mater Chem 2005;15(38): 4106−8.
[245] Malmali M, McCormick A, Cussler EL, Prince J, Reese M. Lower pressure ammonia synthesis. In: NH_3 fuel conference [Internet]. Minneapolis (MN); 2017. Available from: https://nh3fuelassociation.org/2017/10/01/lower-pressure-ammonia-synthesis/.
[246] McCormick A, Cussler E, Daoutidis P, Dauenhauer P, Schmidt L, Ruan R, et al. Potential strategies for distributed sustainable ammonia production. In: NH_3 fuel conference [Internet]. Chicago (IL); 2015. Available from: https://nh3fuelassociation.org/wp-content/uploads/2016/08/mccormick-nh3-fuel-conference-21sep2015.pdf.
[247] Hummelshøj JS, Sørensen RZ, Kustova MY, Johannessen T, Nørskov JK, Christensen CH. Generation of nanopores during desorption of NH_3 from $Mg(NH_3)_6Cl_2$. J Am Chem Soc 2006;128(1):16−7.
[248] Christensen CH, Johannessen T, Sørensen RZ, Nørskov JK. Towards an ammonia-mediated hydrogen economy? Catal Today 2006;111(1−2):140−4.
[249] Liu CY, Aika K. Absorption and desorption behavior of ammonia with alkali earth halide and mixed halide. Chem Lett 2002;8(5):798−9.
[250] Peng P, Li Y, Cheng Y, Deng S, Chen P, Ruan R. Atmospheric pressure ammonia synthesis using non-thermal plasma assisted catalysis. Plasma Chem Plasma Process 2016;36(5):1201−10.

[251] Helminen J, Helenius J, Paatero E, Turunen I. Adsorption equilibria of ammonia gas on inorganic and organic sorbents at 298. 15 K. J Chem Eng Data 2001; 46(2):391−9.
[252] Beach J, Kintner J, Welch A, Ganley J, O'Hayre R. Fast-ramping reactor for CO_2-free NH_3 synthesis. In: NH_3 fuel conference [Internet]. Minneapolis (MN); 2017. Available from: https://nh3fuelassociation.org/2017/10/01/fast-ramping-reactor-for-co2-free-nh3-synthesis/.
[253] Takeuchi M, Tsukamoto T, Kondo A, Matsuoka M. Investigation of NH_3 and NH_4^+ adsorbed on ZSM-5 zeolites by near and middle infrared spectroscopy. Catal Sci Technol 2015;5(9):4587−93.
[254] Takeuchi M, Tsukamoto T, Kondo A, Bao Y, Matsuoka M. Near infrared study on the adsorption states of NH_3 and NH_4^+ on hydrated ZSM-5 zeolites. J Near Infrared Spectrosc 2019;27(3):241−9.
[255] Liu CY, Aika K-I. Ammonia adsorption on ion exchanged Y-zeolites as ammonia storage material. J Japan Pet Inst. 2003;46(5):301−7.
[256] Bogaerts A, Neyts EC. Plasma technology: an emerging technology for energy storage. ACS Energy Lett 2018; 3(4):1013−27.
[257] Song Y, Johnson D, Peng R, Hensley DK, Bonnesen PV, Liang L, et al. A physical catalyst for the electrolysis of nitrogen to ammonia. Sci Adv 2018;4(4).
[258] Peng P, Schiappacasse C, Zhou N, Addy M, Cheng Y, Zhang Y, et al. Sustainable non-thermal plasma-assisted nitrogen fixation - Synergistic catalysis. ChemSusChem 2019;1−12.
[259] Carreon ML. Plasma catalytic ammonia synthesis: state of the art and future directions. J Phys D Appl Phys 2019;52(48).
[260] Mehta P, Barboun P, Go DB, Hicks JC, Schneider WF. Catalysis enabled by plasma activation of strong chemical bonds: a review. ACS Energy Lett 2019;4(5): 1115−33.
[261] Hong J, Prawer S, Murphy AB. Plasma catalysis as an alternative route for ammonia production: status, mechanisms, and prospects for progress. ACS Sustainable Chem Eng 2018;6(1):15−31.
[262] Peng P, Chen P, Schiappacasse C, Zhou N, Anderson E, Chen D, et al. A review on the non-thermal plasma-assisted ammonia synthesis technologies. J Clean Prod 2018;177:597−609.
[263] Kim H-H, Teramoto Y, Negishi N, Ogata A. A multidisciplinary approach to understand the interactions of nonthermal plasma and catalyst: a review. Catal Today 2015;256(Part 1):13−22.
[264] Neyts EC, Ostrikov K, Sunkara MK, Bogaerts A. Plasma catalysis: synergistic effects at the nanoscale. Chem Rev 2015;115(24):13408−46.
[265] Neyts EC, Bogaerts A. Understanding plasma catalysis through modelling and simulation — a review. J Phys D Appl Phys 2014;47(22):1−18.
[266] Mehta P, Barboun P, Herrera FA, Kim J, Rumbach P, Go DB, et al. Overcoming ammonia synthesis scaling relations with plasma-enabled catalysis. Nat Catal 2018;1(4):269−75.
[267] Hansen FY, Henriksen NE, Billing GD, Guldberg A. Catalytic synthesis of ammonia using vibrationally excited nitrogen molecules: theoretical calculation of equilibrium and rate constants. Surf Sci 1992;264(1−2):225−34.
[268] Rouwenhorst KHR, Kim H-H, Lefferts L. Vibrationally excited activation of N_2 in plasma-enhanced catalytic ammonia synthesis: a kinetic analysis. ACS Sustainable Chem Eng 2019;7(20):17515−22.
[269] Brandenburg R, Bogaerts A, Bongers W, Fridman A, Fridman G, Locke BR, et al. White paper on the future of plasma science in environment, for gas conversion and agriculture. Plasma Process Polym April 2018: 1−18. 2018.
[270] Kim H-H, Teramoto Y, Ogata A, Takagi H, Nanba T. Atmospheric-pressure nonthermal plasma synthesis of ammonia over ruthenium catalysts. Plasma Process Polym 2017;14(6):1−9.
[271] Kyriakou V, Garagounis I, Vasileiou E, Vourros A, Stoukides M. Progress in the electrochemical synthesis of ammonia. Catal Today 2017;286:2−13.
[272] van der Ham CJM, Koper MTM, Hetterscheid DGH. Challenges in reduction of dinitrogen by proton and electron transfer. Chem Soc Rev 2014;43(15):5183−91.
[273] Cui X, Tang C, Zhang Q. A review of electrocatalytic reduction of dinitrogen to ammonia under ambient conditions. Adv Energy Mater 2018;8(22):1800369.
[274] Shipman MA, Symes MD. Recent progress towards the electrosynthesis of ammonia from sustainable resources. Catal Today 2017;286:57−68.
[275] Bao D, Zhang Q, Meng F-L, Zhong H-X, Shi M-M, Zhang Y, et al. Electrochemical reduction of N_2 under ambient conditions for artificial N_2 fixation and renewable energy storage using N_2/NH_3 cycle. Adv Mater 2017;29(3):1604799.
[276] Yao Y, Zhu S, Wang H, Li H, Shao M. A spectroscopic study on the nitrogen electrochemical reduction reaction on gold and platinum surfaces. J Am Chem Soc 2018;140(4):1496−501.
[277] Abghoui Y, Skúlasson E. Transition metal nitride catalysts for electrochemical reduction of nitrogen to ammonia at ambient conditions. Procedia Comput Sci 2015;51(1):1897−906.
[278] Yang X, Nash J, Chang X, Yan Y, Xu B, Kattel S, et al. Quantification of active sites and elucidation of the reaction mechanism of the electrochemical nitrogen reduction reaction on vanadium nitride. Angew Chem Int Ed 2019;1−6.
[279] Giddey S, Badwal SPS, Kulkarni A. Review of electrochemical ammonia production technologies and materials. Int J Hydrogen Energy 2013;38(34):14576−94.
[280] James JD, van Delft YC. Power to ammonia process options: input to power to ammonia value chains and business cases [Internet]. 2017. Available from: https://www.ecn.nl/publications//PdfFetch.aspx?nr=ECN-E−17-039.

[281] Kyriakou V, Garagounis I, Vourros A, Vasileiou E, Stoukides M. An electrochemical Haber-bosch process. Joule 2020;4:1−17.
[282] Amar IA, Lan R, Petit CTG, Tao S. Solid-state electrochemical synthesis of ammonia: a review. J Solid State Electrochem 2011;15(9):1845−60.
[283] Vasileiou E, Kyriakou V, Garagounis I, Vourros A, Manerbino A, Coors WG, et al. Electrochemical enhancement of ammonia synthesis in a BaZr0.7-Ce0.2Y0.1O2.9 solid electrolyte cell. Solid State Ionics 2016;288:357−62.
[284] Yun DS, Joo JH, Yu JH, Yoon HC, Kim JN, Yoo CY. Electrochemical ammonia synthesis from steam and nitrogen using proton conducting yttrium doped barium zirconate electrolyte with silver, platinum, and lanthanum strontium cobalt ferrite electrocatalyst. J Power Sources 2015;284:245−51.
[285] Marnellos G, Stoukides M. Ammonia synthesis at atmospheric pressure. Science 1998;282(5386):98−100.
[286] Xie YH, Wang J De, Liu RQ, Su XT, Sun ZP, Li ZJ. Preparation of La 1.9 Ca 0.1 Zr 2 O 6.95 with pyrochlore structure and its application in synthesis of ammonia at atmospheric pressure. Solid State Ionics 2004; 168(1−2):117−21.
[287] Garagounis V, Stoukides D, Stoukides. Electrochemical synthesis of ammonia: recent efforts and future outlook. Membranes 2019;9(9):112.
[288] Kim K, Yoo CY, Kim JN, Yoon HC, Han JI. Electrochemical synthesis of ammonia from water and nitrogen catalyzed by nano-Fe_2O_3 and $CoFe_2O_4$ suspended in a molten LiCl-KCl-CsCl electrolyte. Kor J Chem Eng 2016;33(6):1777−80.
[289] Licht S, Cui B, Wang B, Li F-F, Lau J, Liu S. Ammonia synthesis by N_2 and steam electrolysis in molten hydroxide suspensions of nanoscale Fe_2O_3. Science 2014; 345(6197):637−40.
[290] Murakami T, Nishikiori T, Nohira T, Ito Y. Electrolytic synthesis of ammonia in molten salts under atmospheric pressure. J Am Chem Soc 2003;125(2): 334−5.
[291] Köleli F, Kayan DB. Low overpotential reduction of dinitrogen to ammonia in aqueous media. J Electroanal Chem 2010;638(1):119−22.
[292] Tsuneto A, Kudo A, Sakata T. Lithium-mediated electrochemical reduction of high pressure N_2 to NH_3. J Electroanal Chem 1994;367(1−2):183−8.
[293] Wang K, Smith D, Zheng Y. Electron-driven heterogeneous catalytic synthesis of ammonia: current states and perspective. Carbon Resour Convers 2018;1(1): 2−31.
[294] Bicer Y, Dincer I. Electrochemical synthesis of ammonia in molten salt electrolyte using hydrogen and nitrogen at ambient pressure. J Electrochem Soc 2017;164(8): H5036−42.
[295] Guo X, Zhu Y, Ma T. Lowering reaction temperature: electrochemical ammonia synthesis by coupling various electrolytes and catalysts. J Energy Chem 2017;26(6): 1107−16.
[296] Murakami T, Nohira T, Araki Y, Goto T, Hagiwara R, Ogata YH. Electrolytic synthesis of ammonia from water and nitrogen under atmospheric pressure using a boron-doped diamond electrode as a nonconsumable anode. Electrochem Solid State Lett 2007;10(4):10−2.
[297] Yang J, Weng W, Xiao W. Electrochemical synthesis of ammonia in molten salts. J Energy Chem 2019;43: 195−207.
[298] Xue X, Chen R, Yan C, Zhao P, Hu Y, Zhang W, et al. Review on photocatalytic and electrocatalytic artificial nitrogen fixation for ammonia synthesis at mild conditions: advances, challenges and perspectives. Nano Res 2019;12(6):1229−49.
[299] Wang Q, Guo J, Chen P. Recent progress towards mild-condition ammonia synthesis. J Energy Chem 2019: 25−36.
[300] Kordali V, Kyriacou G, Lambrou C. Electrochemical synthesis of ammonia at atmospheric pressure and low temperature in a solid polymer electrolyte cell. Chem Commun 2000;17:1673−4.
[301] Xu G, Liu R, Wang J. Electrochemical synthesis of ammonia using a cell with a Nafion membrane and SmFe0.7Cu0.3-x Ni x O3 (x = 0-0.3) cathode at atmospheric pressure and lower temperature. Sci China, Ser B Chem. 2009;52(8):1171−5.
[302] Liu R, Xu G. Comparison of electrochemical synthesis of ammonia by using sulfonated polysulfone and nafion membrane with $Sm1.5Sr0.5NiO_4$. Chin J Chem 2010; 28(2):139−42.
[303] Garagounis I, Kyriakou V, Skodra A, Vasileiou E, Stoukides M. Electrochemical synthesis of ammonia in solid electrolyte cells. Front Energy Res 2014;2(January).
[304] Guo C, Ran J, Vasileff A, Qiao S. Rational design of electrocatalysts and photo(electro)catalysts for nitrogen reduction to ammonia (NH_3) under ambient conditions. Energy Environ Sci 2017;11:45−56.
[305] Zhao R, Xie H, Chang L, Zhang X, Zhu X, Tong X, et al. Recent progress in the electrochemical ammonia synthesis under ambient conditions. Energy 2019;1(2): 1−29.
[306] Kim K, Lee N, Yoo C-Y, Kim J-N, Yoon HC, Han J-I. Communication—electrochemical reduction of nitrogen to ammonia in 2-propanol under ambient temperature and pressure. J Electrochem Soc 2016;163(7): F610−2.
[307] Kim K, Yoo C-Y, Kim J-N, Yoon HC, Han J-I. Electrochemical synthesis of ammonia from water and nitrogen in ethylenediamine under ambient temperature and pressure. J Electrochem Soc 2016;163(14):F1523−6.
[308] Zhou F, Azofra LM, Ali M, Kar M, Simonov AN, McDonnell-Worth C, et al. Electro-synthesis of ammonia from nitrogen at ambient temperature and pressure in ionic liquids. Energy Environ Sci 2017; 10(12):2516−20.
[309] Chen G, Ren S, Zhang L, Cheng H, Luo Y, Zhu K, et al. Advances in electrocatalytic N_2 reduction—strategies to tackle the selectivity challenge. Small Methods 2019; 3(6):1800337.

[310] Cheng S, Gao YJ, Yan YL, Gao X, Zhang SH, Zhuang GL, et al. Oxygen vacancy enhancing mechanism of nitrogen reduction reaction property in Ru/TiO_2. J Energy Chem 2019;39:144−51.

[311] Kugler K, Luhn M, Schramm JA, Rahimi K, Wessling M. Galvanic deposition of Rh and Ru on randomly structured Ti felts for the electrochemical NH_3 synthesis. Phys Chem Chem Phys 2015;17(5):3768−82.

[312] Liu HM, Han SH, Zhao Y, Zhu YY, Tian XL, Zeng JH, et al. Surfactant-free atomically ultrathin rhodium nanosheet nanoassemblies for efficient nitrogen electroreduction. J Mater Chem 2018;6(7):3211−7.

[313] Wang H, Yu H, Wang Z, Li Y, Xu Y, Li X, et al. Electrochemical fabrication of porous Au film on Ni foam for nitrogen reduction to ammonia. Small 2019; 1804769:1−7.

[314] Lan R, Irvine JTS, Tao S. Synthesis of ammonia directly from air and water at ambient temperature and pressure. Sci Rep 2013;3:1−7.

[315] Wang J, Yu L, Hu L, Chen G, Xin H, Feng X. Ambient ammonia synthesis via palladium-catalyzed electrohydrogenation of dinitrogen at low overpotential. Nat Commun 2018;9(1).

[316] Huang H, Xia L, Shi X, Asiri AM, Sun X. Ag nanosheet for efficient electrocatalytic N_2 fixation to NH_3 at ambient conditions. Chem Commun 2018;54(81):11427−30.

[317] Hu L, Khaniya A, Wang J, Chen G, Kaden WE, Feng X. Ambient electrochemical ammonia synthesis with high selectivity on Fe/Fe-oxide catalyst. ACS Catal 2018; 8(10):9312−9.

[318] Xiang X, Wang Z, Shi X, Fan M, Sun X. Ammonia synthesis from electrocatalytic N_2 reduction under ambient conditions by Fe_2O_3 nanorods. ChemCatChem 2018; 10(20):4530−5.

[319] Xu B, Xia L, Zhou F, Zhao R, Chen H, Wang T, et al. Enhancing electrocatalytic N_2 reduction to NH_3 by CeO_2 nanorod with oxygen vacancies. ACS Sustainable Chem Eng 2019;7(3):2889−93.

[320] Fu W, Zhuang P, Oliverlam Chee M, Dong P, Ye M, Shen J. Oxygen vacancies in Ta_2O_5 nanorods for highly efficient electrocatalytic N_2 reduction to NH_3 under ambient conditions. ACS Sustainable Chem Eng 2019; 7(10):9622−8.

[321] Zhang G, Ji Q, Zhang K, Chen Y, Li Z, Liu H, et al. Triggering surface oxygen vacancies on atomic layered molybdenum dioxide for a low energy consumption path toward nitrogen fixation. Nanomater Energy 2019; 59(January):10−6.

[322] Han J, Ji X, Ren X, Cui G, Li L, Xie F, et al. MoO_3 nanosheet for efficient electrocatalytic N_2 fixation to NH_3. J Mater Chem 2018;6(27):12974−7.

[323] Huang L, Wu J, Han P, Al-Enizi AM, Almutairi TM, Zhang L, et al. NbO_2 electrocatalyst toward 32% faradaic efficiency for N_2 fixation. Small Methods 2018;3(6): 1−6.

[324] Han J, Liu Z, Ma Y, Cui G, Xie F, Wang F, et al. Ambient N_2 fixation to NH_3 at ambient conditions: using Nb_2O_5 nanofiber as a high-performance electrocatalyst. Nanomater Energy 2018;52(July):264−70.

[325] Zhang R, Ren X, Shi X, Xie F, Zheng B, Guo X, et al. Enabling effective electrocatalytic N_2 conversion to NH_3 by the TiO_2 nanosheets array under ambient conditions. ACS Appl Mater Interfaces 2018;1(34):28251−5.

[326] Wu X, Xia L, Wang Y, Lu W, Liu Q, Shi X, et al. Mn_3O_4 nanocube: an efficient electrocatalyst toward artificial N_2 fixation to NH_3. Small 2018;1803111:6−11.

[327] Chu K, Liu YP, Li YB, Zhang H, Tian Y. Efficient electrocatalytic N_2 reduction on CoO quantum dots. J Mater Chem 2019;7(9):4389−94.

[328] Zhang R, Guo H, Yang L, Wang Y, Niu Z, Huang H, et al. Electrocatalytic N_2 fixation over hollow VO_2 microspheres at ambient conditions. ChemElectroChem 2019;6(4):1−5.

[329] Li X, Li T, Ma Y, Wei Q, Qiu W, Guo H, et al. Boosted electrocatalytic N_2 reduction to NH_3 by defect-rich MoS_2 nanoflower. Adv Energy Mater 2018;8(30): 1−8.

[330] Zhao X, Lan X, Yu D, Fu H, Liu Z, Mu T. Deep eutectic-solvothermal synthesis of nanostructured Fe_3S_4 for electrochemical N_2 fixation under ambient conditions. Chem Commun 2018;54(92):13010−3.

[331] Chen P, Zhang N, Wang S, Zhou T, Tong Y, Ao C, et al. Interfacial engineering of cobalt sulfide/graphene hybrids for highly efficient ammonia electrosynthesis. Proc Natl Acad Sci USA 2019;116(14):6635−40.

[332] Zhang L, Ji X, Ren X, Ma Y, Shi X, Tian Z, et al. Electrochemical ammonia synthesis via nitrogen reduction reaction on a MoS_2 catalyst: theoretical and experimental studies. Adv Mater 2018;1800191:2−7.

[333] Ren X, Zhao J, Wei Q, Ma Y, Guo H, Liu Q, et al. High-performance N_2-to-NH_3 conversion electrocatalyzed by Mo_2C nanorod. ACS Cent Sci 2018;5(1):116−21.

[334] Yuan X-Z, Zhu S, Gu M, Shao M, Wang H, Wang Y, et al. Chromium oxynitride electrocatalysts for electrochemical synthesis of ammonia under ambient conditions. Small Methods 2018;1800324:1800324.

[335] Zhang R, Zhang Y, Ren X, Cui G, Asiri AM, Zheng B, et al. High-efficiency electrosynthesis of ammonia with high selectivity under ambient conditions enabled by VN nanosheet array. ACS Sustainable Chem Eng 2018; 6(8):9545−9.

[336] Ren X, Cui G, Chen L, Xie F, Wei Q, Tian Z, et al. Electrochemical N_2 fixation to NH_3 under ambient conditions: Mo_2N nanorod as a highly efficient and selective catalyst. Chem Commun 2018;54(61):8474−7.

[337] Sherbow TJ, Thompson EJ, Arnold A, Sayler RI, Britt RD, Berben LA. Electrochemical reduction of N_2 to NH_3 at low potential by a molecular aluminum complex. Chem Eur J 2019;25(2):454−8.

[338] Jeong EY, Yoo CY, Jung CH, Park JH, Park YC, Kim JN, et al. Electrochemical ammonia synthesis mediated by titanocene dichloride in aqueous electrolytes under ambient conditions. ACS Sustainable Chem Eng 2017; 5(11):9662−6.

[339] Lv C, Qian Y, Yan C, Ding Y, Liu Y, Chen G, et al. Defect engineering metal-free polymeric carbon nitride electrocatalyst for effective nitrogen fixation under ambient conditions. Angew Chem Int Ed 2018;57(32): 10246–50.
[340] Yu X, Han P, Wei Z, Huang L, Gu Z, Peng S, et al. Boron-Doped graphene for electrocatalytic N_2 reduction. Joule 2018;2(8):1610–22.
[341] Zhang L, Ding LX, Chen GF, Yang X, Wang H. Ammonia synthesis under ambient conditions: selective electroreduction of dinitrogen to ammonia on black phosphorus nanosheets. Angew Chem Int Ed 2019;1–6.
[342] Zhao J, Ren X, Li X, Fan D, Sun X, Ma H, et al. High-performance N_2-to-NH_3 fixation by a metal-free electrocatalyst. Nanoscale 2019;11(10):4231–5.
[343] Zeng J, Geng Z, Du J, Liu Z, Si R, Li P, et al. Achieving a record-high yield rate of 120.9 μgNH_3 mgcat.−1 h−1 for N_2 electrochemical reduction over Ru single-atom catalysts. Adv Mater 2018;30(40):1803498.
[344] Tao H, Choi C, Ding LX, Jiang Z, Han Z, Jia M, et al. Nitrogen fixation by Ru single-atom electrocatalytic reduction. Inside Chem 2019;5(1):204–14.
[345] Wang X, Wang W, Qiao M, Wu G, Chen W, Yuan T, et al. Atomically dispersed Au1 catalyst towards efficient electrochemical synthesis of ammonia. Sci Bull 2018; 63(19):1246–53.
[346] Lü F, Zhao S, Guo R, He J, Peng X, Bao H, et al. Nitrogen-coordinated single Fe sites for efficient electrocatalytic N_2 fixation in neutral media. Nanomater Energy 2019; 61(February):420–7.
[347] Zhao S, Lu X, Wang L, Gale J, Amal R. Carbon-based metal-free catalysts for electrocatalytic reduction of nitrogen for synthesis of ammonia at ambient conditions. Adv Mater 2019;31(13):1–9.
[348] Liu H, Wei L, Liu F, Pei Z, Shi J, Wang ZJ, et al. Homogeneous, heterogeneous, and biological catalysts for electrochemical N_2 reduction toward NH_3 under ambient conditions. ACS Catal 2019:5245–67.
[349] Wang S, Ichihara F, Pang H, Chen H, Ye J. Nitrogen fixation reaction derived from nanostructured catalytic materials. Adv Funct Mater 2018;28(50):1–26.
[350] Hao YC, Guo Y, Chen LW, Shu M, Wang XY, Bu TA, et al. Promoting nitrogen electroreduction to ammonia with bismuth nanocrystals and potassium cations in water. Nat Catal 2019;2(5):448–56.
[351] Nazemi M, El-Sayed MA. Electrochemical synthesis of ammonia from N_2 and H_2O under ambient conditions using pore-size-controlled hollow gold nanocatalysts with tunable plasmonic properties. J Phys Chem Lett 2018;9(17):5160–6.
[352] Wang M, Liu S, Zhong J, Yan C. Over 56.55% Faradaic efficiency of ambient ammonia synthesis enabled by positively shifting the reaction potential. Nat Commun 2019;10(1):1–8.
[353] Xue Z-H, Zhang S-N, Lin Y-X, Su H, Zhai G-Y, Han J-T, et al. Electrochemical reduction of N_2 into NH_3 by donor-acceptor couples of Ni and Au nanoparticles with a 67.8% faradaic efficiency. J Am Chem Soc 2019;0(ja) [null-null].
[354] Andersen SZ, Čolić V, Yang S, Schwalbe JA, Nielander AC, McEnaney JM, et al. A rigorous electrochemical ammonia synthesis protocol with quantitative isotope measurements. Nature 2019;570:504–8.
[355] Butler T, Vermeylen F, Lehmann CM, Likens GE, Puchalski M. Increasing ammonia concentration trends in large regions of the USA derived from the NADP/AMoN network. Atmos Environ 2016;146(3):132–40.
[356] Shah SB, Grabow GL, Westerman PW. Ammonia adsorption in five types of fle 2006;22(September 2005):919–23.
[357] Dabundo R, Lehmann MF, Treibergs L, Tobias CR, Altabet MA, Moisander PH, et al. The contamination of commercial15N_2 gas stocks with15N-labeled nitrate and ammonium and consequences for nitrogen fixation measurements. PloS One 2014;9(10).
[358] Greenlee LF, Renner JN, Foster SL. The use of controls for consistent and accurate measurements of electrocatalytic ammonia synthesis from dinitrogen. ACS Catal 2018; 8(9):7820–7.
[359] Ren Y, Yu C, Tan X, Han X, Huang H, Huang H, et al. Is it appropriate to use the nafion membrane in electrocatalytic N_2 reduction? Small Methods 2019;1900474:1900474.
[360] Li L, Tang C, Yao D, Zheng Y, Qiao S-Z. Electrochemical nitrogen reduction: identification and elimination of contamination in electrolyte. ACS Energy Lett 2019; 4(9):2111–6.
[361] Suryanto BHR, Du H, Wang D, Chen J, Simonov AN, Macfarlane DR. Challenges and prospects in the catalysis of electroreduction of nitrogen to ammonia. Nat Catal 2019;2(1):290–6.
[362] Montoya JH, Tsai C, Vojvodic A, Jens KN. The challenge of electrochemical ammonia synthesis: a new perspective on the role of nitrogen scaling relations. ChemSusChem 2015;8(13):2180–6.
[363] Montemore MM, Medlin JW. Scaling relations between adsorption energies for computational screening and design of catalysts. Catal Sci Technol 2014;4(11): 3748–61.
[364] Höskuldsson ÁB, Abghoui Y, Gunnarsdóttir AB, Skúlason E. Computational screening of rutile oxides for electrochemical ammonia formation. ACS Sustainable Chem Eng 2017;5(11):10327–33.
[365] Abghoui Y, Skúlason E. Electrochemical synthesis of ammonia via Mars-van Krevelen mechanism on the (111) facets of group III–VII transition metal mononitrides. Catal Today [Internet] 2017;286:78–84. Available from: https://doi.org/10.1016/j.cattod.2016.06.009.
[366] Abghoui Y, Sigtryggsson SB, Skúlason E. Biomimetic Available from: nitrogen fixation catalyzed by transition metal sulfide surfaces in an electrolytic cell. ChemSusChem 2019;12(18):4265–73.
[367] Zhao J, Chen Z. Single Mo atom supported on defective boron nitride monolayer as an efficient electrocatalyst

for nitrogen fixation: a computational study. J Am Chem Soc 2017;139(36):12480−7.
[368] Choi C, Back S, Kim NY, Lim J, Kim YH, Jung Y. Suppression of hydrogen evolution reaction in electrochemical N_2 reduction using single-atom catalysts: a computational guideline. ACS Catal 2018;8(8):7517−25.
[369] Zhao J, Zhao J, Cai Q. Single transition metal atom embedded into a MoS_2 nanosheet as a promising catalyst for electrochemical ammonia synthesis. Phys Chem Chem Phys 2018;20(14):9248−55.
[370] Guo R, Hu M, Zhang W, He J. Boosting electrochemical nitrogen reduction performance over binuclear Mo atoms on N-doped nanoporous graphene: a theoretical investigation. Molecules 2019;24(9).
[371] Kibsgaard J, Nørskov JK, Chorkendorff I. The difficulty of proving electrochemical ammonia synthesis. ACS Energy Lett 2019:2986−8.
[372] Zhang L, Mallikarjun Sharada S, Singh AR, Rohr BA, Su Y, Qiao L, et al. A theoretical study of the effect of a non-aqueous proton donor on electrochemical ammonia synthesis. Phys Chem Chem Phys 2018; 20(7):4982−9.
[373] Singh AR, Rohr BA, Schwalbe JA, Cargnello M, Chan K, Jaramillo TF, et al. Electrochemical ammonia synthesis - the selectivity challenge. ACS Catal 2017;7(1): 706−9.
[374] Chen X, Li N, Kong Z, Ong WJ, Zhao X. Photocatalytic fixation of nitrogen to ammonia: state-of-the-art advancements and future prospects. Mater Horizons 2018;5(1):9−27.
[375] Zhang S, Zhao Y, Shi R, Waterhouse GIN, Zhang T. Photocatalytic ammonia synthesis: recent progress and future. Energy 2019;1(2):100013.
[376] Vu MH, Sakar M, Do TO. Insights into the recent progress and advanced materials for photocatalytic nitrogen fixation for ammonia (NH_3) production. Catalysts 2018;8(12).
[377] Ithisuphalap K, Zhang H, Guo L, Yang Q, Yang H, Wu G. Photocatalysis and photoelectrocatalysis methods of nitrogen reduction for sustainable ammonia synthesis. Small Methods 2019;3(6):1800352.
[378] Schrauzer GN, Guth TD. Photolysis of water and photoreduction of nitrogen on titanium Dioxide1. J Am Chem Soc 1977;99(22):7189−93.
[379] Zhao Y, Zhao Y, Shi R, Wang B, Waterhouse GIN, Wu LZ, et al. Tuning oxygen vacancies in ultrathin TiO_2 nanosheets to boost photocatalytic nitrogen fixation up to 700 nm. Adv Mater 2019;31(16):1−9.
[380] Yang J, Guo Y, Jiang R, Qin F, Zhang H, Lu W, et al. High-efficiency "working-in-tandem" nitrogen photofixation achieved by assembling plasmonic gold nanocrystals on ultrathin titania nanosheets. J Am Chem Soc 2018; 140(27):8497−508.
[381] Liu S, Wang Y, Wang S, You M, Hong S, Wu TS, et al. Photocatalytic fixation of nitrogen to ammonia by single Ru atom decorated TiO_2 nanosheets. ACS Sustainable Chem Eng 2019;7(7):6813−20.
[382] Lashgari M, Zeinalkhani P. Photocatalytic N_2 conversion to ammonia using efficient nanostructured solar-energy-materials in aqueous media: a novel hydrogenation strategy and basic understanding of the phenomenon. Appl Catal Gen 2017;529:91−7.
[383] Li X, Wang W, Jiang D, Sun S, Zhang L, Sun X. Efficient solar-driven nitrogen fixation over carbon−tungstic-acid hybrids. Chem Eur J 2016;22(39):13819−22.
[384] Zhang N, Jalil A, Wu D, Chen S, Liu Y, Gao C, et al. Refining defect states in W18O49 by Mo doping: a strategy for tuning N_2 activation towards solar-driven nitrogen fixation. J Am Chem Soc 2018;140(30):9434−43.
[385] Cao Y, Hu S, Li F, Fan Z, Bai J, Lu G, et al. Photofixation of atmospheric nitrogen to ammonia with a novel ternary metal sulfide catalyst under visible light. RSC Adv 2016;6(55):49862−7.
[386] Sun S, Li X, Wang W, Zhang L, Sun X. Photocatalytic robust solar energy reduction of dinitrogen to ammonia on ultrathin MoS_2. Appl Catal B Environ 2017;200:323−9.
[387] Li H, Shang J, Ai Z, Zhang L. Efficient visible light nitrogen fixation with BiOBr nanosheets of oxygen vacancies on the exposed {001} Facets. J Am Chem Soc 2015; 137(19):6393−9.
[388] Wang S, Hai X, Ding X, Chang K, Xiang Y, Meng X, et al. Light-switchable oxygen vacancies in ultrafine Bi_5O_7 Br nanotubes for boosting solar-driven nitrogen fixation in pure water. Adv Mater 2017;29(31):1−7.
[389] Hu S, Chen X, Li Q, Li F, Fan Z, Wang H, et al. Fe^{3+} doping promoted N_2 photofixation ability of honeycombed graphitic carbon nitride: the experimental and density functional theory simulation analysis. Appl Catal B Environ 2017;201:58−69.
[390] Shiraishi Y, Shiota S, Kofuji Y, Hashimoto M, Chishiro K, Hirakawa H, et al. Nitrogen fixation with water on carbon-nitride-based metal-free photocatalysts with 0.1% solar-to-ammonia energy conversion efficiency. ACS Appl Energy Mater 2018;1(8):4169−77.
[391] Wang Z, Hu X, Liu Z, Zou G, Wang G, Zhang K. Recent developments in polymeric carbon nitride-derived photocatalysts and electrocatalysts for nitrogen fixation. ACS Catal 2019;9(11):10260−78.
[392] Medford AJ, Hatzell MC. Photon-driven nitrogen fixation: current progress, thermodynamic considerations, and future outlook. ACS Catal 2017;7(4):2624−43.
[393] Huang P, Liu W, He Z, Xiao C, Yao T, Zou Y, et al. Single atom accelerates ammonia photosynthesis. Sci China Chem 2018;61(9):1187−96.
[394] Volpin ME, Shur VB, Ilatovskaya MA. Fixation of nitrogen by systems based on dicyclopentadienyltitanium dichloride. Bull Acad Sci USSR Div Chem Sci 1964; 13(9):1644.
[395] Volpin ME, Ilatovskaya MA, Kosyakova LV, Shur VB. Catalytic fixation of nitrogen. Chem Commun 1968; (18):1074−5.
[396] Yandulov DV, Schrock RR. Catalytic reduction of dinitrogen to ammonia at a single molybdenum center. Science 2003;301(5629):76−8.

[397] Arashiba K, Miyake Y, Nishibayashi Y. A molybdenum complex bearing PNP-type pincer ligands leads to the catalytic reduction of dinitrogen into ammonia. Nat Chem 2010;3(2):120–5.
[398] Tanaka H, Arashiba K, Kuriyama S, Sasada A, Nakajima K, Yoshizawa K, et al. Unique behaviour of dinitrogen-bridged dimolybdenum complexes bearing pincer ligand towards catalytic formation of ammonia. Nat Commun 2014;5.
[399] Rodriguez MM, Bill E, Brennessel WW, Holland PL. N_2 reduction and hydrogenation to ammonia by a molecular iron-potassium complex. Science 2011;334(6057):780–3.
[400] Anderson JS, Rittle J, Peters JC. Catalytic conversion of nitrogen to ammonia by an iron model complex. Nature 2013;501(7465):84–7.
[401] Kuriyama S, Arashiba K, Nakajima K, Matsuo Y, Tanaka H, Ishii K, et al. Catalytic transformation of dinitrogen into ammonia and hydrazine by iron-dinitrogen complexes bearing pincer ligand. Nat Commun 2016;7.
[402] Pool JA, Lobkovsky E, Chirik PJ. Hydrogenation and cleavage of dinitrogen to ammonia with a zirconium complex. Nature 2004;427(6974):527–30.
[403] Yandulov DV, Schrock RR. Studies relevant to catalytic reduction of dinitrogen to ammonia by molybdenum triamidoamine complexes. Inorg Chem 2005;44(4):1103–17.
[404] Neese F. The Yandulov/Schrock cycle and the nitrogenase reaction: pathways of nitrogen fixation studied by density functional theory. Angew Chem Int Ed 2006; 45(2):196–9.
[405] Chin JM, Schrock RR, Müller P. Synthesis of diamidopyrrolyl molybdenum complexes relevant to reduction of dinitrogen to ammonia. Inorg Chem 2010;49(17): 7904–16.
[406] Dance I. Mimicking nitrogenase. Dalton Trans 2010; 39(12):2972–83.
[407] McEnaney JM, Singh AR, Schwalbe JA, Kibsgaard J, Lin JC, Cargnello M, et al. Ammonia synthesis from N_2 and H_2O using a lithium cycling electrification strategy at atmospheric pressure. Energy Environ Sci 2017; 10(7):1621–30.
[408] Swearer DF, Knowles NR, Everitt HO, Halas NJ. Light-driven chemical looping for ammonia synthesis. ACS Energy Lett 2019;4(7):1505–12.
[409] Gao W, Guo J, Wang P, Wang Q, Chang F, Pei Q, et al. Production of ammonia via a chemical looping process based on metal imides as nitrogen carriers. Nat Energy 2018;3(12):1067–75.
[410] Gálvez ME, Halmann M, Steinfeld A. Ammonia production via a two-step Al_2O_3/AlN thermochemical cycle. 1. Thermodynamic, environmental, and economic analyses. Ind Eng Chem Res 2007;46(7):2042–6.
[411] Cao G, Fisica D, Universitaria C, Sestu SS, Ca M, Sanna S, et al. Synthesis of bulk MgB 2 superconductors by pulsed electric current. AIChE J 2006;58(10): 3203–13.
[412] Michalsky R, Pfromm PH. An ionicity rationale to design solid phase metal nitride reactants for solar ammonia production. J Phys Chem C 2012;116(44): 23243–51.
[413] Michalsky R, Pfromm PH, Steinfeld A. Rational design of metal nitride redox materials for solar-driven ammonia synthesis. Interface Focus 2015;5(3):1–10.
[414] Shan N, Chikan V, Pfromm P, Liu B. Fe and Ni dopants facilitating ammonia synthesis on Mn4N and mechanistic insights from first-principles methods. J Phys Chem C 2018;122(11):6109–16.
[415] Laassiri S, Zeinalipour-Yazdi CD, Catlow CRA, Hargreaves JSJ. The potential of manganese nitride based materials as nitrogen transfer reagents for nitrogen chemical looping. Appl Catal B Environ 2018;223: 60–6.
[416] Michalsky R, Parman BJ, Amanor-Boadu V, Pfromm PH. Solar thermochemical production of ammonia from water, air and sunlight: thermodynamic and economic analyses. Energy 2012;42(1):251–60.
[417] Michalsky R, Avram AM, Peterson BA, Pfromm PH, Peterson AA. Chemical looping of metal nitride catalysts: low-pressure ammonia synthesis for energy storage. Chem Sci 2015;6(7):3965–74.
[418] Wang QR, Guan YQ, Gao WB, Guo JP, Chen P. Thermodynamic properties of ammonia production from hydrogenation of alkali and alkaline earth metal amides. ChemPhysChem 2019;20(10):1376–81.
[419] Kim K, Lee SJ, Kim DY, Yoo CY, Choi JW, Kim JN, et al. Electrochemical synthesis of ammonia from water and nitrogen: a lithium-mediated approach using lithium-ion conducting glass ceramics. ChemSusChem 2018; 11(1):120–4.
[420] Kim K, Chen Y, Han J-I, Yoon HC, Li W. Lithium-mediated ammonia synthesis from water and nitrogen: a membrane-free approach enabled by an immiscible aqueous/organic hybrid electrolyte system. Green Chem 2019;21(14):3839–45.
[421] Tsuneto A, Kudo A, Sakata T. Efficient electrochemical reduction of N_2 to NH_3 catalyzed by lithium. Chem Lett 1993;22:851–4.
[422] Lazouski N, Schiffer ZJ, Williams K, Manthiram K. Understanding continuous lithium-mediated electrochemical nitrogen reduction. Joule 2019;3(4):1127–39.
[423] Lazouski N, Manthiram K. Ambient lithium-mediated ammonia synthesis. Trends Chem 2019;1(1):141–2.